Universiteit
Leiden
The Netherlands

Development of affinity binders for non-invasive in vivo imaging of neurodegenerative disorders

Rutgers, K.S.

Citation
Rutgers, K. S. (2011, June 30). *Development of affinity binders for non-invasive in vivo imaging of neurodegenerative disorders*. Retrieved from https://hdl.handle.net/1887/17750

Version:	Corrected Publisher's Version
License:	Licence agreement concerning inclusion of doctoral thesis in the Institutional Repository of the University of Leiden
Downloaded from:	https://hdl.handle.net/1887/17750

Note: To cite this publication please use the final published version (if applicable).

DEVELOPMENT OF AFFINITY BINDERS FOR NON-INVASIVE *IN VIVO* IMAGING OF NEURODEGENERATIVE DISORDERS

Kim Rutgers

Cover design: Mirjam Hoekman

Layout and printing: Off Page, www.offpage.nl

ISBN: 978-94-90371-90-6

Copyright © 2011 by Kim Rutgers. All rights reserved.
Copyright on the individual chapters rests with author(s), with the following exceptions:
Chapter 2: Elsevier B.V.
Chapter 3: Elsevier B.V.

No part of this book may be reproduced, stored in a retrieval system, or transmitted in any form or by any means, without prior permission of the author.

DEVELOPMENT OF AFFINITY BINDERS FOR NON-INVASIVE *IN VIVO* IMAGING OF NEURODEGENERATIVE DISORDERS

Proefschrift

ter verkrijging van
de graad van Doctor aan de Universiteit Leiden,
op gezag van Rector Magnificus prof. mr. P.F. van der Heijden,
volgens besluit van het College voor Promoties
te verdedigen op donderdag 30 juni 2011
klokke 13:45 uur

door

Kim Sharon Rutgers
geboren te Nijmegen
in 1975

PROMOTIECOMMISSIE

Promotores:	Prof. Dr. M.A. van Buchem
	Prof. Dr. Ir. S.M. van der Maarel
Co-promoter:	Dr. L. van der Weerd
Overige leden:	Dr. A.G. de Boer[1]
	Prof. Dr. R.A.C. Roos
	Prof. Dr. C.T Verrips[2]

[1] Department of Pharmacology, Leiden-Amsterdam Center for Drug Research, Leiden University, Netherlands

[2] Department of Molecular Cell Biology, Utrecht University, Utrecht, Netherlands

The studies presented in this thesis were performed at the department of Human Genetics, Neurology, Pathology, Radiology, and Pharmacology at the Leiden University Medical Centre, Leiden, The Netherlands, the department of Molecular Cell Biology, Utrecht University, Utrecht, The Netherlands, the department of Neurology, Massachusetts General Hospital and Harvard Medical School, Charlestown, MA, US and the department of Pathology, C.S. Kubik Laboratory for Neuropathology, Massachusetts General Hospital and Harvard Medical School, Charlestown, MA, US. This work was financially supported by grants from the IOP Genomics Senter [IGE05005], the National Institutes of Health (NIH AG021084 and AG005134) and by the Centre for Medical Systems Biology within the framework of the Netherlands Genomics Initiative (NGI)/Netherlands Organization for Scientific Research (NWO). Publication of this thesis was financially supported the Centre for Medical Systems Biology (CMSB), the J.E. Jurriaanse stichting and Internationale Stichting Alzheimer Onderzoek (ISAO).

In heaven all the interesting people are missing.

(Friedrich Nietzsche)

TABLE OF CONTENTS

Chapter 1	General introduction	9
Chapter 2	Differential recognition of vascular and parenchymal beta amyloid deposition	27
Chapter 3	Transmigration of beta amyloid specific heavy chain antibody fragments across the in-vitro blood-brain barrier	57
Chapter 4	Binding characteristics and in vivo detection of beta amyloid deposits using heavy chain antibody fragments as potential molecular imaging agents	57
Chapter 5	General discussion	81
Addendum	Summary	95
	Samenvatting	99
	Curriculum Vitae	103
	Dankwoord	105

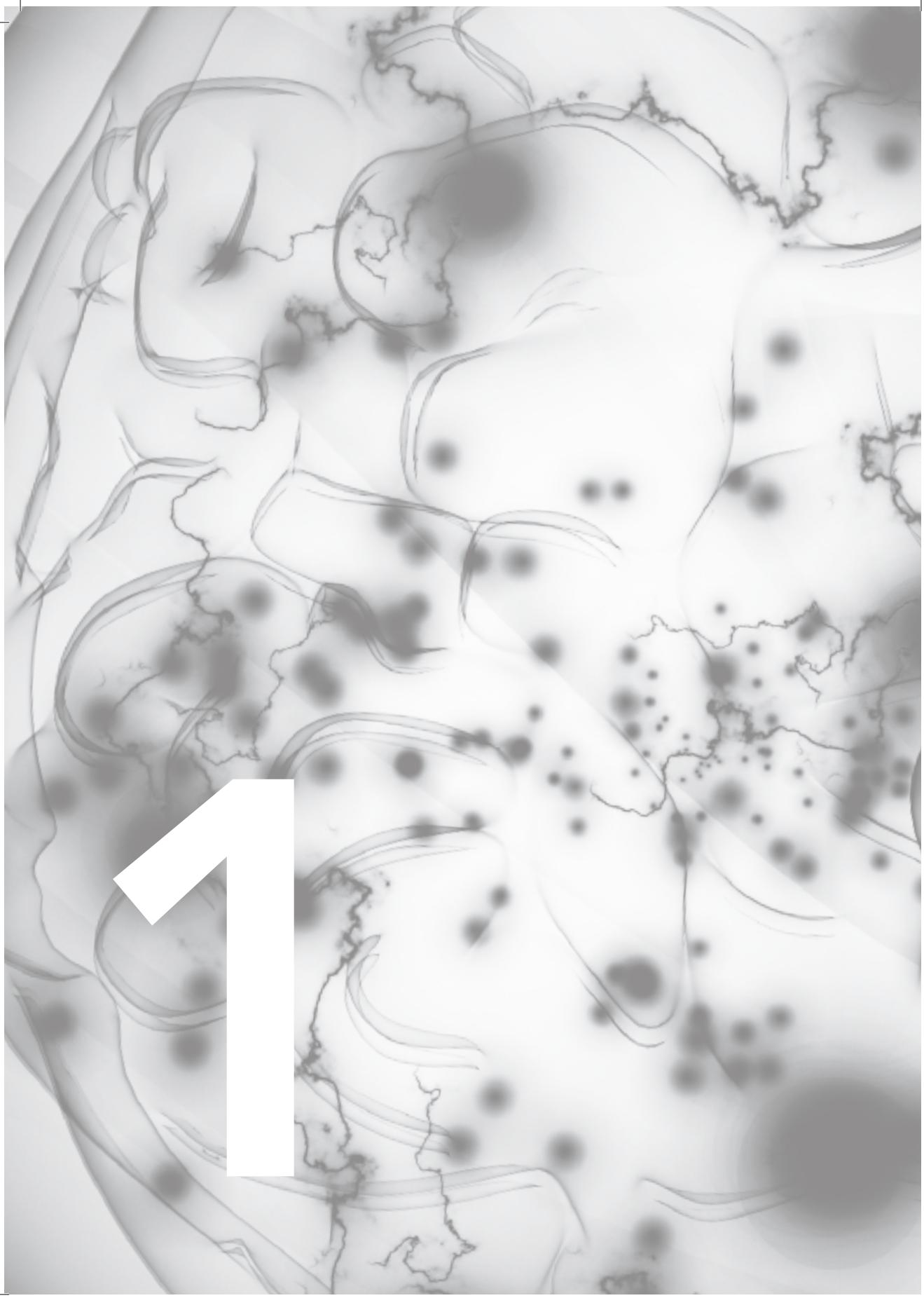
1

CHAPTER 1 | GENERAL INTRODUCTION

INTRODUCTION

Aggregation and accumulation of amyloid-forming proteins are causal to an emerging group of progressive and chronic entities. Soluble proteins normally present in body fluids form, by conformational changes, insoluble aggregates. Although the amino-acid sequences of this group of proteins are diverse, when aggregated, they are all arranged in an equal structured fashion i.e. the cross-B spine [1]. These protein deposits result in a histological feature termed amyloid. The protein aggregation diseases with amyloid involvement, collectively known as amyloidoses, include Alzheimer's disease (AD) and cerebral amyloid angiopathy (CAA).

ALZHEIMER'S DISEASE

AD is the most common form of dementia and one of the major health problems in the world. More than 35 million people worldwide suffer from AD, with age being the main risk factor [2]. This number is rapidly increasing in developed countries, caused by the growing part of elderly in demographic distribution of the population.

AD is clinically characterized by progression from episodic memory problems to an inexorable global cognitive decline that makes patients in the final stage of AD bedridden and completely care dependent, with death occurring 9 years after diagnosis on average.

AD was first described by Alzheimer in 1907. The first clues of the mechanisms behind this disease were obtained by post-mortem analysis of human AD brains. These investigations led to the identification of the histological hallmarks of AD; senile plaques consisting of extracellular amyloid-β (Aβ) deposits and neurofibrillary tangles associated with tau aggregates in the regions of the brain responsible for memory and cognition (Figure 1) [3].

AD is categorized in two subtypes: early onset autosomal-dominant cases (<5%) and late onset sporadic cases (>95%). Genes involved in genetically grounded AD

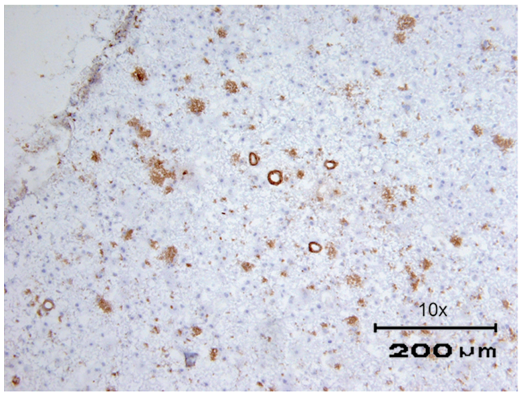

Figure 1 Immunohistochemistry of the cerebral cortex of an AD patient with CAA. The cryosection shown is stained with the conventional antibody 4G8. Immunoreactivety of 4G8 with Aβ, located in the vessel walls (CAA) and in parenchymal plaques, is visible [11].

are *APP, presenilin (PS)-1* and *(PS)-2*. For sporadic AD, genetic variations in the *APOE* gene play an important role [4]. The risk of sporadic AD increases with the number of *APOEε4* alleles [5]. The other genetic risk factor known for sporadic AD is polymorphisms of one of the inflammatory genes, for instance *TNF-α* [6].

In addition to the AD hallmarks mentioned above, fibrillar amyloid deposition is also frequently observed in medium-sized and small cerebral vessel walls, a condition known as cerebral amyloid angiopathy (CAA). Vascular dysfunction as a consequence of these amyloid depositions is postulated as a major mechanism of neurodegeneration, and this makes vascular amyloid deposition an important contributor to the disease pathogenesis (Figure 1)[7-10].

CEREBRAL AMYLOID ANGIOPATHY

CAA was first described in 1983 and is characterized by extracellular Aβ deposition in the cerebral and leptomeningeal vessel walls [12]. Seven of the twenty proteins known to be involved in amyloid deposit formation have been shown to cause CAA. The most frequently observed form of CAA in aged individuals is caused by Aβ aggregates; this makes it the most common cause of non-hypertensive intracerebral hemorrhage in elderly. Analogous to AD, mutations in the Aβ precursor protein (APP), PS1 and PS2 genes underlie familial forms of CAA. The most severe CAA is observed in cases with the Flemisch, Iowa and Dutch mutations in APP [13,14].

HEREDITARY CEREBRAL HEMORRHAGE WITH AMYLOIDOSIS-DUTCH TYPE

Hereditary cerebral hemorrhage with amyloidosis-Dutch type (HCHWA-D) was first described in 1964 and is characterized by severe CAA with secondary hemorrhages and/or infarcts with a mid-life age of onset [15]. As a consequence, HCHWA-D patients suffer from hemorrhagic strokes and dementia [16]. The cause of this disorder is a point mutation (guanine-to-cytosine transversion) at codon 693 of the APP gene at chromosome 21. This nucleotide transversion causes a glutamine-for-glutamic acid replacement at residue 22 of Aβ [13,17]. Dutch type Aβ ($Aβ_d$) is more prone to aggregation, more resistant to proteolytic degradation and is less efficiently cleared into the blood than wild-type Aβ ($Aβ_w$), supporting a pathogenic role by impaired clearance [18-22].

Although only 5% of all AD cases are familial and HCHWA-D is a rare disorder, both diseases implicate Aβ as a causative agent since the genetic mutations present in those diseases are associated with Aβ processing. As a consequence, diseases in which a genetic anomaly grounds the illness are a good model for research.

AMYLOID BETA

Aβ peptides consists of 39 to 43 amino acids and the vast majority, near 90%, of secreted Aβ ends at residue 40. Only <10% accounts for Aβ42 and Aβ38 peptides are the least abundant [23,24]. The pathological pattern of distribution varies amongst the different Aβ species. Aβ42 is predominantly present in parenchymal deposits, whereas Aβ40 is mainly present as vascular Aβ particularly in the large leptomeningeal vessels [25]. The small cortical arteries and arterioles affected by Aβ consist of a combination of Aβ40 and Aβ42 and amyloid associated with the capillary network is primarily composed of Aβ42 [26].

Aβ is derived from the C-terminal region of the type I membrane-spanning glycoprotein amyloid precursor protein (APP), which is ubiquitously expressed. The APP gene resides on chromosome 21 and is normally processed by the non-amyloidogenic pathway: APP is sequentially cleaved by α-secretase, resulting in $APPs_{\alpha}$ and $APP\text{-}CTF_{\alpha,}$ and γ-secretase which yields the small p3 fragment and the AICD (Figure 2). $APPs_{\alpha}$ has been suggested to exhibit synapse-promoting and

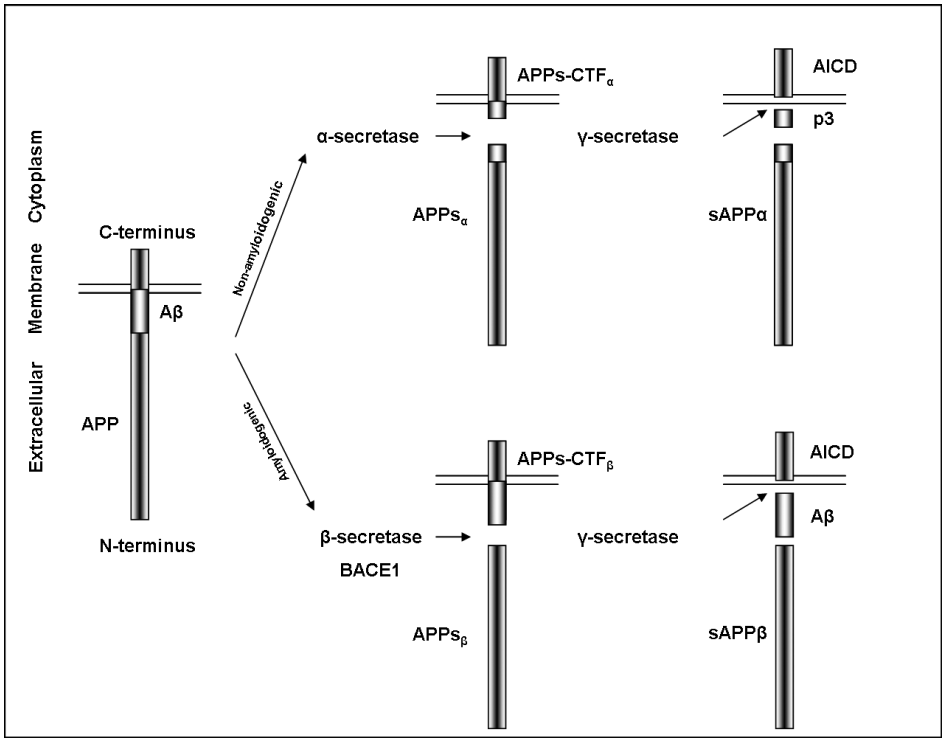

Figure 2 Proteolytic processing of APP. In the non-amyloidogenic pathway APP is sequential processed by α- and γ-secretase. α-secretase cleaves within the Aβ domain, preventing production of the intact Aβ peptide. In the amyloidogenic pathway APP is sequential processed by β- and γ-secretase. This pathway generates Aβ.

neuroprotective properties and, although controversial, AICD has been proposed to be a nuclear signalling molecule [27-30].

Aβ is generated through the amyloidogenic pathway: APP is sequentially cleaved by β-secretase (BACE1) at the N-terminus, generating the ectodomain $APPs_{\beta}$ and $APP\text{-}CTF_{\beta}$ and by and γ-secretase (a complex of presenilins, nicastrin, pen-2 and andaph-1) at the C-terminus liberating AICD and Aβ [31]. The cleavage site of γ-secretase is not precise and therefore Aβ peptides of lengths 39 to 43 can be formed (Figure 2). Aβ is proposed to be associated with synaptic activity, depressing excitatory synaptic transmission onto neurons [32].

Aß TOXICITY: FIBRILS, OLIGOMERS, MONOMERS

The exact nature of Aβ toxicity is still an object of debate. Aβ protein is normally present in the brain and cerebrospinal fluid of healthy individuals throughout life [33, 34, 35, 36, 37]. Therefore, the mere presence of Aβ is not responsible for setting off the Aβ inflicted neurodegeneration pathway. The ability to self-associate appears to be essential for neurotoxicity of Aβ. Aβ can exist in several different conformations depending on the solvent. In physiological buffers β-sheet and random coil structures are observed and in a membrane like environment the peptide adopts the α-helix conformation. Fibrilogenesis has been shown to be linked to an α to β-sheet conversion. Replacement of any residue within the sequence residues 17-23 by proline increases Aβ solubility and reduces the presence of the β-sheet conformation and fibril formation [38]. Aβ monomers can aggregate to form oligomers or bigger aggregates with different conformations. Amyloid protofibril and fibril formation can be induced by small nuclei of such aggregates [39,40]. In the amyloid plaques, that characterize the brains of patients with AD, Aβ is organized into insoluble fibrils with a diameter of 6–10 nm. Synthetic Aβ possesses the ability to self-aggregate in vitro into insoluble fibrils similar to those present in the human brain [41,42].

It was demonstrated that aggregation of Aβ is essential for its toxicity and it was assumed that since amyloid fibrils were measurable, these assemblies instigate this toxicity. However, the number of senile plaques, consisting of Aβ fibrils, in a dedicated area of the AD brain correlates poorly with synaptic loss or neuronal death, in that particular region, and the degree of cognitive impairment [43].

Rather, the presence of similar SDS-stable dimers and trimers in the soluble fraction of human brain and in extracts of amyloid plaques provided evidence for the involvement of these soluble non-fibrillar Aβ oligomers in AD. Furthermore, small Aβ oligomers exhibit in general much higher cytotoxicity than Aβ fibrils and in brain-slice preparations, these oligomers appear to be toxic to synapses [44, 45, 46, 47, 48-51, 52]. Moreover, recent studies associate the soluble Aβ oligomer levels with the degree of synaptic loss and severity of cognitive impairment [40,53-56,57]. Equivalent to the poor correlation between the amyloid plaque density in the human brain and severity of dementia [58, 59, 60], in APP transgenic mice memory impairment and changes in neuron

form and function can be observed well before Aβ plaque deposition [61, 62, 63, 64, 65,66, 67]. Thus rather than the histological visible Aβ fibrils, there is indication that the Aβ oligomers are implicated in Aβ toxicity. Therefore, intends of therapeutic approaches for the early targeting of Aβ neurotoxicity should be directed against those oligomers.

Small molecules could be valuable tools for AD therapy. Antibodies targeted against Aβ can prevent oligomerization or disrupt pre-formed oligomers and allow the brain's degradative machinery to remove these toxic agents. The difficulty in targeting these toxic agents is that all imaging or therapy moieties have to be able to pass the blood brain barrier (BBB).

THE BLOOD BRAIN BARRIER

The brain forms a protected microenvironment by a vascular barrier system that regulates the passage between the bloodstream and the brain parenchyma. This so-called blood brain barrier supplies the brain with nutrients and filters toxic compounds back into the bloodstream [68]. It mediates carrier-mediated transport of glucose, amino acids and active transport of ions [69-71]. The BBB is composed of a monolayer capillary brain endothelial cells (BEC). These BEC are surrounded by pericytes and astrocytic endfeet. The astrocytes are responsible for the preservation of specific BBB characteristics of endothelial cells [72,73]. The BEC are characterized by a lack of fenestrations, a high degree of polarization and an interconnection sealed by tight (TJ) and adherens junctions [74]. The TJ are responsible for low paracellular permeability of the BBB [75]. The BBB restricts free passage of compounds to small lipid-soluble molecules (<400 Da) with less than nine hydrogen bonds [76].

The BBB complicates the development of diagnostic tools or pharmacological agents for neurodegenerative diseases considerably by prohibiting free entrance of diagnostic or therapeutic of compounds into the brain. For the development of imaging and drug-targeting agents for the brain BBB passage is a key prerogative. Therefore the use of an in vitro system to assess crossing ability of the developed agents is a necessity in early research and a first step towards in vivo imaging behind the BBB.

An in vitro model has to mimic the in vivo situation as closely as possible and therefore the model has to contain all the BBB specific characteristics expressed by BBB specific cell-types. In order to maintain all BBB properties it is essential to use co-cultures of fully differentiated primary cultures of Bovine Cerebral Endothelial Cells (BCEC) and astrocytes. Studies have indicated that it is difficult to induce and maintain BBB properties in other than primary endothelial cells of cerebral origin [77, 78]. The use of primary cultures is time consuming and there is a high variation between isolations [79]. However, Gaillard *et al* established a protocol of freezing the fractions of brain capillaries and astrocytes to synchronize the culture procedures [80]. This protocol results in a higher flexibility and an increase in possible experiments from the same starting material, and as a consequence a reduction in variation between experiments. Furthermore, immortalized cells and tumor cell lines, frequently chosen as a substitute

for primary cultures, mimic a BBB with disease-like properties and are therefore sub-optimal for the use in a BBB model [79].

Co-culturing of astrocytes is crucial for the in vitro BBB model since astrocytes induce and maintain BBB properties in endothelial cells [72, 73]. The efficacy of the presence of astrocytes on the BBB properties of the model, correlates negatively with the distance between the astrocytes and the endothelial cells. Therefore, astrocytes were cultured on the bottom side of the filter instead of on the bottom of the well increasing the trans endothelial resistance considerably [80]

The in vitro BBB model system used in this study is functionally characterized and extensively studied for its BBB mimicking properties. Fully differentiated primary cultures of and astrocytes were grown on semi-permeable filter inserts, with astrocytes on the bottom site of the filter (Figure 3) [80]. This in vitro BBB system is used to assess the ability of heavy chain antibody fragments, directed against Aβ, to cross the blood brain barrier.

HEAVY CHAIN ANTIBODY FRAGMENTS

The mammalian immune system generates an enormous repertoire of highly specific antibodies for virtually each in Nature existing biological compound. In order to use these antibodies clinically, the molecular size, immunogenicity, binding affinity, solubility and pharmacokinitics were modified. Therefore, the success of these

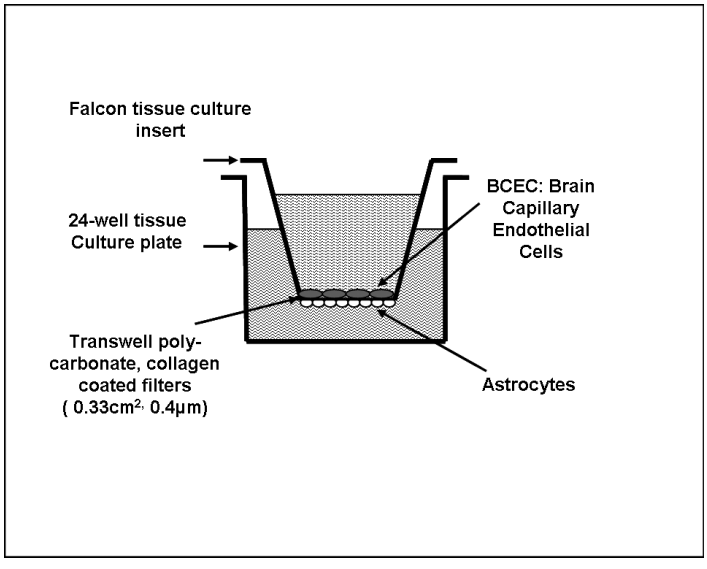

Figure 3 Schematic drawing of the in vitro BBB model. The model consists of 12-well tissue culture plate with falcon tissue culture inserts, the astrocytes and BCECs are seeded on transwell poly carbonate, collagen coated filters (0.33cm^2, 0.4µm).

conventional antibodies can be vastly contributed to the progress in molecular engineering techniques in the last decade [81].

In addition to the conventional immunoglobulin repertoire, *Camelidae* express unusually shaped antibodies which are devoid of light chains: the so-called heavy chain antibodies. While conventional antibodies are heterodimers in which the variable domain of the heavy chain (V_H) is pared with the variable domain of the light chain (V_L) (Figure 4). These variable domains, which embody the antigen binding domains, are held together by a hydrophobic interface. Their single N-terminal domain (VHH) is fully capable of antigen binding (Figure 4) [82]. V_HHs have a molecular size of ~15 kDa which makes them the smallest naturally occurring antigen-binding units known to date with antigen affinities fully comparable with those reported for conventional antibodies [83]. The substitution of four amino acids in framework II creates a more hydrophilic surface resulting in high natural solubility which makes VHH highly suitable for phage-display [84,85].

The VHH is encoded by a single gene fragment, ensuring straightforward cloning into the phagemid vector. This enables expression of the antibody fragment on the phage particle [86]. The VHH can be selected from naive, immune or synthetic libraries [87, 88, 89]. The disadvantage of selecting from these libraries, in the absence of affinity maturation, is that it yields generally VHH with lower affinity for their antigen. Therefore, in order to obtain high affinity VHH construction of, and additional selection from, an immune library is preferred.

It has been shown that V_HHs can be expressed in, and subsequently purified from, *E. coli* periplasm at higher levels than the equivalent of conventional antibodies [90]. In addition, a good production of V_HHs can also be obtained in yeast, plant and mammalian cells [91, 92].

Furthermore, the immune system of camelids has an intrinsic propensity to generate enzyme blocking agents [93]. Heavy chain antibodies can possess a complementarity determining region (CDR) 3 that has the ability to form fingerlike extensions which are able to protrude into cavities on antigens. This was concluded from studies on hen egg lysozyme, in which extending loops of the VHH were able to occupy the enzymatic cleft. In contrast a Fab-fragment has a relatively flat interaction face, outside the active site of lysosyme [94] (figure 4).

V_HHs possess several favorable characteristics when compared with the single variable fragments (scFv) derived from conventional antibodies (figure 4). They have a high stability, good refolding capacity, and are able to penetrate tissue rapidly [95, 96, 97]. In addition, V_HHs can be easily fused to other proteins, in order to adjust and amplify their utility for specific diagnostic or therapeutic applications [98]. For diagnostic applications VHHs can be labeled with various compounds used in diverse imaging techniques, depending on their application. For example α-GFP V_HHs were fused with monomeric Red Fluorescent Protein (mRFP). This generated a visible GFP-binding antibody [99].

For therapeutic application, V_HHs can be fused to molecules with an effector function. For example a V_HH with specificity for an antigen involved in tumor development was coupled to a lactamase and in vivo regression of the tumors, which the antibody was

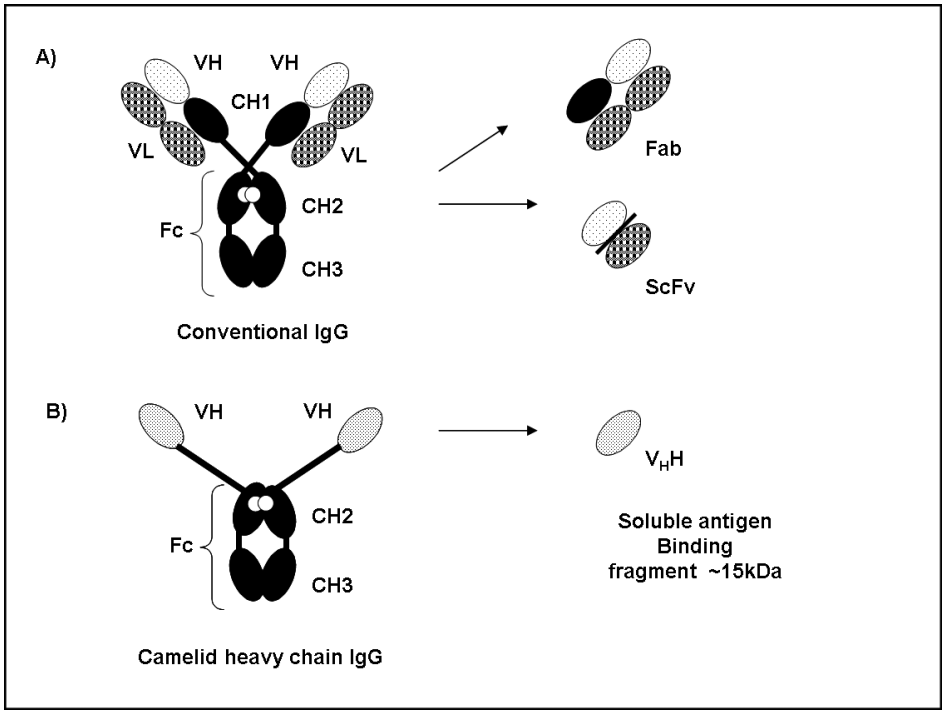

Figure 4 Comparison of the antigen binding fragments from the classical and the heavy chain antibody. A) Schematic representation of the conventional antibody in which the V_H and V_L are paired. The antigen binding domains of the traditional antibodies are obtained after proteolysis (Fab) or from cloning in which a synthetic linker stabilizes the VH-VL dimer (ScFv). B) Schematic representation of a Camelid heavy-chain IgG, that is devoid of the light chains. The variable domain of a heavy chain antibody (V_HH) is the smallest intact antigen-binding fragment known. Drawn after Muyldermans et al [95].

directed against, was shown in a mouse model [100]. Furthermore, in vivo experiments were performed with chimeric V_HHs eliminating trypanosome infections in mouse model systems [101, 102]. The conserved epitopes are located deep in the dense bacterial coat. Larger antigen-binding fragments were not able to penetrate this layer of coat protein. To circumvent this inaccessibility V_HHs were used. The V_HHs were able to penetrate the high density coat protein that covers the entire surface of the parasite [103].

Additionally, VHHs can be cloned in tandem, separated by a linker, generating bivalent antibodies. When two identical VHH are cloned in tandem (homo-bihead), this often yields an antibody with a higher avidity for the antigen [104]. V_HHs directed against different antigens can also be cloned in tandem (Hetero-biheads), generating bi-specific reagents e.g tandem cloning with a V_HHs directed against serum albumin can improve the serum half life [105].

Because of their small size, VHH rapidly pass the renal filter, resulting in a fast blood clearance. In addition, their small size facilitates rapid tissue penetration and

propensity to cross the blood-brain-barrier (BBB) [106 107]. The former characteristics are advantageous for non-invasive diagnostic in vivo imaging of neurological (behind the BBB) disorders.

OUTLINE

As described above the properties of heavy chain antibody fragments make them potential candidates for use in *in vivo* diagnosis of AD and CAA. In ***chapter two*** the generation of antibody fragments, directed against Aß is described. The antibody fragments were selected from non-immune and two immune libraries. The vascular tissue complex immune library: which was obtained by immunizing the Lama's with the blood vessels of a HCHWA-D patient. And the grey matter complex immune library, in which the Lama's were immunized with the grey matter of a DS patient.

Next, in ***chapter three***, the previously generated amyloid beta affinity binders were assessed for their ability to cross the blood-brain barrier using an established *in vitro* blood brain barrier co-culture system. This *in vitro* BBB co-culture system consists of bovine brain capillary endothelial (BCEC) cells and newborn rat astrocytes and has shown to mimic the BBB in vitro [80].

In ***chapter four*** the VHH are assessed on their *in vivo* properties. First the VHH were tested for their ability to recognize Aβ *in vivo* in an APP/PS1 mouse model by direct topical application of the alexa 594 labeled VHH. In addition, blood clearance and biodistribution of the VHH were monitored using direct radioactive labeling with ^{99m}Technicium. Furthermore the fluorescent labeled VHH were evaluated on their specific *in vivo* binding properties after injection in the tail vein, the blood-brain barrier was circumvented either by craniotomy combined with intravital microscopy or disrupted using intracarotid co-injections of mannitol.

REFERENCE LIST

1. Sawaya, M.R. *et al.* Atomic structures of amyloid cross-beta spines reveal varied steric zippers. *Nature* **447**, 453-457 (2007).
2. Ashford, J.W. APOE genotype effects on Alzheimer's disease onset and epidemiology. *J. Mol. Neurosci.* **23**, 157-165 (2004).
3. Alzheimer, A., Stelzmann, R.A., Schnitzlein, H.N. & Murtagh, F.R. An English translation of Alzheimer's 1907 paper, "Uber eine eigenartige Erkankung der Hirnrinde". *Clin. Anat.* **8**, 429-431 (1995).
4. Richard, F. Genetic susceptibility factors for Alzheimer's disease. (2001).
5. Corder, E.H. Gene dose of apolipoprotein E type 4 allele and the risk of Alzheimer's disease in late onset families. (1993).
6. McCusker, S.M. Association between polymorphism in regulatory region of gene encoding tumour necrosis factor alpha and risk of Alzheimer's disease and vascular dementia: a case-control study. (2001).
7. Farkas, E. & Luiten, P.G. Cerebral microvascular pathology in aging and Alzheimer's disease. *Prog. Neurobiol.* **64**, 575-611 (2001).
8. de la Torre, J.C. Alzheimer's disease is a vasocognopathy: a new term to describe its nature. *Neurol. Res.* **26**, 517-524 (2004).

9. Gorelick, P.B. Risk factors for vascular dementia and Alzheimer disease. *Stroke* **35**, 2620-2622 (2004).
10. Petty, M.A. & Wettstein, J.G. Elements of cerebral microvascular ischaemia. *Brain Res. Brain Res. Rev.* **36**, 23-34 (2001).
11. Rutgers, K.S. *et al.* Differential recognition of vascular and parenchymal beta amyloid deposition. *Neurobiol. Aging* (2009).
12. Glenner, G.G. & Wong, C.W. Alzheimer's disease: initial report of the purification and characterization of a novel cerebrovascular amyloid protein. *Biochem. Biophys. Res. Commun.* **120**, 885-890 (1984).
13. Levy, E. *et al.* Mutation of the Alzheimer's disease amyloid gene in hereditary cerebral hemorrhage, Dutch type. *Science* **248**, 1124-1126 (1990).
14. Revesz, T. *et al.* Cerebral amyloid angiopathies: a pathologic, biochemical, and genetic view. *J. Neuropathol. Exp. Neurol.* **62**, 885-898 (2003).
15. van Duinen, S.G. *et al.* Hereditary cerebral hemorrhage with amyloidosis in patients of Dutch origin is related to Alzheimer disease. *Proc. Natl. Acad. Sci. U. S. A* **84**, 5991-5994 (1987).
16. Bornebroek, M. *et al.* Hereditary cerebral hemorrhage with amyloidosis-Dutch type: better correlation of cognitive deterioration with advancing age than with number of focal lesions or white matter hyperintensities. *Alzheimer Dis. Assoc. Disord.* **10**, 224-231 (1996).
17. Bakker, E. *et al.* DNA diagnosis for hereditary cerebral hemorrhage with amyloidosis (Dutch type). *Am. J. Hum. Genet.* **49**, 518-521 (1991).
18. Wisniewski, T., Ghiso, J. & Frangione, B. Peptides homologous to the amyloid protein of Alzheimer's disease containing a glutamine for glutamic acid substitution have accelerated amyloid fibril formation. *Biochem. Biophys. Res. Commun.* **179**, 1247-1254 (1991).
19. Clements, A., Walsh, D.M., Williams, C.H. & Allsop, D. Effects of the mutations Glu22 to Gln and Ala21 to Gly on the aggregation of a synthetic fragment of the Alzheimer's amyloid beta/A4 peptide. *Neurosci. Lett.* **161**, 17-20 (1993).
20. Fabian, H., Szendrei, G.I., Mantsch, H.H. & Otvos, L., Jr. Comparative analysis of human and Dutch-type Alzheimer beta-amyloid peptides by infrared spectroscopy and circular dichroism. *Biochem. Biophys. Res. Commun.* **191**, 232-239 (1993).
21. Monro, O.R. *et al.* Substitution at codon 22 reduces clearance of Alzheimer's amyloid-beta peptide from the cerebrospinal fluid and prevents its transport from the central nervous system into blood. *Neurobiol. Aging* **23**, 405-412 (2002).
22. Tsubuki, S., Takaki, Y. & Saido, T.C. Dutch, Flemish, Italian, and Arctic mutations of APP and resistance of Abeta to physiologically relevant proteolytic degradation. *Lancet* **361**, 1957-1958 (2003).
23. Selkoe, D.J. Alzheimer's disease: genes, proteins, and therapy. *Physiol Rev.* **81**, 741-766 (2001).
24. Thinakaran, G. & Koo, E.H. Amyloid precursor protein trafficking, processing, and function. *J. Biol. Chem.* **283**, 29615-29619 (2008).
25. Roher, A.E. *et al.* beta-Amyloid-(1-42) is a major component of cerebrovascular amyloid deposits: implications for the pathology of Alzheimer disease. *Proc. Natl. Acad. Sci. U. S. A* **90**, 10836-10840 (1993).
26. Kokjohn, T.A. & Roher, A.E. Amyloid precursor protein transgenic mouse models and Alzheimer's disease: understanding the paradigms, limitations, and contributions. *Alzheimers. Dement.* **5**, 340-347 (2009).
27. Annaert, W. & De Strooper, B. Presenilins: molecular switches between proteolysis and signal transduction. *Trends Neurosci.* **22**, 439-443 (1999).
28. Cao, X. & Sudhof, T.C. A transcriptionally [correction of transcriptively] active complex of APP with Fe65 and histone acetyltransferase Tip60. *Science* **293**, 115-120 (2001).
29. Cupers, P. *et al.* The discrepancy between presenilin subcellular localization and gamma-secretase processing of amyloid precursor protein. *J. Cell Biol.* **154**, 731-740 (2001).
30. Hebert, S.S. *et al.* Regulated intramembrane proteolysis of amyloid precursor protein and regulation of expression of putative target genes. *EMBO Rep.* **7**, 739-745 (2006).
31. Nunan, J. & Small, D.H. Proteolytic processing of the amyloid-beta protein

precursor of Alzheimer's disease. *Essays Biochem.* **38**, 37-49 (2002).

32. Kamenetz, F. *et al.* APP processing and synaptic function. *Neuron* **37**, 925-937 (2003).
33. Haass, C. *et al.* Amyloid beta-peptide is produced by cultured cells during normal metabolism. *Nature* **359**, 322-325 (1992).
34. Seubert, P. *et al.* Isolation and quantification of soluble Alzheimer's beta-peptide from biological fluids. *Nature* **359**, 325-327 (1992).
35. Vigo-Pelfrey, C., Lee, D., Keim, P., Lieberburg, I. & Schenk, D.B. Characterization of beta-amyloid peptide from human cerebrospinal fluid. *J. Neurochem.* **61**, 1965-1968 (1993).
36. Ida, N. *et al.* Analysis of heterogeneous A4 peptides in human cerebrospinal fluid and blood by a newly developed sensitive Western blot assay. *J. Biol. Chem.* **271**, 22908-22914 (1996).
37. Walsh, D.M., Tseng, B.P., Rydel, R.E., Podlisny, M.B. & Selkoe, D.J. The oligomerization of amyloid beta-protein begins intracellularly in cells derived from human brain. *Biochemistry* **39**, 10831-10839 (2000).
38. De Strooper, B. *et al.* Production of intracellular amyloid-containing fragments in hippocampal neurons expressing human amyloid precursor protein and protection against amyloidogenesis by subtle amino acid substitutions in the rodent sequence. *EMBO J.* **14**, 4932-4938 (1995).
39. Kayed, R. *et al.* Common structure of soluble amyloid oligomers implies common mechanism of pathogenesis. *Science* **300**, 486-489 (2003).
40. Klein, W.L., Krafft, G.A. & Finch, C.E. Targeting small Abeta oligomers: the solution to an Alzheimer's disease conundrum? *Trends Neurosci.* **24**, 219-224 (2001).
41. Castano, E.M. *et al.* In vitro formation of amyloid fibrils from two synthetic peptides of different lengths homologous to Alzheimer's disease beta-protein. *Biochem. Biophys. Res. Commun.* **141**, 782-789 (1986).
42. Kirschner, D.A. *et al.* Synthetic peptide homologous to beta protein from Alzheimer disease forms amyloid-like fibrils in vitro. *Proc. Natl. Acad. Sci. U. S. A* **84**, 6953-6957 (1987).
43. Wilcock, G.K. & Esiri, M.M. Plaques, tangles and dementia. A quantitative study. *J. Neurol. Sci.* **56**, 343-356 (1982).
44. Roher, A.E. *et al.* Morphology and toxicity of Abeta-(1-42) dimer derived from neuritic and vascular amyloid deposits of Alzheimer's disease. *J. Biol. Chem.* **271**, 20631-20635 (1996).
45. Enya, M. *et al.* Appearance of sodium dodecyl sulfate-stable amyloid beta-protein (Abeta) dimer in the cortex during aging. *Am. J. Pathol.* **154**, 271-279 (1999).
46. Funato, H., Enya, M., Yoshimura, M., Morishima-Kawashima, M. & Ihara, Y. Presence of sodium dodecyl sulfate-stable amyloid beta-protein dimers in the hippocampus CA1 not exhibiting neurofibrillary tangle formation. *Am. J. Pathol.* **155**, 23-28 (1999).
47. McLean, C.A. *et al.* Soluble pool of Abeta amyloid as a determinant of severity of neurodegeneration in Alzheimer's disease. *Ann. Neurol.* **46**, 860-866 (1999).
48. Dahlgren, K.N. *et al.* Oligomeric and fibrillar species of amyloid-beta peptides differentially affect neuronal viability. *J. Biol. Chem.* **277**, 32046-32053 (2002).
49. McLean, C.A. *et al.* Soluble pool of Abeta amyloid as a determinant of severity of neurodegeneration in Alzheimer's disease. *Ann. Neurol.* **46**, 860-866 (1999).
50. Cleary, J.P. *et al.* Natural oligomers of the amyloid-beta protein specifically disrupt cognitive function. *Nat. Neurosci.* **8**, 79-84 (2005).
51. Lesne, S. *et al.* A specific amyloid-beta protein assembly in the brain impairs memory. *Nature* **440**, 352-357 (2006).
52. Walsh, D.M. *et al.* Certain inhibitors of synthetic amyloid beta-peptide (Abeta) fibrillogenesis block oligomerization of natural Abeta and thereby rescue long-term potentiation. *J. Neurosci.* **25**, 2455-2462 (2005).
53. Caughey, B. & Lansbury, P.T. Protofibrils, pores, fibrils, and neurodegeneration: separating the responsible protein aggregates from the innocent bystanders. *Annu. Rev. Neurosci.* **26**, 267-298 (2003).

54. Haass, C. & Selkoe, D.J. Soluble protein oligomers in neurodegeneration: lessons from the Alzheimer's amyloid beta-peptide. *Nat. Rev. Mol. Cell Biol.* **8**, 101-112 (2007).
55. LaFerla, F.M., Green, K.N. & Oddo, S. Intracellular amyloid-beta in Alzheimer's disease. *Nat. Rev. Neurosci.* **8**, 499-509 (2007).
56. Ferreira, S.T., Vieira, M.N. & De Felice, F.G. Soluble protein oligomers as emerging toxins in Alzheimer's and other amyloid diseases. *IUBMB. Life* **59**, 332-345 (2007).
57. Walsh, D.M. & Selkoe, D.J. A beta oligomers - a decade of discovery. *J. Neurochem.* **101**, 1172-1184 (2007).
58. Katzman, R. Alzheimer's disease. *N. Engl. J. Med.* **314**, 964-973 (1986).
59. Terry, R.D. *et al.* Physical basis of cognitive alterations in Alzheimer's disease: synapse loss is the major correlate of cognitive impairment. *Ann. Neurol.* **30**, 572-580 (1991).
60. Dickson, D.W. *et al.* Correlations of synaptic and pathological markers with cognition of the elderly. *Neurobiol. Aging* **16**, 285-298 (1995).
61. Moechars, D. *et al.* Early phenotypic changes in transgenic mice that overexpress different mutants of amyloid precursor protein in brain. *J. Biol. Chem.* **274**, 6483-6492 (1999).
62. Hsia, A.Y. *et al.* Plaque-independent disruption of neural circuits in Alzheimer's disease mouse models. *Proc. Natl. Acad. Sci. U. S. A* **96**, 3228-3233 (1999).
63. Chapman, P.F. *et al.* Impaired synaptic plasticity and learning in aged amyloid precursor protein transgenic mice. *Nat. Neurosci.* **2**, 271-276 (1999).
64. Mucke, L. *et al.* High-level neuronal expression of abeta 1-42 in wild-type human amyloid protein precursor transgenic mice: synaptotoxicity without plaque formation. *J. Neurosci.* **20**, 4050-4058 (2000).
65. Westerman, M.A. *et al.* The relationship between Abeta and memory in the Tg2576 mouse model of Alzheimer's disease. *J. Neurosci.* **22**, 1858-1867 (2002).
66. Dineley, K.T., Xia, X., Bui, D., Sweatt, J.D. & Zheng, H. Accelerated plaque accumulation, associative learning deficits, and up-regulation of alpha 7 nicotinic receptor protein in transgenic mice co-expressing mutant human presenilin 1 and amyloid precursor proteins. *J. Biol. Chem.* **277**, 22768-22780 (2002).
67. Wu, C.C. *et al.* Selective vulnerability of dentate granule cells prior to amyloid deposition in PDAPP mice: digital morphometric analyses. *Proc. Natl. Acad. Sci. U. S. A* **101**, 7141-7146 (2004).
68. Persidsky, Y., Ramirez, S.H., Haorah, J. & Kanmogne, G.D. Blood-brain barrier: structural components and function under physiologic and pathologic conditions. *J. Neuroimmune. Pharmacol.* **1**, 223-236 (2006).
69. Yudilevich, D.L. & De Rose, N. Blood-brain transfer of glucose and other molecules measured by rapid indicator dilution. *Am. J. Physiol* **220**, 841-846 (1971).
70. Oldendorf, W.H. Carrier-mediated blood-brain barrier transport of short-chain monocarboxylic organic acids. *Am. J. Physiol* **224**, 1450-1453 (1973).
71. Davson, H. Review lecture. The blood-brain barrier. *J. Physiol* **255**, 1-28 (1976).
72. Arthur, F.E., Shivers, R.R. & Bowman, P.D. Astrocyte-mediated induction of tight junctions in brain capillary endothelium: an efficient in vitro model. *Brain Res.* **433**, 155-159 (1987).
73. Janzer, R.C. & Raff, M.C. Astrocytes induce blood-brain barrier properties in endothelial cells. *Nature* **325**, 253-257 (1987).
74. Hawkins, B.T. & Davis, T.P. The blood-brain barrier/neurovascular unit in health and disease. *Pharmacol. Rev.* **57**, 173-185 (2005).
75. Bazzoni, G. & Dejana, E. Endothelial cell-to-cell junctions: molecular organization and role in vascular homeostasis. *Physiol Rev.* **84**, 869-901 (2004).
76. Pardridge, W.M. Blood-brain barrier delivery. *Drug Discov. Today* **12**, 54-61 (2007).
77. Lechardeur, D. & Scherman, D. Functional expression of the P-glycoprotein mdr in primary cultures of bovine cerebral capillary endothelial cells. *Cell Biol. Toxicol.* **11**, 283-293 (1995).

78. Wolburg, H. *et al.* Modulation of tight junction structure in blood-brain barrier endothelial cells. Effects of tissue culture, second messengers and cocultured astrocytes. *J. Cell Sci.* **107 (Pt 5)**, 1347-1357 (1994).

79. Hurst, R.D. & Fritz, I.B. Properties of an immortalised vascular endothelial/glioma cell co-culture model of the blood-brain barrier. *J. Cell Physiol* **167**, 81-88 (1996).

80. Gaillard, P.J. *et al.* Establishment and functional characterization of an in vitro model of the blood-brain barrier, comprising a co-culture of brain capillary endothelial cells and astrocytes. *Eur. J. Pharm. Sci.* **12**, 215-222 (2001).

81. Shen, J. *et al.* Single variable domain antibody as a versatile building block for the construction of IgG-like bispecific antibodies. *J. Immunol. Methods* **318**, 65-74 (2007).

82. Hamers-Casterman, C. *et al.* Naturally occurring antibodies devoid of light chains. *Nature* **363**, 446-448 (1993).

83. Zhang, J. *et al.* Pentamerization of single-domain antibodies from phage libraries: a novel strategy for the rapid generation of high-avidity antibody reagents. *J. Mol. Biol.* **335**, 49-56 (2004).

84. Muyldermans, S., Atarhouch, T., Saldanha, J., Barbosa, J.A. & Hamers, R. Sequence and structure of VH domain from naturally occurring camel heavy chain immunoglobulins lacking light chains. *Protein Eng* **7**, 1129-1135 (1994).

85. Vu, K.B., Ghahroudi, M.A., Wyns, L. & Muyldermans, S. Comparison of llama VH sequences from conventional and heavy chain antibodies. *Mol. Immunol.* **34**, 1121-1131 (1997).

86. Hoogenboom, H.R. Overview of antibody phage-display technology and its applications. *Methods Mol. Biol.* **178**, 1-37 (2002).

87. Verheesen, P. *et al.* Reliable and controllable antibody fragment selections from Camelid non-immune libraries for target validation. *Biochim. Biophys. Acta* **1764**, 1307-1319 (2006).

88. Tanha, J. *et al.* Optimal design features of camelized human single-domain antibody libraries. *J. Biol. Chem.* **276**, 24774-24780 (2001).

89. Yau, K.Y. *et al.* Selection of hapten-specific single-domain antibodies from a non-immunized llama ribosome display library. *J. Immunol. Methods* **281**, 161-175 (2003).

90. Tanha, J., Dubuc, G., Hirama, T., Narang, S.A. & MacKenzie, C.R. Selection by phage display of llama conventional V(H) fragments with heavy chain antibody V(H)H properties. *J. Immunol. Methods* **263**, 97-109 (2002).

91. Frenken, L.G., Hessing, J.G., Van den Hondel, C.A. & Verrips, C.T. Recent advances in the large-scale production of antibody fragments using lower eukaryotic microorganisms. *Res. Immunol.* **149**, 589-599 (1998).

92. Harmsen, M.M. & de Haard, H.J. Properties, production, and applications of camelid single-domain antibody fragments. *Appl. Microbiol. Biotechnol.* **77**, 13-22 (2007).

93. De Genst, E. *et al.* Molecular basis for the preferential cleft recognition by dromedary heavy-chain antibodies. *Proc. Natl. Acad. Sci. U. S. A* **103**, 4586-4591 (2006).

94. Desmyter, A. *et al.* Crystal structure of a camel single-domain VH antibody fragment in complex with lysozyme. *Nat. Struct. Biol.* **3**, 803-811 (1996).

95. Muyldermans, S. Single domain camel antibodies: current status. *J. Biotechnol.* **74**, 277-302 (2001).

96. Cortez-Retamozo, V. *et al.* Efficient tumor targeting by single-domain antibody fragments of camels. *Int. J. Cancer* **98**, 456-462 (2002).

97. Dumoulin, M. *et al.* A camelid antibody fragment inhibits the formation of amyloid fibrils by human lysozyme. *Nature* **424**, 783-788 (2003).

98. Conrath, K.E. *et al.* Beta-lactamase inhibitors derived from single-domain antibody fragments elicited in the camelidae. *Antimicrob. Agents Chemother.* **45**, 2807-2812 (2001).

99. Rothbauer, U. *et al.* Targeting and tracing antigens in live cells with fluorescent nanobodies. *Nat. Methods* **3**, 887-889 (2006).

100. Cortez-Retamozo, V. *et al.* Efficient cancer therapy with a nanobody-based conjugate. *Cancer Res.* **64**, 2853-2857 (2004).

101. Stijlemans, B. *et al.* Efficient targeting of conserved cryptic epitopes of infectious agents by single domain antibodies. African trypanosomes as paradigm. *J. Biol. Chem.* **279**, 1256-1261 (2004).

102. Baral, T.N. *et al.* Experimental therapy of African trypanosomiasis with a nanobody-conjugated human trypanolytic factor. *Nat. Med.* **12**, 580-584 (2006).

103. van, M.N. The effect of normal human serum on trypanosomes of distinct antigenic type (ETat 1 to 12) isolated from a strain of Trypanosoma brucei rhodesiense. (1976).

104. Conrath, K.E. *et al.* Beta-lactamase inhibitors derived from single-domain antibody fragments elicited in the camelidae. *Antimicrob. Agents Chemother.* **45**, 2807-2812 (2001).

105. Coppieters, K. *et al.* Formatted anti-tumor necrosis factor alpha VHH proteins derived from camelids show superior potency and targeting to inflamed joints in a murine model of collagen-induced arthritis. *Arthritis Rheum.* **54**, 1856-1866 (2006).

106. Harmsen, M.M., Van Solt, C.B., Fijten, H.P. & Van Setten, M.C. Prolonged in vivo residence times of llama single-domain antibody fragments in pigs by binding to porcine immunoglobulins. *Vaccine* **23**, 4926-4934 (2005).

107. Muruganandam, A., Tanha, J., Narang, S. & Stanimirovic, D. Selection of phage-displayed llama single-domain antibodies that transmigrate across human blood-brain barrier endothelium. *FASEB J.* **16**, 240-242 (2002).

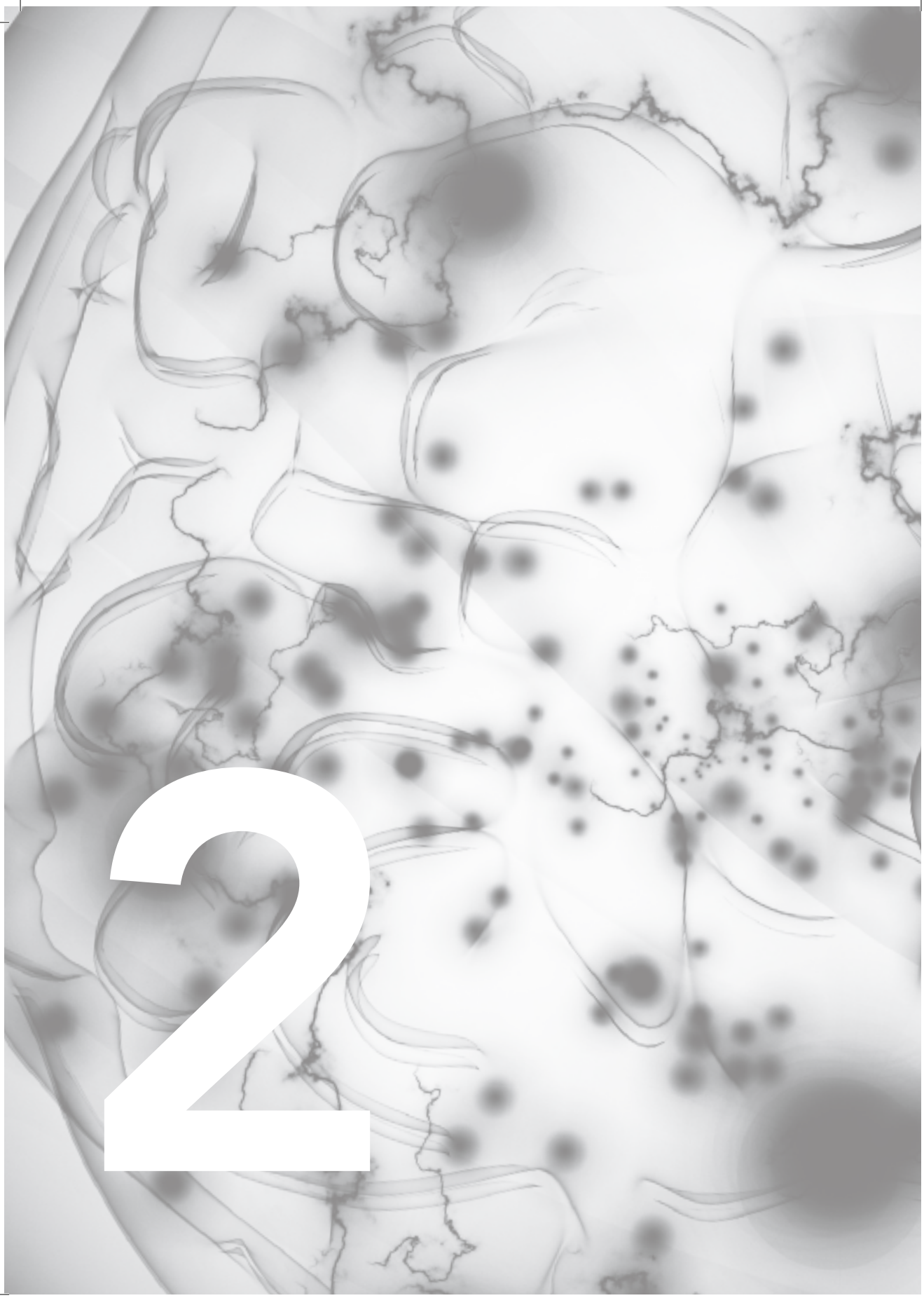
2

CHAPTER 2 | DIFFERENTIAL RECOGNITION OF VASCULAR AND PARENCHYMAL BETA AMYLOID DEPOSITION

2

DIFFERENTIAL RECOGNITION OF VASCULAR AND PARENCHYMAL BETA AMYLOID DEPOSITION

Kim S. Rutgers, M.Sc.[1], Alexandra van Remoortere, Ph.D.[2], Mark A. van Buchem, M.D., Ph.D.[3], C. Theo Verrips, Ph.D.[4], Steven M. Greenberg, M.D., Ph.D.[5], Brian J. Bacskai, Ph.D.[5], Matthew P. Frosch, M.D., Ph.D.[6], Sjoerd G. van Duinen, M.D., Ph.D.[7,8], Marion L. Maat-Schieman M.D., Ph.D.[8], Silvère M. van der Maarel, Ph.D.[1]

1. Department of Human Genetics, Leiden University Medical Center, Leiden, Netherlands
2. Department of Parasitology, Leiden University Medical Center, Leiden, Netherlands
3. Department of Radiology, Leiden University Medical Center, Leiden, Netherlands
4. Department of Molecular Cell Biology, Utrecht University, Utrecht, Netherlands
5. Department of Neurology, Massachusetts General Hospital and Harvard Medical School, Charlestown, MA, US
6. Department of Pathology, C.S. Kubik Laboratory for Neuropathology, Massachusetts General Hospital and Harvard Medical School
7. Department of Pathology, Leiden University Medical Center, Leiden, Netherlands
8. Department of Neurology, Leiden University Medical Center, Leiden, Netherlands

Keywords: Alzheimer's disease, Amyloid beta, Antibody, Histochemistry, Imaging, Immunoreactivity
Running title: Beta amyloid recognition in the brain

ABSTRACT

By phage display, llama-derived heavy chain antibody fragments were selected from non-immune and immune libraries and tested for their affinity and specificity for beta amyloid by phage-ELISA, immunohistochemistry and surface plasmon resonance.

We identified 8 distinct heavy chain antibody fragments specific for beta amyloid. Whilst three of them recognized vascular and parenchymal beta amyloid deposits, the remaining five heavy chain antibody fragments recognized vascular beta amyloid specifically, failing to bind to parenchymal beta amyloid.

These heavy chain antibody fragments, selected from different libraries, demonstrated differential affinity for different epitopes when used for immunohistochemistry. These observations indicate that the llama heavy chain antibody fragments are the first immunologic probes with the ability to differentiate between parenchymal and vascular beta amyloid aggregates. This indicates that vascular and parenchymal beta amyloid deposits are heterogeneous in epitope presence/availability. The properties of these heavy chain antibody fragments make them potential candidates for use in *in vivo* differential diagnosis of Alzheimer disease and cerebral amyloid angiopathy. Continued use and characterization of these reagents will be necessary to fully understand the performance of these immunoreagents.

1. INTRODUCTION

Alzheimer disease (AD) is the most common cause of dementia and is characterized by the aggregation of beta amyloid (Aβ) in the form of plaques and neurofibrillary degeneration, including neurofibrillary tangles, dystrophic neurites and neuropil threads. The amyloid cascade theory proposes that Aβ plays a central role in the pathogenesis of AD [15]. The deposition of Aβ as primary neuropathologic feature is shared by AD and cerebral amyloid angiopathy (CAA), although the location of the deposits differ between the two diseases [15,26].

CAA describes a group of disorders that is characterized by heterogeneous amyloidogic protein deposition in cerebral vessel walls. CAA is the most common cause of non-hypertensive intracerebral hemorrhage in the elderly [23]. Hereditary cerebral hemorrhage with amyloidosis-Dutch type (HCHWA-D) is a hereditary form of CAA and commonly considered a paradigm for CAA by virtue of being the first familial CAA to be characterized and by far the best described [3].

Although AD and CAA frequently coexist in a patient, they generally are distinct clinical and histological entities [7]. Growing evidence suggests that patients with severe CAA suffer from cognitive impairment, independent of the presence of AD pathology [10,22].

Currently, neuropathologic examination is required for definitive diagnosis of AD and CAA. Conventional clinical tests are relatively insensitive for the early changes of cerebral amyloidoses, and the changes that are detected are non-specific. With a new generation of neuroprotective agents emerging, there is a need to detect these diseases in early stages.

Molecular imaging techniques specific to amyloid and other structural changes associated with neurodegenerative disease may begin to overcome this predicament, with these techniques relying on agents that are capable of detecting molecular and cellular changes in vivo. It has been demonstrated that agents targeted at Aβ and detectable by PET can detect cerebral Aβ accumulations in patients with AD and CAA[17]. However, these agents detect both vascular and parenchymal Aβ, and are thus not well suited to differentiate between AD and CAA.

A relatively new source of immunologic agents has been derived from the Camelid heavy-chain antibody repertoire (HCAb). In addition to conventional immunoglobulins, *Camilidae* express antibodies which are devoid of light chains. Their single N-terminal domain (VHH) is fully capable of antigen binding with affinities comparable with those reported for conventional antibodies [14,30]. VHHs have several potential advantages as immunologic tool which might allow them to be used for non-invasive, early and differential in vivo Aß detection in the brain: because of their small size VHHs rapidly pass the renal filter resulting in a fast blood clearance and rapid tissue penetration; they are reported to be able to cross the blood-brain-barrier (BBB); and they have not shown any immunogenicity in mice [25].

Here we describe the selection of VHHs against Aß generated from non-immunized animals and from animals immunized with vascular amyloid deposits

from a patient with HCHWA-D or grey matter from a patient with Down Syndrome and AD pathologic findings. The intent was to obtain high affinity VHHs specific for distinctive AD or CAA Aβ epitopes. The VHHs selected from the non-immune library solitarily recognize vascular Aβ depositions, similar to VHHs selected from the vascular CAA library. In contrast, the VHHs generated from the grey matter AD library show predominantly high affinity for Aβ epitopes that are specific for, or enriched in parenchymal plaques in addition to vascular deposits.

2. MATERIALS AND METHODS

2.1 Selection of antibody fragment by phage display

For the selection of non-immune VHHs an existing llama-derived phagemid library was used, kindly provided by BAC, The Netherlands [8]. VHHs were selected in two rounds of micropanning by direct immobilization of Aβ1-42, essentially described before [28]. The selection procedure of the second round of selection was identical to the first round with the exception that 10^9 input phages and 1ug of antigen was used.

Two Llama-derived immune phagemid libraries were generated. For the vascular CAA library immunization was performed with recombinant beta-amyloid (Aβ1-42, r-peptide, Georgia, USA) and with affected blood vessels of a HCHWA-D patient. For the grey matter AD library, brain parenchyma homogenates of a DS patient with extensive plaque formation was used as the immunogen. Phage display selection from the immune libraries were performed as described for the naive library with the exception that for the vascular CAA library selections 0.2-10ug of different antigens (Aβ1-42, Aβ1-16, Aβ11-22, Aβ25-35 and Aβ17-42, r-peptide, Georgia, USA) and 10ul phages ($4.8x10^8$ phages) were used as input. For Aβ1-42 one round of selection was sufficient. One round of selection was performed with the grey matter AD library, with 10 and 50ul input phages and 0.1-10ug antigen (Aβ1-42) coated.

2.2 Phage ELISA and diversity screening of selected VHHs

Phage productions and ELISA were performed as described before [28]. In order to assess the diversity of the selected naive VHHs, DNA fingerprints were obtained as described before. For the immune VHHs the diversity was screened by means of surface Plasmon resonance (SPR) analysis.

2.3 Epitope mapping of Aβ specific VHHs

Epitope mapping was performed by phage ELISA experiment s as described before [28]. The reactivity of the phage-VHHs is tested on synthetic Aβ fragments 1-40, 1-42, 1-16, 11-22, 22-35, 25-35, 17-42 (rPeptide, Georgia, USA) and control protein. The phage-ELISA data were analyzed by one-way ANOVA followed by a LSD posthoc test. Threshold value for statistical significance was set at $p = 0.05$. SPSS 15.0.1 was used for all analysis (SPSS for Windows, Rel. 15.0.1. 2006, SPSS Inc, Chicago, Illinois, USA).

2.4 Subcloning, Production and purification of VHHs

The VHH genes specific for Aβ were subcloned into the pUR 5850VSV production vector [27], produced in *E. coli* and purified from the periplasmic supernatants as described [19]. This vector contains a C-terminal His6 tag for purification and myc tag for detection. Talon metal affinity resin columns (Clontech, CA, USA) were used for purification according to the supplier's instructions.

2.5 Patient material

Autopsy brain tissue of patients with a genetically confirmed diagnosis of HCHWA-D and patients with AD, CAA, DS or HCHWA-I, and controls were used. The neuropathological evaluation was confirmed by S.G.v.D. and M.L.C.M-S. All HCHWA-D patients gave informed consent to use their tissues for research purposes. Tissue from all other patients and the controls was encoded and used in agreement with the code as defined in the Netherlands (Code Goed Gebruik). For the study of cases from Massachusetts General Hospital, all neuropathologic evaluation was confirmed by M.P.F; tissue was collected and used in the study in accordance with institutional approval for de-identified autopsy tissue.

2.6 Immunohistochemistry

Frozen brain tissue sections (5µm) of DS, HCHWA-D, HCHWA-I, AD, CAA patients and normal control tissue were rinsed in PBS, fixed with ice-cold acetone for 10 min, incubated with peroxidase blocking reagent (Dako Cytomation) for 20 min, washed in PBS and incubated with the anti-Aβ VHHs (0.625-20ng/ul) in 1% BSA/PBS overnight in a wet chamber. Thereafter, sections were rinsed with PBS and incubated with mouse-anti-VSV (1:1000) or mouse-anti-c-myc (1:6000) for 1 hour and subsequently with EnVision^{+} ® system labelled Polymer-Hrp anti-Mouse (Dako Cytomation) for 30 min. Detection was performed with Liquid DAB^{+} Substrate Chromogen System (Dako Cytomation). Hemotoxylin counterstaining was performed and the sections were dehydrated and mounted in micromount mounting medium (Surgipath, Richmond, IL, USA). 4G8 (1:200) and R1282 (1:1500) were used as a positive control for Aβ staining [12]. Final preparations were analyzed with an Olympus Provis AX70TF light microscope and images were obtained using the Olympus digital DP12 camera.

2.7 Surface plasmon resonance spectroscopy (SPR)

All SPR binding studies were conducted at 25ºC in HBS-EP running buffer using a Biacore 3000 biosensor system (GE Healthcare). Aβ1-42 was amine coupled (EDC/NHS) to a CM-5 sensor chip (research grade, GE) using 10 mM NaAc (pH 4.0) as coupling buffer, and HBS-EP as running buffer. Immobilization levels between 150 and 1000 RU could be obtained, however only surfaces of at least 350 RU gave reproducible results. Therefore, we analyzed VHH binding on surfaces at 350, 450 and 1000RU. As a reference channel an unrelated peptide, of the same size as Aβ1-42,

derived from the poly A-binding protein nuclear 1 (containing an alpha-helical domain) was immobilized [20]. Binding experiments of VHHs were performed, using increasing concentration series from 5 nM to 4 µM at a flow rate of 30 µl/min and injection time of 8,3 min to reach equilibrium binding. The surfaces were regenerated after each cycle with two 60-s pulses of 1 M GnHCl and 10 mM NaOH, followed by a stabilization time of 5 min. Biacore data were analyzed with BiaEvaluation v. 4.1 (GE). Reference surface and blanks were subtracted from all binding curves. The dissociation constant (K_D) for the interaction between VHHs and Aβ 1-42 was measured from saturation binding experiments. The value for K_D was obtained using a non-linear least squares analysis (steady state analysis) with $AB_{eq}=AB_{max}$ (1/(1+KD/[A]) where AB_{eq} is the average of the response signal at equilibrium in defined intervals for each concentration of VHHs [A] and AB_{max} is the maximum response that can be obtained for VHHs binding depending on the number of binding sites available on the Aβ1-42.

3. RESULTS

3.1 Selection and screening of VHHs

To obtain VHHs from the non-immune library against beta amyloid, two successive rounds of selection were performed by phage display. Synthetic Aß 1-42 was directly coated onto Nunc maxisorp plates in both rounds. The progress of selection was monitored by colony count of the enriched polyclonal outputs. In each round an increase in output/input ratio was observed, indicative for enrichment of VHHs directed against Aß 1-42 in the polyclonal phage-pool. After the second round of selection 96 monoclonal phage-clones were randomly chosen. Clones were arrayed and tested for Aß 1-42 affinity by dot blot analysis (data not shown). Several clones showed specific binding to the antigen. Their diversity was screened by DNA fingerprint analysis showing a large diversity in fingerprint patterns. Subsequently, a subset of clones with different fingerprints was sequenced, resulting in a subset of different VHHs specific for Aß 1-42. Two of the VHHs, ni3A and ni8B, were chosen for further characterization.

In order to select high affinity VHHs potentially specific for epitopes unique to CAA Aβ, phage selection was also performed utilizing the vascular CAA immune library. For Aß 1-42 specific VHH, one round of selection was sufficient to obtain high affinity VHHs directed against CAA Aβ epitopes: the output of the selection plate was significantly higher compared with the background plate after one round of selection. In order to aim at a panel of VHHs directed against diverse Aß epitopes, phage selection was performed with different Aβ fragments. Two successive rounds of selection were necessary judged by the colony count.

Because of the heterogeneous character of Aβ presentation in CAA and AD we also aimed to select VHHs from a library that was generated by immunizing a llama with a protein homogenate of brain parenchyma with extensive AD pathology. We anticipated that, if there are conformational differences between vascular and parenchymal amyloid

deposition, this library would yield VHHs with high affinity for AD Aβ epitopes that are specific for parenchymal plaques. Judged by colony count, one round of selection was sufficient for the selection of specific VHHs from this library.

After the selection procedure from the vascular and brain parenchyma libraries, >300 monoclonal phage-clones were randomly chosen from each selection and screened by phage ELISA. Many clones showed specific binding to the antigen. Their diversity was screened by means of off rate differences in SPR analysis. As a consequence of the concentration independence of this parameter, production differences between VHH clones are not of influence. A large diversity in SPR curves was detected. Subsequently, a subset of clones with different off rates was sequenced. This yielded several unique high affinity VHHs specific for their respective antigens (va2E, vaE2 and va1G for the vascular library and pa4D, pa11E and pa2H for the parenchymal library). All selected VHHs were subcloned into the pUR5850-VSV production vector to increase the production yield. The characteristics of all VHHs selected for further analysis are summarized in (table 1).

3.2 Epitope mapping of Aβ specific VHHs

Epitope mapping of the VHHs was performed by phage ELISA experiments. Ni3A and ni8B have a significantly higher affinity preference for Aβ 1-42 compared to all other antigens. Va2E recognizes 1-42 and 17-42 significantly better than other fragments, although Aβ 1-40 recognition is clearly detected. VaE2 and va1G are not phage-VHH ELISA reactive. Pa4D, pa11E, pa2H have affinity preference for Aβ 1-42 and Aβ 1-40 (figure 1). Thus, VHHs selected from the different libraries show distinct epitope specificity, consistent with the distinct immunogens used prior to the phage-ELISA experiment.

Table 1 Overview of VHHs selected from the non-immune, vascular CAA and parenchymal libraries, with their characteristics. + weak intensity, ++ strong intensity, +++ very strong intensity.

			Immunohistochemistry					
			Vascular Aβ reactivity		ParenchymalAβ reactivity		KD Average (nM)	STDV (nM)
VHH	Library	Antigen used for selection	HCHWA-D	AD	HCHWA-D	AD		
ni3A	Non-immune	Aß 1-42	++	++	-	-	39	12
ni8B	Non-immune	Aß 1-42	++	++	-	-	109	36
va2E	Vascular	Aß 17-42	++	+	-	-	650	157
vaE2	vascular	Aß 1-42	++	+	-	-	1180	443
va1G	vascular	Aß 11-22	++	+	-	-	179	73
pa4D	grey matter	Aß 1-42	++	+++	-	+++	100	9
pa11E	grey matter	Aß 1-42	+++	+++	-	+++	129	45
pa2H	grey matter	Aß 1-42	+++	+++	-	+++	160	21

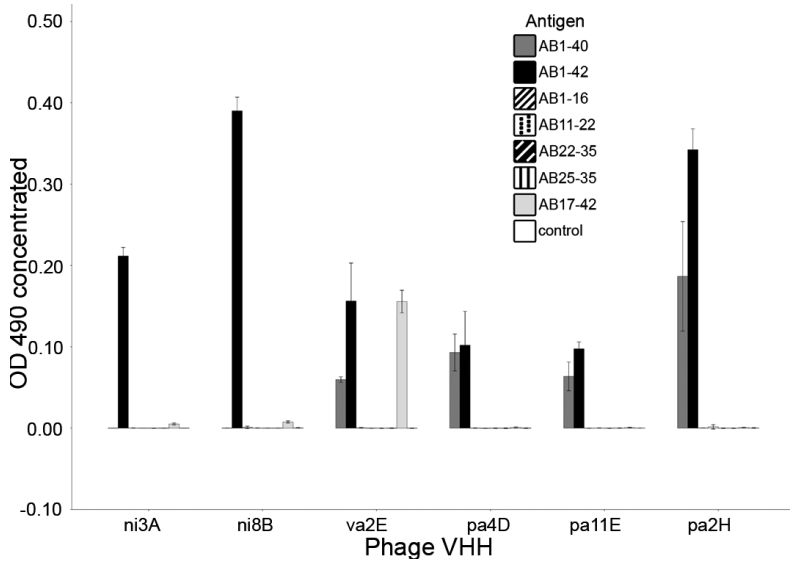

Figure 1 Epitope mapping of Aβ specific VHHs. Depicted are Phage-VHH Elisa results. Data is represented as the corrected OD (minus negative control) measured at 490nm.

3.3 Determination of affinity constants using SPR biosensor analysis

The binding of the various VHHs over a dynamic range of concentrations from 5 nM to 4 μM were determined on three different densities of immobilized Aβ1-42 (350, 450 and 1000 RUs) to evaluate the affinity constant (KD). Sensorgrams with double referenced binding curves of VHH pa11E are shown for the 450 and 1000 RU surface density (Figure 2A and 2C, respectively) and steady state binding (Req) levels were determined (indicated by an asterisks in figure 2A and 2C). The Req levels were plotted versus concentration (Fig 2B and 2D) and subsequently the KD values were determined using steady state analysis. The average of the KDs for all VHHs is summarized in Table 1 and range between 39 and 1200nM. The KD value of each VHH was found to be consistent and independent of the immobilization level of Aβ1-42.

3.4 Immunohistochemistry

The VHHs directed against Aß which were derived from the non-immune library (ni3A, ni8B) showed specific staining of vascular Aβ, with equal affinity for these deposits in cases of AD, HCHWA-D and CAA (figure 3), (table 1).

In order to confirm specificity for Aß and to rule out a contribution from the well-established non-specific endothelial cross-reactivity of the VHHs, immunohistochemistry was performed on control tissue lacking evidence of Aβ deposits. Additionally, staining with a traditional anti-Aβ antibody (4G8/R1282) was performed on adjacent tissue sections. The absence of staining in control tissue and an identical vascular and/or parenchymal staining pattern obtained with 4G8/R1282 in all patients (figure 4) confirmed

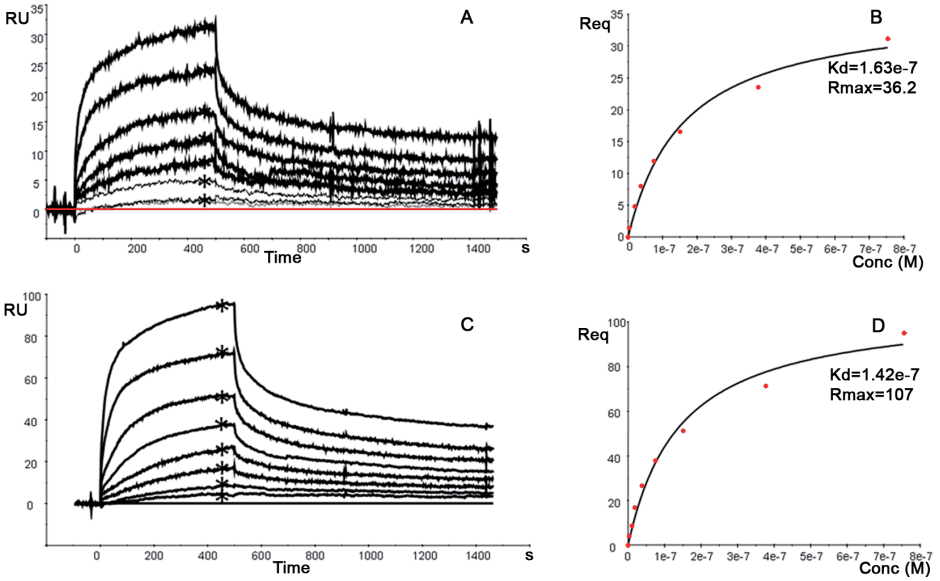

Figure 2 Example of the binding measurements performed with VHH 11E 0nM to 750nM) to 450 RUs(A) and 100RUs (C) immobilized Aβ 1-42. The sensorgrams were double referenced and Req values were determined (indicated by an asterisk) and plotted versus the concentration (B,D) to evaluate the KD using the steady state analysis provided by BiaEval 4.1.

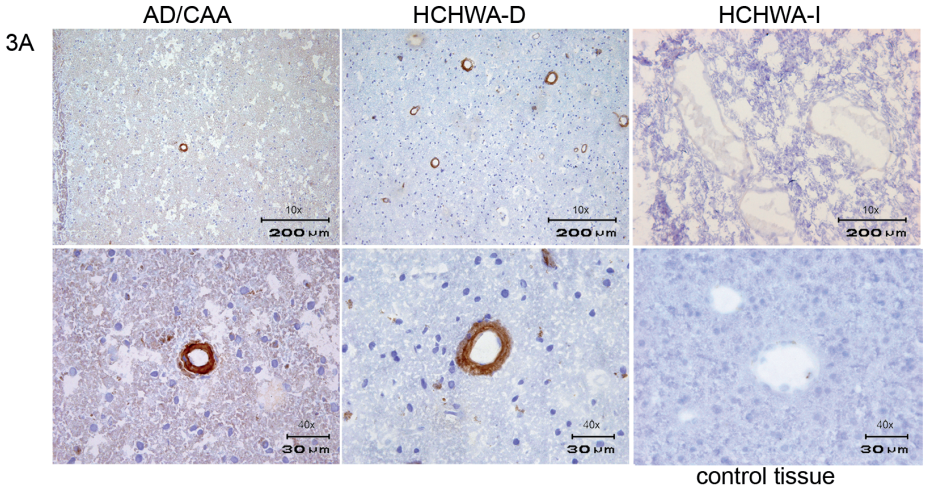

Figure 3 Immunohistochemistry of VHH ni3A derived from non-immune library. In the upper panel a 10x magnification of AD, HCHWA-D, HCHWA-I cryosections is shown. The lower panel is showing a 40x magnification of AD, HCHWA-D and control tissue cryosections. Ni3A shows immunoreactivity with vascular Aß in AD and HCHWA-D patient sections. No immunoreactivity was present in HCHWA-I patient sections and control tissue sections.

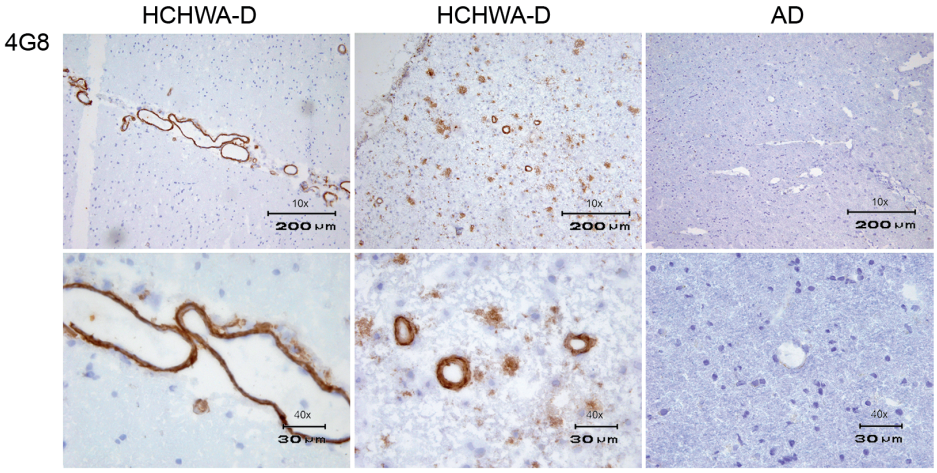

Figure 4 Immunohistochemistry with the conventional monoclonal antibody 4G8. The upper panel is showing a 10x magnification and the lower panel a 40x magnification of, from left to right, HCHWA-D with vascular Aβ immunoreactivity, AD with vascular and parenchymal immunoreactivity and control tissue. Identical vascular Aβ staining was observed with VHHs ni3A, ni8B, va2E, vaE2 and va1G. Identical parenchymal staining patterns, in addition to vascular Aβ immune reactivity was observed with VHHs pa2H, pa11E, pa4D.

Aß specificity. Because conformational specificity has been reported for VHHs selected against Aβ, selected VHHs were also tested on tissue sections of HCHWA-I patients in which the amyloid consists of mutant cystatin [9,13]. Selected VHHs showed absence of staining on HCHWA-I sections and consequently do not detect amyloid epitopes shared by all species of amyloid. Therefore, the selected VHHs are considered to be ß-amyloid sequence specific (figures 3, 5, 6), (table 1).

VHHs selected from the vascular CAA library (vaE2, va1G and va2E) showed vascular Aβ immuno-reactivity. In contrast with the non-immune VHHs they displayed a higher affinity for vascular Aβ in HCHWA-D patients when compared with AD (figure 5, table 1).

The VHHs selected from the grey matter AD library (pa2H, pa11E, and pa4D), recognized Aβ epitopes that are specific for, or enriched in parenchymal plaques. In contrast with the VHHs selected from the vascular CAA library, they showed specificity for parenchymal Aβ depositions of AD patients. (figure 6, table 1).

As VHHs derived from post-immunization libraries seemed to show a preference for Aβ deposits which corresponded to the disease state used for immunization, while those from the non-immune library did not show a preference for AD or HCHWA-D Aβ deposits, all VHHs were tested in a larger panel of sporadic CAA patients. An example of immune reactivity of pa2H and ni8B in a series of 4 sporadic CAA patients is shown in figure 7. Pa2H and ni8B also in these patients recognized CAA, like all other VHH derived from the non-immune and parenchymal libraries. We therefore consider the affinity preference for these VHHs to be disease- and not patient-specific.

Furthermore, the overall preference for HCHWA-D of the vascular CAA library derived VHH was further corroborated with the observation that only one sporadic CAA patient showed vascular reactivity for these VHHs (data not shown).

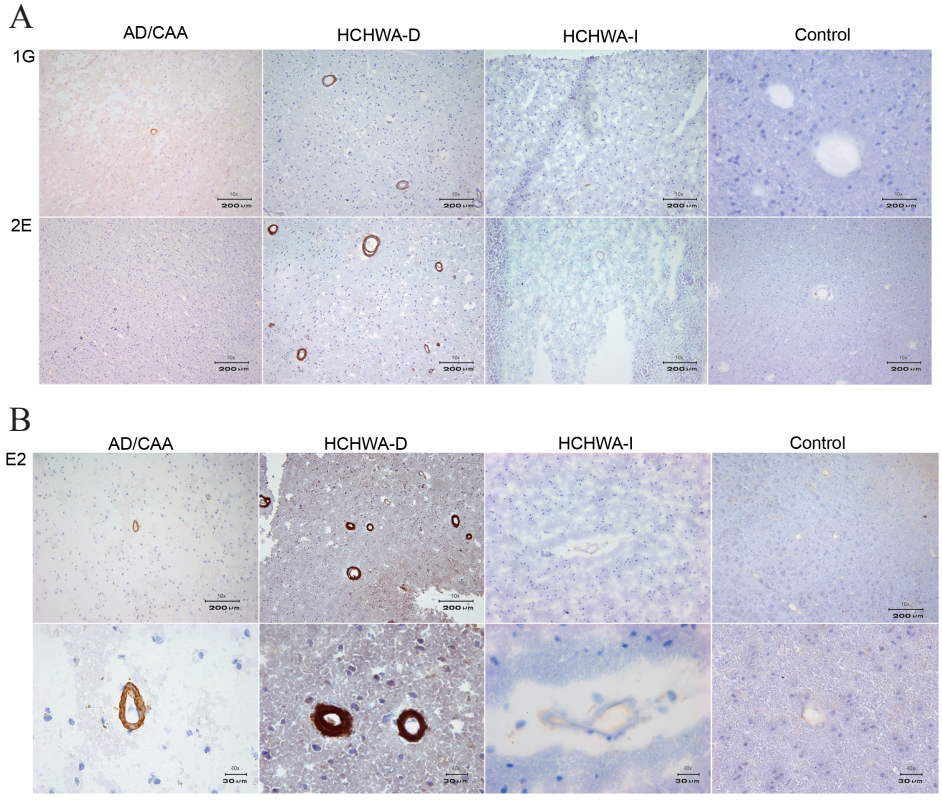

Figure 5 Immunohistochemistry of VHH va1G, va2E and vaE2 derived from the vascular amyloid library. **A)** The upper panel shows a 10x magnification of the immunohistochemical staining with va1G on AD, HCHWA-D, HCHWA-I and control tissue cryosections. In the lower panel a 10x magnification of the immunoreacitivity with va2E on, from left to right, AD, HCHWA-D, HCHWA-I tissue sections and a 40x magnification of the control tissue is shown. **B)** The upper panel shows a 10x magnification of the immunoreactivity with vaE2 on AD, HCHWA-D, HCHWA-I and control tissue cryosections. In the lower panel a 40x magnification of the immunoreactivity with vaE2 is shown for the same tissue sections. The VHHs in panel A and B show vascular beta amyloid reactivity, with an overall Aβ affinity preference for HCHWA-D patients, especially va2E, which has no immune reactivity for Aß in AD.

4. DISCUSSION

AD is the most common form of dementia and CAA is a major cause of intracerebral hemorrhage in elderly [23]. Both are progressive neurodegenerative diseases that share Aβ deposition as etiological event: a misbalance in the homeostasis between Aβ production and clearance that promotes accumulation of Aβ in the brain is supposed to

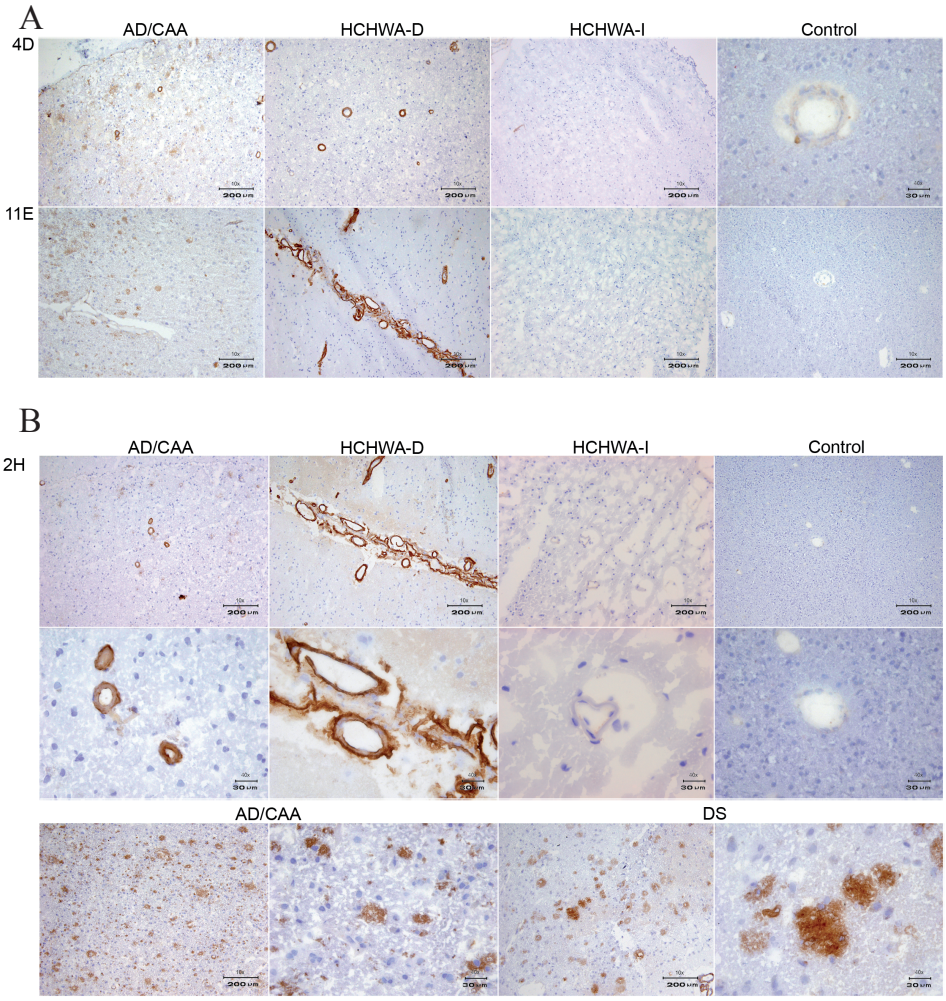

Figure 6 Immunohistochemistry of VHH pa4D, pa11E and pa2H, derived from the grey matter library. **A)** The upper panel shows a 10x magnification of the immunoreactivity with pa4D on AD, HCHWA-D, HCHWA-I and a 10x magnification of control tissue cryosections. In the lower panel a 10x magnification of the staining with pa11E on the same tissue sections from left to right, AD, HCHWA-D, HCHWA-I tissue sections and a 40x magnification of the control tissue is shown. **B)** All the panels show immunoreactivity VHH pa2H, from on AD, HCHWA-D, HCHWA-I and control tissue cryosections. The upper panel is showing a 10x magnification. In the middle panel the 40x magnification is shown. The lower panel shows 10 and 40x magnifications AD and DS cryosections. The VHHs displayed in panel A and B show high affinity for parenchymal Aβ epitopes, in addition to vascular affinity.

represent the earliest event in the disease process in many patients [2,24]. Therefore, Aβ is a pathologic hallmark of AD, CAA and related neurodegenerative diseases. Although cerebral accumulation and aggregation of Aβ is the primary neuropathologic feature shared by AD and CAA the two diseases are heterogeneous in Aβ etiology and clinical

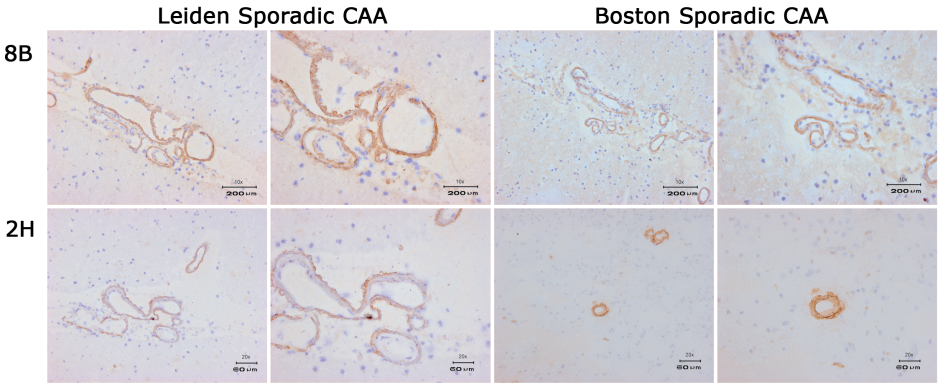

Figure 7 Immunohistochemistry of VHH pa2H and ni8B. VHHs are tested on four different sporadic CAA patients. Two of the patients are Leiden CAA patients and two are Boston CAA patients.

presentation [15,26]. The availability of diagnostic probes for early detection of cerebral Aß in living patients which preferably discriminate between vascular and parenchymal aggregates would contribute significantly to the early diagnosis and treatment of this group of disorders.

In this study a panel of immunologic reagents directed against Aß were examined with the long term objective of developing tools for the early non-invasive differential in vivo imaging of AD and CAA. VHHs have several potential advantages which might allow them to be used for in vivo imaging of neurological disorders. VHHs have a molecular mass of ~15 kDa and because of their small size VHHs show quick tissue penetration, are rapidly cleared from the blood and can have the propensity to cross the BBB. [16,21,30]. Furthermore, in animal models, VHHs have shown little immunogenicity and can be produced in a quick en economical manner in microorganisms [1,5,6,8]

In this study, we compared the performance of VHHs selected from immune- and non-immune libraries in immunohistochemistry. First VHHs were selected from a non-immune and vascular CAA library. This selection from the vascular CAA library resulted in VHHs that only recognize vascular Aβ depositions and fail to recognize parenchymal depositions of Aβ. Because the major component of vascular Aβ in these diseases is Aβ40, high affinity of the VHHs for Aβ40 could explain this selective recognition of vascular beta amyloid [11]. We therefore tested affinity preference of our selected VHHs for different Aβ peptides by phage-ELISA. Surprisingly, most VHHs showed highest preference for Aβ1-42. From these results we conclude that although in both vessels and parenchyma progressive cerebral accumulation and aggregation of Aβ is present, Aβ deposition at these two types of structures seems to differ in Aβ epitope availability.

In order to obtain VHHs that preferentially recognize Aβ epitopes that are specific for, or enriched in parenchymal plaques, we immunized a llama with brain parenchyma of a patient with extensive AD pathology. In contrast to the VHHs selected from the

vascular library, VHHs selected from this library show high affinity for Aβ present in parenchymal plaques in addition to vascular affinity. The results from the vascular and parenchymal immune libraries suggest that different epitopes are present or exposed in vascular and parenchymal Aβ deposits. While vascular Aβ epitopes recognized by the VHHs are not available in parenchymal Aβ deposition, Aβ epitopes available and recognized in the brain parenchyma are also present in vascular Aβ deposition. This phenomenon may be related to differences in the conformation state of the Aβ present in the vessels and the parenchyma.

In addition to this discrimination between vascular and parenchymal Aβ, VHHs selected from the grey matter AD library recognize parenchymal Aβ selectively in patients with AD pathology but not in HCHWA-D patients. This finding suggests that these VHHs discriminate amyloid plaques from plaques containing (predominantly) non-fibrillar Aβ.

Overall, the VHHs selected from the different libraries showed distinct patterns of specificity when used for immunohistochemistry, with the highest Aβ immune reactivity being observed in the disease condition that was used for immunization. This is consistent with the phage-ELISA data and therefore supporting the presence/availability and recognition by the VHHs of different epitopes present in CAA and AD. Nevertheless, the discriminatory propensity of the VHHs derived from the non-immune and CAA libraries was consistent in sporadic and hereditary CAA.

The formation of highly insoluble fibrils with a β-pleated structure (amyloid) is a common biochemical characteristic shared by proteins with diverse amino acid sequences. This aggregation and fibrillization process is observed in many neurological/neurodegenerative disorders [29]. In AD and CAA, Aβ is the major constituent of these aggregates, while in HCHWA-I the amyloid consists mainly of cystatin C (L68Q) [9]. Given the absence of immunohistochemical staining of HCHWA-I protein depositions, we conclude our VHHs are specific for Aβ in its amyloidogenic confirmation. This distinguishes them from some of the recently published antibodies which recognize the amyloid structure independent of its protein composition [18].

Plasma IgGs specific for known toxic Aβ and amyloidogenic non-Aβ species are common in healthy individuals and some of these antibody levels decline with age and AD progression [4]. It has been suggested that these Aβ sequence- or conformation-specific antibodies can prevent or delay Aβ pathology, possibly through a number of different pathways. Although additional studies are required to establish the therapeutic significance of specific Aβ antibodies, a preventive measure toward AD may come from further development of conformation-specific Aβ antibodies such as the VHH described in this study.

In conclusion, we selected sequence specific VHHs against Aß. Different immunization strategies resulted in the selection of high affinity VHHs specific for different Aβ epitopes. To our knowledge, the VHHs presented here are the first immunologic agents that are capable of discriminating vascular and parenchymal Aß deposits, though further studies are required to elucidate the basis of this specificity. Additionally, because of the favourable in vivo characteristics of VHHs, these reagents

have the potential to serve as tools for in vivo imaging to discriminate between vascular and parenchymal beta amyloid deposition.

5. ACKNOWLEDGEMENTS

We would like to thank Finnbogi R. Thormodsson, PhD, Faculty of Medicine, University of Iceland, Reykjavik, for providing cryo-sections of HCHWA-I patients and Ingrid Hegeman-Kleinn for technical assistance. We also would like to thank Kim Retera, PhD, VU Medical Center, Amsterdam, for Biacore analysis support. This work was supported by grants from the IOP Genomics Senter [IGE05005], the National Institutes of Health (NIH AG021084 and AG005134) and by the Centre for Medical Systems Biology within the framework of the Netherlands Genomics Initiative (NGI)/ Netherlands Organization for Scientific Research (NWO).

5.1 Disclosure statement for authors

All coauthors have seen and agree with the contents of the manuscript and that the manuscript is not under review at any other publication. Two authors (SMM and CTV) hold a patent on two of the HCAb fragments (ni3A and ni8B) described in this study.

REFERENCE LIST

1. Arbabi-Ghahroudi,M., Tanha,J. & MacKenzie,R. Prokaryotic expression of antibodies. Cancer Metastasis Rev. 24, 501-519 (2005).
2. Blennow,K., de Leon,M.J. & Zetterberg,H. Alzheimer's disease. Lancet 368, 387-403 (2006).
3. Bornebroek,M. et al. Hereditary cerebral hemorrhage with amyloidosis-Dutch type: better correlation of cognitive deterioration with advancing age than with number of focal lesions or white matter hyperintensities. Alzheimer Dis. Assoc. Disord. 10, 224-231 (1996).
4. Britschgi,M. & Wyss-Coray,T. Blood protein signature for the early diagnosis of Alzheimer disease. Arch. Neurol. 66, 161-165 (2009).
5. Coppieters,K. et al. Formatted anti-tumor necrosis factor alpha VHH proteins derived from camelids show superior potency and targeting to inflamed joints in a murine model of collagen-induced arthritis. Arthritis Rheum. 54, 1856-1866 (2006).
6. Cortez-Retamozo,V. et al. Efficient tumor targeting by single-domain antibody fragments of camels. Int. J. Cancer 98, 456-462 (2002).
7. Ellis,R.J. et al. Cerebral amyloid angiopathy in the brains of patients with Alzheimer's disease: the CERAD experience, Part XV. Neurology 46, 1592-1596 (1996).
8. Frenken,L.G. et al. Isolation of antigen specific llama VHH antibody fragments and their high level secretion by Saccharomyces cerevisiae. J. Biotechnol. 78, 11-21 (2000).
9. Ghiso,J., Jensson,O. & Frangione,B. Amyloid fibrils in hereditary cerebral hemorrhage with amyloidosis of Icelandic type is a variant of gamma-trace basic protein (cystatin C). Proc. Natl. Acad. Sci. U. S. A 83, 2974-2978 (1986).
10. Grabowski,T.J., Cho,H.S., Vonsattel,J.P., Rebeck,G.W. & Greenberg,S.M. Novel amyloid precursor protein mutation in an Iowa family with dementia and severe

cerebral amyloid angiopathy. Ann. Neurol. 49, 697-705 (2001).

11. Gravina,S.A. et al. Amyloid beta protein (A beta) in Alzheimer's disease brain. Biochemical and immunocytochemical analysis with antibodies specific for forms ending at A beta 40 or A beta 42(43). J. Biol. Chem. 270, 7013-7016 (1995).
12. Haass,C. et al. Amyloid beta-peptide is produced by cultured cells during normal metabolism. Nature 359, 322-325 (1992).
13. Habicht,G. et al. Directed selection of a conformational antibody domain that prevents mature amyloid fibril formation by stabilizing Abeta protofibrils. Proc. Natl. Acad. Sci. U. S. A 104, 19232-19237 (2007).
14. Hamers-Casterman,C. et al. Naturally occurring antibodies devoid of light chains. Nature 363, 446-448 (1993).
15. Hardy,J. & Selkoe,D.J. The amyloid hypothesis of Alzheimer's disease: progress and problems on the road to therapeutics. Science 297, 353-356 (2002).
16. Harmsen,M.M., Van Solt,C.B., Fijten,H.P. & Van Setten,M.C. Prolonged in vivo residence times of llama single-domain antibody fragments in pigs by binding to porcine immunoglobulins. Vaccine 23, 4926-4934 (2005).
17. Johnson,K.A. et al. Imaging of amyloid burden and distribution in cerebral amyloid angiopathy. Ann. Neurol. 62, 229-234 (2007).
18. Kayed,R. et al. Common structure of soluble amyloid oligomers implies common mechanism of pathogenesis. Science 300, 486-489 (2003).
19. Kazemier,B., de Haard,H., Boender,P., van Gemen,B. & Hoogenboom,H. Determination of active single chain antibody concentrations in crude periplasmic fractions. J. Immunol. Methods 194, 201-209 (1996).
20. Kerwitz,Y. et al. Stimulation of poly(A) polymerase through a direct interaction with the nuclear poly(A) binding protein allosterically regulated by RNA. EMBO J. 22, 3705-3714 (2003).
21. Muruganandam,A., Tanha,J., Narang,S. & Stanimirovic,D. Selection of phage-displayed llama single-domain antibodies that transmigrate across human blood-brain barrier endothelium. FASEB J. 16, 240-242 (2002).
22. Natte,R. et al. Dementia in hereditary cerebral hemorrhage with amyloidosis-Dutch type is associated with cerebral amyloid angiopathy but is independent of plaques and neurofibrillary tangles. Ann. Neurol. 50, 765-772 (2001).
23. Revesz,T. et al. Sporadic and familial cerebral amyloid angiopathies. Brain Pathol. 12, 343-357 (2002).
24. Seubert,P. et al. Secretion of beta-amyloid precursor protein cleaved at the amino terminus of the beta-amyloid peptide. Nature 361, 260-263 (1993).
25. Stijlemans,B. et al. Efficient targeting of conserved cryptic epitopes of infectious agents by single domain antibodies. African trypanosomes as paradigm. J. Biol. Chem. 279, 1256-1261 (2004).
26. van Duinen,S.G. et al. Hereditary cerebral hemorrhage with amyloidosis in patients of Dutch origin is related to Alzheimer disease. Proc. Natl. Acad. Sci. U. S. A 84, 5991-5994 (1987).
27. van Koningsbruggen,S. et al. Llama-derived phage display antibodies in the dissection of the human disease oculopharyngeal muscular dystrophy. J. Immunol. Methods 279, 149-161 (2003).
28. Verheesen,P. et al. Reliable and controllable antibody fragment selections from Camelid non-immune libraries for target validation. Biochim. Biophys. Acta 1764, 1307-1319 (2006).
29. Westermark,P. et al. Amyloid fibril protein nomenclature -- 2002. Amyloid. 9, 197-200 (2002).
30. Zhang,J. et al. Pentamerization of single-domain antibodies from phage libraries: a novel strategy for the rapid generation of high-avidity antibody reagents. J. Mol. Biol. 335, 49-56 (2004).

3

CHAPTER 3 | TRANSMIGRATION OF BETA AMYLOID SPECIFIC HEAVY CHAIN ANTIBODY FRAGMENTS ACROSS THE IN-VITRO BLOOD-BRAIN BARRIER

TRANSMIGRATION OF BETA AMYLOID SPECIFIC HEAVY CHAIN ANTIBODY FRAGMENTS ACROSS THE IN-VITRO BLOOD-BRAIN BARRIER

3

Kim S. Rutgers, M.Sc.[1], Rob J. Nabuurs, M.Sc.[2], Sjoerd S. van den Berg, M.Sc.[1], Geert J. Schenk, M.Sc.[6], C. Theo Verrips, Ph.D.[3], Sjoerd G. van Duinen, M.D., Ph.D.[4,5], Marion L. Maat-Schieman M.D., Ph.D[5], Mark A. van Buchem, M.D., Ph.D.[2], A. Bert G. de Boer Ph.D.[6], Silvère M. van der Maarel, Ph.D.[1]

1. Department of Human Genetics, Leiden University Medical Center, Leiden, Netherlands
2. Department of Radiology, Leiden University Medical Center, Leiden, Netherlands
3. Department of Molecular Cell Biology, Utrecht University, Utrecht, Netherlands
4. Department of Pathology, Leiden University Medical Center, Leiden, Netherlands
5. Department of Neurology, Leiden University Medical Center, Leiden, Netherlands
6. Department of Pharmacology, Leiden-Amsterdam Center for Drug Research, Leiden University, Netherlands

Running title: BBB passage of Aβ specific antibody fragments
Keywords: Blood brain barrier, Alzheimer's disease, Amyloid beta, Antibody, Imaging, Cerebral Amyloid Angiopathy

ABSTRACT

Previously selected amyloid beta recognizing VHH affinity binders derived from the Camelid heavy chain antibody repertoire were tested for their propensity to cross the blood-brain barrier using an established in vitro blood brain barrier co-culture system. Of all tested VHH, ni3A showed highest transmigration efficiency which is, in part, facilitated by a 3 amino acid substitution in its N-terminal domain. Additional studies indicated that the mechanism of transcellular passage of ni3A is by active transport. As VHH ni3A combines the ability to recognize amyloid beta and to cross the blood-brain barrier, it has potential as a tool for non-invasive in vivo imaging and as efficient local drug targeting moiety in patients suffering from cerebral amyloidosis such as Alzheimer's disease and cerebral amyloid angiopathy.

1. INTRODUCTION

Alzheimer's disease (AD) is the most prevalent form of dementia and clinically characterized by an irreversible process of cognitive decline 1. Cerebral amyloid angiopathy (CAA), is the main cause of non-hypertensive intracerebral hemorrhage in the elderly 13. AD and CAA share amyloid beta (Aβ) accumulation and aggregation as one of their primary neuropathologic characteristics 5,16. Furthermore, a definitive diagnose can only be made with certainty by post-mortem histological analysis of brain tissue. Ideally, treatment of AD and CAA patients has to be started before significant cognitive loss has occurred. However, this requires novel diagnostic methods, ideally non-invasive, allowing the early detection of these diseases. Therefore, several classical antibodies, targeted at Aβ, have been developed for detection and treatment of cerebral amyloidosis, but their utilization in vivo has been hampered by their size which prevents them from crossing the blood-brain barrier (BBB) effectively.

Camelidae co-express unusually shaped antibodies which are devoid of light chains next to their conventional immunoglobulin repertoire. These antibodies, referred to as heavy chain antibodies (HCAb), are composed of two identical heavy chains. Their antigen-binding properties are therefore only defined by the variable domains of these heavy chains (VHH). Interestingly, these VHH by themselves are fully capable of antigen binding 4.

VHH have a molecular mass of ~15 kDa with affinities similar to those achieved with conventional antibodies 19. VHH rapidly pass the renal filter, resulting in a rapid tissue penetration and fast blood clearance 6. Moreover, it was demonstrated that they can cross the BBB: VHH FC5 binds to human cerebromicrovascular endothelial cells (HCEC) and transmigrates across an in vitro human BBB model 10. Therefore, VHH are considered to have potential as tools for early non-invasive diagnosis using targeted contrast agents and delivery of therapeutic agents in patients with neurodegenerative disorders.

Targeted drug delivery and non-invasive early diagnosis using targeted contrast agents in neurodegenerative disorders are complicated by the regulated interface created by the BBB. The BBBs primary function is to maintain homeostasis of the brain and protects it against undesirable compounds and cells. For the identification of compounds that can cross the BBB the availability of in vitro BBB (co)-culture systems is imperative. Previously, we reported on an in vitro BBB co-culture system consisting of bovine brain capillary endothelial (BCEC) cells and newborn rat astrocytes. This established BBB model has been studied thoroughly and was shown to mimic the BBB in vitro, having small paracellular permeability, expression of various transporters and a relatively high transendothelial electrical resistance (TEER) 3.

In a previous study, we described VHH which we selected against Aβ by phage display 14. As a first step toward in vivo application, we here analyzed their propensity to cross the BBB in vitro and the influence of three specific amino acid substitutions on this crossing ability. The combination of both properties, i.e. the ability to cross the BBB and to recognize Aβ, would render these VHH promising tools for non invasive in vivo imaging and efficient local drug targeting in patients with AD or CAA.

2. MATERIALS AND METHODS

2.1 VHH used in this study

The VHH used in this study were described previously 14. VHH ni3A, ni8B and va2E are selected against Aβ. VHH ni3A and ni8B are derived from a non-immune library; va2E is selected from an immune library created after immunisation with post-mortem cerebral blood vessels of a Hereditary Cerebral Hemorrhage With Amyloidosis – Duchtype (HCHWA-D) patient. VHH FC5 encoding mRNA and amino acid sequences are deposited in the GenBank no. AF441486 and no. AAL58846, respectively and was produced synthetically.

2.2 Subcloning and Production

The VHH genes were subcloned into the pUR5850VSV production vector 17. Thereafter, the VHH were produced in E. coli and purified from the periplasmic supernatants as described earlier 8. To test the necessity of the presence of three atypical amino acids in the N-terminus (framework 1; FR1) of ni3A for its ability to cross the BBB, a chimearic VHH 3A2E was constructed by PCR amplification of FR1 of ni3A and the region starting from complementarity determining region 1 (CDR1) until FR4 of va2E, and subsequent cloning of the chimearic PCR product into the pUR5071myc and pUR5850VSV vectors. All vectors were sequence verified (LGTC, Leiden, Netherlands). Production was performed as described previously 7.

The open reading frame of the similarly sized control protein alpha-synuclein (SNCA) was PCR amplified from human brain cDNA, cloned, sequence verified and its encoded product was produced in the pET28 production system (Novagen, Madison, WI, USA). Primer sequences are available upon request. All proteins were purified using Talon metal affinity resin (Clontech, Palo Alto, CA, USA) according to the instructions of the manufacturer.

2.3 Immunohistochemistry

Frozen brain tissue sections (5µm) of Down syndrome (DS), HCHW-AD, AD patients and non-demented control tissue were rinsed in PBS, fixed with ice-cold acetone for 10 min, incubated with peroxidase blocking reagent (Dako Cytomation) for 20 min, washed in PBS and incubated with the anti-Aβ VHH (10ng/ul) in 1% BSA/ PBS overnight in a wet chamber. Thereafter, the sections were rinsed with PBS and incubated with mouse-anti-VSV or mouse-anti-c-myc for 1 hour and EnVision+ ® system labelled Polymer-Hrp anti-Mouse (Dako Cytomation) for 30 min. Detection was performed with Liquid DAB+ Substrate Chromogen System (Dako Cytomation). In addition, hemotoxylin counterstaining was performed and the sections were dehydrated and mounted in micromount mounting medium (Surgipath, Richmond, IL, USA). 4G8 (Covance, Princeton, New Jersey, USA) was used as a positive control for Aβ staining.

2.4 In vitro blood-brain barrier system

The in vitro BBB model was prepared as described before 2,3. Briefly, brain capillaries were isolated from cortices of bovine brain, acquired at a slaughterhouse (de Boer, Nieuwerkerk a/d IJssel, The Netherlands). The capillary fraction was prepared by homogenization, captured by percolation with nylon meshes and subsequently digested by enzymes. Astrocytes were isolated from cortices of brains of newborn Wistar rats (Harlan B.V., Zeist, The Netherlands) and used for co-culture purposes and the preparation of astrocyte conditioned medium. Brain capillaries were cultured on collagen and fibronectin coated culture flasks in 50% astrocyte conditioned medium to brain capillary endothelial cells (BCEC). The astrocytes were seeded on the bottom of the filter. Two days later the BCEC were passaged on collagen coated Transwell polycarbonate filters (surface area: 0.33cm2, pore size: 0.4 µm, Corning Costar, Cambridge, MA, USA) and cultured to tight monolayers in 50% astrocyte conditioned medium in 5 days.

2.5 In vitro blood-brain barrier transport

Transport studies were performed after 10 days of seeding and subsequently 5 days of seeding on the filters in DMEM+ 10% fetal calf serum (Bio Whittaker Europe, Verviers, Belgium) at 370C. Transport studies were initiated by adding 10µg VHH to the upper chamber of the in vitro BBB system. 60ul aliquots were taken from the bottom chamber at 5, 15, 30, 60 and 90 min. As a control a protein with the same size as a VHH (SNCA) was used. Membrane integrity was monitored with transendothelial electrical resistance (TEER) measurements, which is considered to be a reliable and sensitive method to monitor the paracellular BBB permeability. The threshold was set at a resistance of 200 Ohm x cm2. After 120 min the cells were washed 3 times 300µl DMEM+S, harvested and lysed with MPER (Pierce Biotechnology, Rockford, IL, USA). For determination of the amount of VHH/protein that transmigrated across the model, 25µl aliquots collected from the bottom chamber were immobilized on a Ni-NTA HisSorb 96-well plate (QIAGEN Benelux, Venlo, The Netherlands) diluted in 1% BSA with a final volume of 200µl, at 40C overnight. Plates were washed 4 times with PBS 0.05% Tween (PBST) and incubated with anti-c-Myc / anti-VSV monoclonal antibody diluted in 1% BSA for 1hour at room temperature. After washing, plates were incubated with polyclonal Rabbit anti-Mouse Immuno globulins conjugated with HRP (DakoCytomation). Plates were washed and detection was performed by adding 100ml OPD (3,7mM o-phenyldiamine, 50mM Na2HPO4.H2O, 25mM citric acid) supplemented with 0.01% H2O2 to the wells. When the reaction was clearly visible, 50ml 1M H2SO4/well was added to stop the reaction. The extinction at 490nm was measured utilizing a Biotec synergy HT plate reader. All statistical analyses were performed by unpaired 2 tailed t-test using GraphPad Prism version 5.00 for Windows (GraphPad Software, San Diego California USA). Threshold value for statistical significant differences was set at 5%.

3. RESULTS

3.1 Subcloning and purification of specific VHH

Two independent VHH clones, ni3A and ni8B respectively, were chosen for this study 14. These VHH were subcloned into the pUR5850-VSV production vector. Ni3A has an unusual intrinsic efficiency in crossing the BBB (see below, figure 3). In order to investigate the necessity of the presence of three, for VHH unusual amino acid residues in the N terminus of ni3A, [R15-D-G-D], with respect to crossing the BBB, heterogeneous VHH 3A2E was constructed. 3A2E consists of the N-terminus from ni3A fused, at the boundary between FR1 and CDR1, with the C-terminus of va2E and therefore also contains these unusual amino acid residues. VHH va2E also recognizes Aβ but was selected from a different phage display library 14. After production in E. coli the pure VHH were isolated from the periplasmic fraction and purified by immobilized metal affinity chromatography on Talon beads. An overview of the single and chimaeric VHH constructs is shown in figure 1.

3.2 Immunohistochemistry

Frozen brain tissue sections of AD, DS and HCHWA-D patients showed specific Aβ staining of 3A2E indicating that the Aβ recognizing propensity of va2E was preserved in this chimaeric molecule (figure 2). The specificity of the Aβ staining was confirmed by the absence of staining in control brain tissue sections and an identical staining pattern was obtained with, the commercially available Aβ antibody, 4G8 in all patients. In contrast to 4G8, only vascular staining was observed with 3A2E, equal to ni3A and ni8B, as previously described 14.

3.3 In vitro blood-brain barrier transport

VHH ni3A, ni8B and FC5 were assessed for their ability to transmigrate across the BBB in vitro. While FC5 was previously described to cross the BBB as it was selected

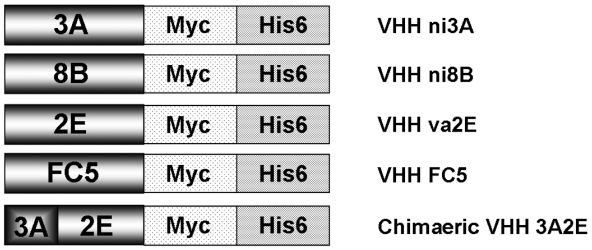

Figure 1 Overview single and chimaeric VHH constructs. Depicted is a schematic representation of the VHHs used for the different experiments. First (up -> down) the monovalent VHHs ni3A, ni8B, va2E and FC5 are shown. At the bottom, the chimearic VHH 3A2E is depicted. VHHs are equipped with a c-Myc (Myc) tag for secondary antigen recognition and a hexa histidine tag (His6) for affinity purification.

Figure 2 Immunohistochemistry of the cerebral cortex of an AD patient, HCHWA-D patient and control tissue. Cryosections stained with chimaeric VHH 3A2E are shown. From left to right a 10x magnification of frozen tissue sections of an AD and HCHWA-D patient, and control tissue are depicted. 3A2E retains its functionality of recognizing vascular Aβ.

for this propensity, we didn't anticipate that ni3A showed higher transmigration velocity than FC5 10. Yet, the transmigration rate of ni3A and ni8B was significantly higher compared to FC5 (respectively $p<0.01$ and $p=0.01$) (figure 3).

Although VHH ni3A differs by 3 amino acids in its N terminus from ni8B but has furthermore identical CDRs, a significantly higher transmigration velocity was observed by ni3A ($p<0.01$) (figure 3). In order to elucidate the capacity of ni3A to cross the BBB system with high efficiency, two additional VHH were tested: VHH va2E and chimaeric VHH 3A2E. The difference in crossing efficiency between va2E and the unrelated control protein of similar molecular weight (SNCA) did not reach statistical significance ($p=0.22$) (figure 3). Chimaeric VHH 3A2E has the same FR1 as ni3A and the 2E-specific C-terminus. Chimaeric VHH 3A2E displayed a significantly higher transmigration rate compared to 2E ($p=0.02$) (figure 3), indicating that the 3 amino acids subtracted from ni3A facilitate the crossing efficiency of VHH. At 4oC there was no significant passage of the VHH ni3A, indicating that the transmigration of ni3A is by active transport (figure 4).

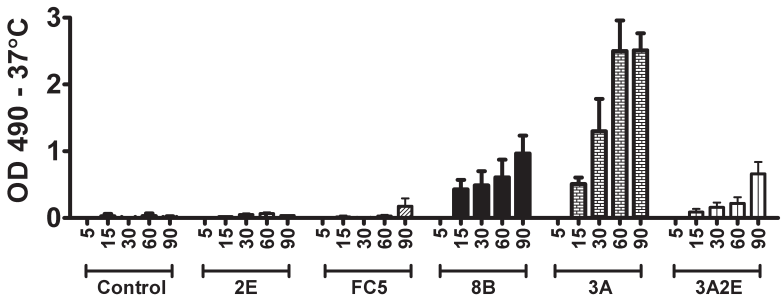

Figure 3 Transmigration of VHHs across the in-vitro BBB system. Transmigration at 37°C. Measurements were taken 5, 15, 30, 60 and 90 minutes after addition of the VHH samples to the system. Data is represented as OD490 at consecutive time points.

4. DISCUSSION

The availability of effective treatment for neurodegenerative disorders like AD and CAA is currently lacking but dearly needed. This lack of available therapy is partly based on our poor understanding of the pathogenesis of these diseases. The absence of reliable and sensitive biomarkers that permit studying cerebral amyloidosis in its early phases has certainly contributed to this situation. Cerebral Aβ accumulation and aggregation is one of the primary neuropathologic characteristics of AD and CAA and is assumed to play a key role in the pathogenesis of these diseases. Consequently Aβ is considered to be an important biomarker of cerebral amyloidosis 5,16. Recently, molecular imaging techniques have been developed that permit detection of brain amyloidosis in vivo. Currently, positron emission tomography (PET) using amyloid-binding radiotracer compounds are being used for detecting cerebral amyloidosis in patients worldwide 9,15,18. However, these agents detect both vascular and parenchymal Aβ, and are thus not well suited to differentially recognize AD and CAA. Therefore, the development of imaging moieties that can be used to differentiate between vascular and parenchymal amyloid in living patients could help detecting CAA and/or AD in vivo.

Previously we reported VHH which differentially recognize vascular and parenchymal Aβ deposition 14. In this study we assessed the ability of these recently selected VHH for their ability to serve as imaging moieties and vehicles for tissue targeting. These VHH have the potential to serve as delivery vectors for efficient local drug targeting and for diagnostic purposes. It is believed that VHH have advantages to serve as imaging agents and/or transport moieties behind the BBB as they may overcome some of the current hurdles to transmigrate over the regulated interface created by the BBB 6,11. In this study, an established in vitro co-culture model of the BBB was used to test different Aβ recognizing VHH for their ability to cross the BBB. Previously it was shown that in order to acquire a high quality in vitro co-culture model of the BBB one needs an optimal isolation method of bovine brain capillaries, and specific culture procedures for primary bovine brain capillary endothelial cells (BCEC) and rat-astrocytes 3. The co-culture systems used in this study are superior to others with respect to paracellular permeability and the maintenance of influx and efflux transportsystems 12.

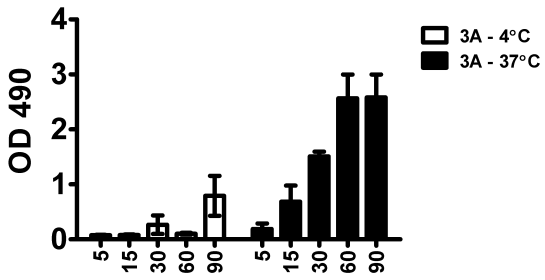

Figure 4 Transmigration of ni3A across the in-vitro BBB system at 4oC and 37°C. Measurements were taken 5, 15, 30, 60 and 90 minutes after addition of the samples to the system. Data is represented as OD490 at consecutive time points. At 4oC, passage of the ni3A could not be observed, indicating that the mechanism of transcellular passage of ni3A is by active transport

As VHH FC5 was previously reported to cross the BBB in vitro, we compared the crossing efficiency of FC5 to VHH ni3A selected against Aβ. To our great surprise, ni3A showed higher transmigration efficiency than FC5 at 37 oC. At 4oC there was barely passage of ni3A. This temperature sensitive transport suggests that the mechanism of transcellular passage of ni3A is by active transport.

Ni3A passes the system with the highest efficiency compared to all other VHH tested. Because ni3A is only three amino acids different from ni8B in FR1, and they present different crossing efficiencies, we hypothesized that those amino acid residues could potentially be key for the crossing propensity. It is interesting to note that these three amino acid diversion of ni3A is a special feature that is not present in any germline VHH gene. In order to test this hypothesis, VHH 3A2E was constructed, a chimaeric VHH in which we combined FR1 of ni3A with the carboxyterminus (CDR1-FR4) of va2E, a VHH which was selected against Aβ from an immune library and showed no crossing ability.

In vitro BBB passage of va2E was significantly and positively facilitated by the replacement of the three ni3A –specific amino acids. Although the unique amino acids in ni3A are not sufficient for efficient transmigration we conclude that they positively affect the transmigration rate. Apparently, a combination of N-terminal amino acid substitutions and other ni3A and ni8B-specific downstream sequences allow ni3A to outperform other VHH in its transmigration efficacy. In support, chimearic 3A2E and ni8B, both having only one of these features, show intermediate transmigration efficiencies.

In conclusion, in this study VHH ni3A shows in addition to a high affinity for Aβ, the ability to cross the BBB in vitro. This transport is temperature sensitive and facilitated by 3 unique amino acids. Ni3A has potential as in vivo imaging agent and local drug targeting moiety. Further studies will need to focus on its mechanism of transmigration and its application in vivo.

5. ACKNOWLEDGEMENTS

This work was supported by grants from the IOP Genomics Senter [IGE05005] and by the Center of Medical Systems Biology (CMSB2) and the Netherlands Consortium for Systems Biology (NCSB) established by The Netherlands Genomics Initiative/ Netherlands Organization for Scientific Research (NGI/NWO).

5.1 Disclosure statement for authors

All coauthors have seen and agree with the contents of the manuscript and that the manuscript is not under review at any other publication. Two authors (SMM and CTV) hold a patent on two of the HCAb fragments (ni3A and ni8B) described in this study.

REFERENCE LIST

1. Alzheimer, A., Stelzmann, R.A., Schnitzlein, H.N. & Murtagh, F.R. An English translation of Alzheimer's 1907 paper, "Uber eine eigenartige Erkankung der Hirnrinde". Clin. Anat. 8, 429-431 (1995).
2. Gaillard, P.J. & de Boer, A.G. 2B-Trans technology: targeted drug delivery across the blood-brain barrier. Methods Mol. Biol. 437, 161-175 (2008).
3. Gaillard, P.J. et al. Establishment and functional characterization of an in vitro model of the blood-brain barrier, comprising a co-culture of brain capillary endothelial cells and astrocytes. Eur. J. Pharm. Sci. 12, 215-222 (2001).
4. Hamers-Casterman, C. et al. Naturally occurring antibodies devoid of light chains. Nature 363, 446-448 (1993).
5. Hardy, J. & Selkoe, D.J. The amyloid hypothesis of Alzheimer's disease: progress and problems on the road to therapeutics. Science 297, 353-356 (2002).
6. Harmsen, M.M., Van Solt, C.B., Fijten, H.P. & Van Setten, M.C. Prolonged in vivo residence times of llama single-domain antibody fragments in pigs by binding to porcine immunoglobulins. Vaccine 23, 4926-4934 (2005).
7. Kazemier, B., de Haard, H., Boender, P., van Gemen, B. & Hoogenboom, H. Determination of active single chain antibody concentrations in crude periplasmic fractions. J. Immunol. Methods 194, 201-209 (1996).
8. Kazemier, B., de Haard, H., Boender, P., van Gemen, B. & Hoogenboom, H. Determination of active single chain antibody concentrations in crude periplasmic fractions. J. Immunol. Methods 194, 201-209 (1996).
9. Klunk, W.E. et al. Imaging brain amyloid in Alzheimer's disease with Pittsburgh Compound-B. Ann. Neurol. 55, 306-319 (2004).
10. Muruganandam, A., Tanha, J., Narang, S. & Stanimirovic, D. Selection of phage-displayed llama single-domain antibodies that transmigrate across human blood-brain barrier endothelium. FASEB J. 16, 240-242 (2002).
11. Muyldermans, S., Cambillau, C. & Wyns, L. Recognition of antigens by single-domain antibody fragments: the superfluous luxury of paired domains. Trends Biochem. Sci. 26, 230-235 (2001).
12. Prieto, P. et al. The assessment of repeated dose toxicity in vitro: a proposed approach. The report and recommendations of ECVAM workshop 56. Altern. Lab Anim 34, 315-341 (2006).
13. Revesz, T. et al. Sporadic and familial cerebral amyloid angiopathies. Brain Pathol. 12, 343-357 (2002).
14. Rutgers, K.S. et al. Differential recognition of vascular and parenchymal beta amyloid deposition. Neurobiol. Aging (2009).
15. Small, G.W. et al. PET of brain amyloid and tau in mild cognitive impairment. N. Engl. J. Med. 355, 2652-2663 (2006).
16. van Duinen, S.G. et al. Hereditary cerebral hemorrhage with amyloidosis in patients of Dutch origin is related to Alzheimer disease. Proc. Natl. Acad. Sci. U. S. A 84, 5991-5994 (1987).
17. van Koningsbruggen, S. et al. Llama-derived phage display antibodies in the dissection of the human disease oculopharyngeal muscular dystrophy. J. Immunol. Methods 279, 149-161 (2003).
18. Verhoeff, N.P. et al. In-vivo imaging of Alzheimer disease beta-amyloid with [11C]SB-13 PET. Am. J. Geriatr. Psychiatry 12, 584-595 (2004).
19. Zhang, J. et al. Pentamerization of single-domain antibodies from phage libraries: a novel strategy for the rapid generation of high-avidity antibody reagents. J. Mol. Biol. 335, 49-56 (2004).

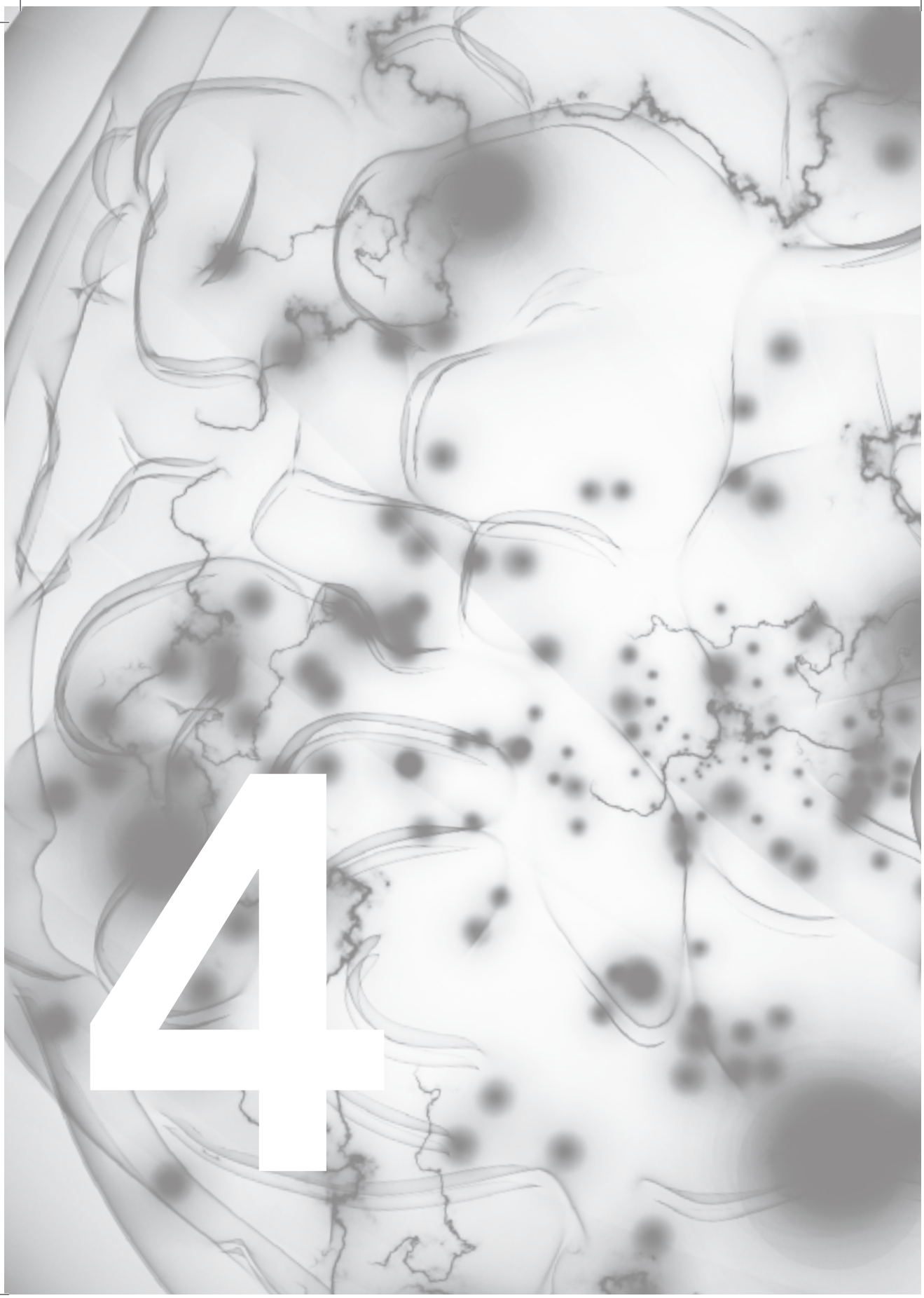
4

CHAPTER 4 | BINDING CHARACTERISTICS AND IN VIVO DETECTION OF BETA AMYLOID DEPOSITS USING HEAVY CHAIN ANTIBODY FRAGMENTS AS POTENTIAL MOLECULAR IMAGING AGENTS

BINDING CHARACTERISTICS AND IN VIVO DETECTION OF BETA AMYLOID DEPOSITS USING HEAVY CHAIN ANTIBODY FRAGMENTS AS POTENTIAL MOLECULAR IMAGING AGENTS

4

Rob J.A. Nabuurs, M.Sc.[#1], Kim S. Rutgers, M.Sc.[#2], Mick M. Welling Ph.D.[1], Thanos Metaxas, Ph.D.[4], Maaike E. de Backer, Ph.D[1], Brian J. Bacskai, PhD[4], Mark A. van Buchem, M.D.,Ph.D.[1], Silvère M. van der Maarel, Ph.D.[2], Louise van der Weerd Ph.D.[1,5]

[#] Authors have contributed to this work equally.
1. Department of Radiology, Leiden University Medical Center, Leiden, Netherlands
2. Department of Human Genetics, Leiden University Medical Center, Leiden, Netherlands
3. Department of Nuclear Medicine, Leiden University Medical Center, Leiden, Netherlands
4. Department of Neurology, Massachusetts General Hospital and Harvard Medical School, Charlestown, MA, USA
5. Department of Anatomy, Leiden University Medical Center, Leiden, Netherlands

Running title: heavy chain antibody fragments as potential molecular imaging agents
Keywords: Alzheimer's disease, Amyloid beta, Antibody, Imaging, Immunoreactivity, diagnostic tools

ABSTRACT

Previously we demonstrated that two llama-derived heavy chain antibody fragments (referred to as V_HH), ni3A and pa2H, were able to detect either solely vascular β-amyloid (Aβ) or both vascular and parenchymal Aβ depositions, which are pathological hallmarks found in cerebral amyloid angiopathy (CAA) and Alzheimer's disease (AD), respectively. These V_HH could potentially be used as *in vivo* diagnostic imaging agents for detection of exclusively CAA, or a mixture of CAA and AD phenotypes. The aim of this study was to assess the *in vivo* affinity and biodistribution of both V_HH in the APP/PS1 mouse model that presents both parenchymal and vascular plaque.

Both fluorescently labeled V_HH stained positive for murine parenchymal Aβ on tissue sections. In contrast to human tissue, ni3A did not show selective affinity for CAA in the mouse. In a pharmacodynamic study using ^{99m}Tc-labeled V_HH, we observed fast renal clearance. Pa2H showed a significant higher brain uptake 24 hours post injection in transgenic compared to wild type animals, though the absolute amount of brain uptake was too low for *in vivo* imaging of amyloid plaque.

Therefore, we circumvented the blood-brain barrier to assess the *in vivo* binding of fluorescently labeled V_HH to amyloid plaques. Specificity for Aβ plaques *in vivo* was observed for both V_HH without non-specific background staining. Pa2H, which showed a higher affinity than ni3A, was readily detectable for 24 hours or more after injection.

In conclusion, these data provide evidence that these V_HH have the ability to target Aβ depositions *in vivo*, making them promising tools for further development as diagnostic agents for the distinctive detection of different Aβ deposits in CAA and AD.

INTRODUCTION

The deposition of β-amyloid peptides (Aβ) within the brain plays an important role in the pathogenesis of two major neurodegenerative disorders: Alzheimer's disease (AD) and cerebral amyloid angiopathy (CAA). [16,47] AD is the most common cause of dementia in the elderly population. [4] Besides neurofibrillary degeneration, involving neurofibrillary tangles, histological examination of the post mortem AD brain typically reveals parenchymal Aβ deposits, either as so-called dense core or senile plaques or as oligomeric aggregates named diffuse plaques.[9]

In CAA, Aβ depositions specifically occur within the vascular wall of small cortical and leptomeningeal arteries, and sometimes in the capillaries. These depositions are associated with loss of vessel wall integrity, resulting in an increased risk of brain hemorrhages, both large and small. [35] Furthermore, CAA is thought to be a probable cause of brain ischemia and cognitive impairment independent of stroke. [35] In 90% of the AD patients CAA is coexistent, while CAA by itself is present in 30% of the non-demented population over 60 years of age. [44]

Even though the direct correlation between the amount of cerebral amyloid and its clinical presentation is still under debate, accumulation of Aβ is believed to start even as many as 20 years prior the first noticeable clinical symptoms. [11,19] Therefore, *in vivo* detection of Aβ remains an important biomarker especially sensitive for early diagnosis.

Until now, several amyloid-targeting PET probes have been clinically evaluated, with ^{11}C-PiB being the gold standard for *in vivo* amyloid imaging. ^{11}C-PiB has been shown to detect cerebral amyloid in both AD and CAA subjects as well as mild cognitive impaired (MCI) patients.[23] However, ^{11}C-PiB and other similar PET ligands target both vascular and parenchymal amyloid deposits, and a gross differentiation between AD and CAA can only be made spatially based on the occipital predilection of CAA.[22] Furthermore, currently no functional or target-specific clinical tracer exists that allows detection of oligomeric Aβ as found within diffuse plaques, which are hypothesized to play a major role in the neurodegenerative cascade.[43]

Previously, we have selected heavy chain antibody fragments against Aβ. [33] These recombinant affinity binders are a relatively new source of immunologic agents derived from the Camelid heavy chain antibody repertoire (HCAb), which in contrast to conventional immunoglobulins are devoid of light chains. Their single N-terminal domain (V_HH) is fully capable of antigen binding with affinities comparable with those reported for conventional antibodies. [15,17] The selection yielded V_HH that expressed a high affinity specific for either solely CAA, or all Aβ epitopes as visualized by immunostaining of human AD/CAA brain tissue.[33]

Possible BBB passage of the Aβ-targeting V_HH was recently investigated using an established *in vitro* BBB model, showing that some of the selected V_HH were efficiently transported across the BBB *in vitro*.[32] Therefore, we concluded that these V_HH have great potential to be used for non-invasive, early differential *in vivo* Aβ detection in the brain.

The purpose of this study was to assess the *in vivo* characteristics of two distinct Aβ targeting V_HH, ni3A and pa2H, that are important for their potential use as tools to differentially detect AD and CAA. First, pharmacologic behaviour and biodistribution were examined after administration of radiolabeled V_HH into aged APP/PS1 mice, a transgenic AD mouse model known to accumulate both vascular and parenchymal Aβ depositions. Secondly, fluorescently labeled V_HH were administered after the BBB was circumvented to evaluate their ability to specifically bind to Aβ depositions *in vivo*.

MATERIALS & METHODS

Subcloning and production of ni3A and pa2H

The V_HH used in this study have been described previously.[33] Briefly, V_HH ni3A and pa2H were selected against Aβ(1-42). Ni3A was derived from a non-immune library; pa2H was selected from an immune library created after immunisation with post-mortem cerebral brain parenchyma of a patient with Down's syndrome. V_HH genes were subcloned into the pUR5850VSV production vector and their sequences were verified (LGTC, Leiden, Netherlands).[40] The proteins were produced in *E. coli* and purified from the periplasmic supernatants as described.[24] Ni3A and pa2H were respectively myc- and VSV-tagged for detection, and for both a HIS-tag was used for purification using Talon metal affinity resin (Clontech, Palo Alto, CA, USA) according to the instructions of the manufacturer.

Animal studies

A colony of transgenic mice and wild type littermates was set up using the APPswe/PS1dE9 strain (APP/PS1) (Jackson Laboratory, Bar Harbor, MA, USA); a transgenic mouse model shown to accumulate both vascular and parenchymal Aβ depositions.[20] The animals are maintained under pathogen-free conditions in the animal housing facilities of the LUMC for at least 1 year before the onset of the experiments. Food and water were given *ad libitum* including the day of experimentation. Besides standard genotyping, after each experiment appropriate use was confirmed using a standard Thioflavin T staining for amyloid. All animal studies were carried out in compliance with the Dutch laws related to the conduct of animal experiments and approved by the local Committee for Animal Experiments.

Staining material

All staining procedures were performed using autopsy brain tissue of patients diagnosed with AD or controls as confirmed by neuropathological examination. Tissue was encoded and used in agreement with the code as defined in the Netherlands (Code Goed Gebruik). Murine material was obtained using snap frozen brain tissue of aged APP/PS1 transgenic mice and their wildtype littermates from our colony.

Murine specificity of the selected V_HH

Selectivity for different Aβ depositions has only been reported using human material.[33] To evaluate appropriate use of the APP/PS1 mouse model, the previously described immunostaining protocol was adapted for murine brain material. Frozen brain tissue sections (10µm) of 12 – 16 months old APP/PS1 mice and wildtype littermates were rinsed in PBS, fixed with ice-cold acetone for 10 min, incubated with peroxidase blocking reagent (Dako Cytomation) for 20 min and washed in PBS.

The sections were incubated overnight in a wet chamber with anti-Aβ V_HH in 1% BSA/PBS or only 1% BSA/PBS as a negative control. In addition, the secondary antibodies, mouse-anti-VSV or mouse-anti-c-myc, are labeled with the Biotinylation Reagent. The secondary antibodies and the Biotinylation Reagent, a modified biotinylated anti-mouse immunoglobulin (ARK, Dako Cytomation), were incubated together, resulting in binding of biotinylated antibody to the mouse-anti-VSV or mouse-anti-c-myc. In addition, normal mouse serum used as blocking reagent was added to the mixture. The tissue sections were incubated with the mouse-anti-VSV or mouse-anti-c-myc secondary antibodies, labeled with the Biotinylation Reagent, for 1 hour at room temperature. Subsequently, Streptavidin-peroxidase was applied on the tissue slide and incubated for 15 minutes followed by a reaction with Liquid DAB+ Substrate Chromogen System (Dako Cytomation). The sections were dehydrated and mounted in micromount mounting medium (Surgipath, Richmond, IL, USA). Final preparations were analyzed with an automated scanning microscope (Pannoramic MIDI, 3DHistech Ltd) equipped with Pannoramic Viewer software.

Biodistribution and clearance

Radiolabelling

V_HH were labeled directly with technetium-99m (^{99m}Tc) using a labeling protocol described by Welling *et al.*[46] Briefly, 20 µl of V_HH in PBS solution (450-500 ng/µl) was added to 8 µl of an aseptic mixture of 950 mg/l $Sn(Cl)_2.2H_2O$ and 2 g/l $Na_4P_2O_7.10H_2O$ (Technescan PYP, Covidien, Petten, the Netherlands) in saline. After addition of 4 µl of 10 mg/ml of KBH_4 (crystalline, Sigma Chemical Co, St. Louis, MO) in 0.1 M NaOH, and 100 µl of $Na[^{99m}TcO_4]$ solution (approximately 200-700 MBq/ml, Technekow, Covidien, Petten, the Netherlands) the mixture was gently stirred at room temperature for at least 30 min before use.

Analysis of the labeling solution, referred to as ^{99m}Tc-V_HH, performed as previously described [45], resulted in a radiochemical purity of >95% as shown by ITLC. Upon size exclusion HPLC no unreduced or free $^{99m}TcO_4$ was detected. The majority of labeled material remained stable for the duration of the experiments. (See supplemental data)

Biodistribution and brain uptake

To study the biodistribution of each radiolabeled V_HH over time, 12 – 16 month old APP/PS1 mice and wild type littermates were used. Freshly labeled ^{99m}Tc-V_HH was diluted in sterile saline to be administered with a final concentration of approx 10 µg/

ml. Each animal was anaesthetized by isoflurane (1-2%) inhalation and intravenously injected with 0.2 ml ^{99m}Tc-V_HH solution (5-10 MBq/ml) via the tail vein. At different intervals (t = 3 – 6 – 24 hrs) post injection APP/PS1 (n =4) and wild type animals (n=4) were sacrificed using a lethal dose of pentobarbital (Euthanasol, AST Pharma). 0.5 ml of blood was collected from each animal using cardiac puncture. Animals were further dissected to remove various organs (heart, lungs, liver, kidneys, spleen, thigh muscle). The brain was divided into the cerebrum and cerebellum. All organs and blood were weighted, and the radioactivity was measured using an automated gamma counter (Wizard^2, Perkin Elmer). After decay correction, radioactivity distribution in various tissues at the different time points was expressed as the mean (±SD) percentage of the total injected dose of radioactivity per gram tissue (%ID/g). Blood / cerebrum ratios were calculated to correct for possible confounding effects of activity accountable by residual blood. Cerebrum tissue (target tissue), was further compared with values determined in muscle (non-target) to determine a non-target-to-target ration. In addition, experiments at t = 24 hrs were repeated twice using ^{99m}Tc- pa2H.

Blood clearance and fraction analysis

To examine the blood half-life 5 µl samples were collected from a small incision in the tail at several time points between 3 – 90 minutes post injection of ^{99m}Tc-V_HH into transgenic or wildtype mice (n=4). Radioactivity was measured using a gamma counter as described above, decay-corrected, and calculated in % ID/g. Combined with the cardiac blood samples obtained during the biodistribution experiments, corresponding half-lives were calculated with a standard built-in two phase exponential decay non-linear fitting routine by Graphpad Prism v5.2 for Windows with the plateau constraint set to zero.

Similar, blood fraction analysis was performed by obtaining 10 µl of blood at 10 and 90 minutes post injection. Mixed with 90 µl heparin (34 U/ml saline) to prevent clotting, blood samples were diluted with 1X PBS to a volume of 1 ml, and centrifuged for 10 min at 7,000 rpm. Each sample was divided in two equal volumes: one part containing exclusively supernatant; the other part including supernatant and pellet. Radioactivity for both parts were measured as described above to determine the plasma versus the cell bound radioactivity of ^{99m}Tc-V_HH over time.

Statistical analysis

Statistical analysis of the biodistribution experiments and blood analyses were performed using an unpaired one or two tailed *t* test. Results were considered to be statistically significant when the *P*-value was below 0.05.

Specificity of radiolabeled pa2H

Specificity of V_HH for Aβ after incorporation of the radiolabel was tested by quantitative competition autoradiography. The labeling solution was diluted to 1 ml with 1% BSA in 1X PBS to a final concentration of 1 µg/ml. Fresh frozen 20 µm human and murine brain sections were blocked with 0.1 ml 1% BSA in PBS for 1 hour at 37^{o}C followed by similar incubation with 100µl of the labeling solution, and washed three times with 1X PBS. For competition experiments a similar protocol was

followed besides an additional one hour pre-incubated of the labeling solution with excess of either monomeric or aggregated Aβ(1-40)(rPeptide, Bogart, GA) at 37°C. Aβ fibrils were prepared by 48 hrs incubation of 0.5 mg/ml of protein in 1X PBS in a thermomixer (250 rpm at 37° C) after which the solution became visibly cloudy due to fibril formation. Radioactivity bound to the sections was counted by placing them at a low energy general all-purpose collimator of a gamma camera (Toshiba GCA 7100/ UI, Tokyo, Japan). Counts were collected for 15 minutes in a 256x256 matrix covering the complete slide using a window of 20% at 140 KeV. On each scintigram a similar region of interest (ROI) was fitted for each section to asses binding of ^{99m}Tc- pa2H. Initial 0.1 ml of the diluted labeling solution was used as a reference to calculate the % of radioactivity bound to the sections. Binding of ^{99m}Tc- pa2H in the presence of the competitor is expressed as the % of radioactivity that binds to the section without the competitor. Experiments were performed in threefold.

In vivo Aß targeting by V_HH

Fluorescent labeling with Alexa Fluor 594

V_HH were fluorescently labeled with Alexa Fluor 594 protein labeling kit (Molecular Probes, Invitrogen) according to the manufacturer's guidelines except only half of the recommended amount of dye was used. Alexa594 was chosen as it possesses favourable two photon excitation for further experiments. The protein solution was briefly spinned to remove possible aggregates before extensive dialysis to lose excess free label. The degree of labeling and the protein concentration were determined using the Spectrophotometer Nanodrop ND-1000 (Isogen Life Sciences), and typically ranged between 200 – 600 ng/µl. Protein integrity was confirmed by mass spectrometry.

Immunofluorescence using V_HH-Alexa594

To examine whether the fluorescent labeling had an effect upon antigen recognition, immunohistochemistry was performed on 5µm frozen human and 10 µm murine brain sections. Briefly, tissues were rinsed in PBS, fixated with ice-cold acetone for 10 minutes before overnight incubation with VHH-Alexa594 (415 ng/µl) in 1% BSA/PBS in a wet chamber. Sections were washed three times in PBS for 5 minutes, air dried and mounted (Aqua-Poly/mount, Polysciences Inc). Resulting slides were examined using a Leica DMR5500B fluorescent microscope with TX2 filter block, equipped with a Leica DFC350FX camera.

In vivo Aß imaging by topical application

Four APP/PS1 animals, aged 11-14 months, received permanent cranial windows to allow serial *in vivo* imaging of the brain by multiphoton microscopy according to previously reported protocols. [31,34] Mice were anesthetized with 1-2% isoflurane, positioned into a stereotaxic frame, and a circular craniotomy was performed from bregma to lambda. Careful removal of the dura gained direct access to the leptomeningeal vessels and brain parenchyma allowing subdural application bypassing the BBB. A drop of 40-60 µl of V_HH-Alexa594 (275 – 400 ng/µl) was

applied directly topical onto the exposed brain for 30 minutes. Softly rinsed with 1X PBS, the brain surface was sealed by a glass cover slip mounted onto the skull with dental cement thus creating a window to underlying brain surface. Colocalization of the V_HH-Alexa594 with Aβ depositions was based either upon their typical green autofluorescence or by intraperitoneal injections of Methoxy-X04, a fluorescent substance known to selectively bind to amyloid deposits *in vivo* [25], one day prior surgery. Animals were imaged immediately following surgery (day 0) to be re-imaged for several days thereafter to study the washout. All images were acquired with a Bio-Rad 1024 microscope (Bio-Rad, Hercules,CA) equipped with a Ti:Sapphire laser (Mai Tai; Spectra Physics, Mountain View, CA) set at 810 nm for optimal Alexa594 two photon excitation. External photodetectors (Hamamatsu Photonics, Hamamatsu City, Japan) simultaneously collected blue fluorescent signal from Methoxy-X04, green for autofluorescence, and red from Alexa594 labeled V_HH. Areas were imaged to a depth of approximately 200 µm in 5 µm steps with a 20x objective (UMPlanFl; Olympus, Tokyo, Japan) resulting in microscopic field of 615.8 x 615.6 µm. Maximum intensity projections for the entire image stack were reconstructed using ImageJ freeware.

Specific in vivo Aß binding after BBB disruption

A more systemic approach circumventing the BBB to study the *in vivo* behaviour of the V_HH throughout a larger area within the brain involved intracarotic injections of V_HH-Alexa594 with mannitol to disrupt the BBB, following a protocol previously described by Wadghiri *et al.*[42] In brief, anesthetized aged APP/PS1 mice (n=9) or wild type littermates (n=3) were canulated via the right common carotid artery. Flow through the external carotid artery was prevented by a vascular clamp. A mixture of 100µl pa2H-Alexa594 (573 ng/µl) and 600µl 1X PBS with or without 15% mannitol was administrated using an infusion pump at 60µl/min for 10 minutes (802 Syringe pump, Univentor). After full recovery, animals were euthanized at t = 2 – 24 hrs post injection (200µl Euthanasol, AST Pharma), and intracardially perfused with 4% PFA. Resected brains were cryoprotected by immersion for 4 hrs in 10% sucrose in 4% PFA changed to 30% sucrose overnight. Thirty micrometer cryosections were counterstained for amyloid using a standard Thioflavin T staining. In addition, adjacent sections were immunostained for Aβ using a standard commercial monoclonal antibody immunostaining (6F/3D, DakoCytomation), with one hour immersion in 85% formic acid and 30 minutes in trypsin (Type II-S, Sigma), rinsed with aquadest and 1X PBS in between, followed by overnight staining in 1 ml 1:10 dilution of Aβ-antibody at room temperature. Secondary antibody staining consisted of 2 hours immersion with 1:100 goat-antimouse-Alexa488 (Invitrogen). All sections were mounted with Aqua/Polymount (Aqua-Poly/mount, Polysciences Inc.).

Microscopic images were obtained using the above Leica DM5500B fluorescence microscope, equipped with a A4, L5 and TX2 filtercubes respectively for the detection of Thioflavin T, Alexa488 and Alexa594 using a 10x oil objective. Subsections were photomerged using Adobe Photoshop CS3 to obtain a complete overview of the brain sections.

RESULTS

Murine specificity of the selected V_HH

Immunostained brain sections of aged APP/PS1 and wild type littermates using V_HH ni3A and pa2H were made to assess their capacity to selectively recognize different types of deposits in this transgenic AD mouse model. (Fig. 1) Pa2H stained positive for all forms of Aβ depositions. In this transgenic mouse model, ni3A did not show selective affinity for vascular Aβ; both vascular and parenchymal Aβ depositions were clearly labeled. Compared to ni3A, equivalent staining protocols with pa2H resulted in higher specificity for Aβ combined with a low unspecific background binding. For neither V_HH specific affinity was detected within the brain sections of wildtype animals.

Biodistribution and clearance

Biodistribution and brain uptake

The distribution of a bolus injection of either radiolabeled ni3A or pa2H over time is shown in Tables 1 and 2 respectively. No significant differences in organ uptake between wildtype and transgenic animals were found, except for the brain uptake of pa2H after 24 hours. Although the amount was low (0.038 % I.D./g), cerebral uptake was 40% higher in the transgenic animals.

The cerebrum / blood ratio did not differ, indicating that this uptake difference was not caused by different VHH concentrations within the blood pool. For the cerebellum similar results were found. Using Thioflavin T staining, Aβ depositions were visible in both parts of these transgenic brains. Experiments for this particular endpoint were repeated two times, this resulted in similar findings. In most organs, the radioactivity count dropped twofold between 6 and 24 hours, whereas brain activity remained within the same range.

In general, the majority of each ^{99m}Tc-V_HH was excreted via the kidneys and urinary tract. Renal activity remained high over time, indicating continuous renal clearance of the V_HH followed by steady excretion into the urinary bladder. Cellular involvement as shown by distinctive hepatic clearance or splenal activity was low, though in comparison to ^{99m}Tc-ni3A, ^{99m}Tc-pa2H showed about 3 times higher clearance via liver and spleen. Also, the clearance rate for ^{99m}Tc-pa2H was lower, independent of genotype. However, within the first 3 hours ^{99m}Tc-ni3A resulted in a higher general organ uptake, with exception of the aforementioned liver and spleen.

Blood clearance and fraction analysis

Blood clearance consisted of a fast and a slow component. (Fig.2) A standard fitting routine resulted in the corresponding half-lives and their contribution. (Table 3) In general, the majority of the radiolabeled V_HH (78-89%) was cleared from the blood with a half-life of 10 – 20 minutes. Regarding the slow half-life, clearance of ^{99m}Tc-pa2H was much slower. However, it should be noted that the actual half-life of the slow component of ^{99m}Tc- pa2H could only be calculated with limited accuracy,

Table 1. Biodistribution of ^{99m}Tc-ni3A in mice. A bolus injection of 2 µg ^{99m}Tc-ni3A was administered intravenously into 12-14 month old APP/PS1 mice or their wild type littermates. At three time points after injection the animals were sacrificed and various tissues and entire organs were removed, weighed and counted for radioactivity. Values are expressed as a percentage of the injected dose per gram tissue (mean ± SD).

	t = 3 hr		t = 6 hr		t = 24 hr	
Tissue / organ	**Wildtypes**	**APP/PS1**	**Wildtypes**	**APP/PS1**	**Wildtypes**	**APP/PS1**
blood	1.202 ± 0.379	1.146 ± 0.131	0.778 ± 0.048	0.808 ± 0.115	0.451 ± 0.073	0.363 ± 0.051
heart	0.525 ± 0.129	0.508 ± 0.109	0.347 ± 0.049	0.337 ± 0.127	0.252 ± 0.041	0.216 ± 0.014
lungs	0.850 ± 0.184	0.819 ± 0.208	0.659 ± 0.184	0.743 ± 0.301	0.375 ± 0.113	0.291 ± 0.055
liver	1.078 ± 0.235	1.000 ± 0.293	1.078 ± 0.188	1.223 ± 0.424	0.568 ± 0.149	0.488 ± 0.164
kidneys	15.531 ± 2.986	15.192 ± 3.075	10.266 ± 1.657	14.294 ± 4.337	9.089 ± 6.152	9.901 ± 1.158
spleen	0.590 ± 0.257	0.531 ± 0.084	0.792 ± 0.144	0.753 ± 0.291	0.397 ± 0.056	0.465 ± 0.234
muscle	0.171 ± 0.075	0.120 ± 0.069	0.111 ± 0.088	0.086 ± 0.022	0.043 ± 0.007	0.048 ± 0.008
cerebrum	0.035 ± 0.009	0.035 ± 0.007	0.031 ± 0.007	0.035 ± 0.008	0.018 ± 0.003	0.019 ± 0.001
cerebellum	0.073 ± 0.031	0.063 ± 0.009	0.098 ± 0.009	0.096 ± 0.014	0.029 ± 0.005	0.026 ± 0.002
cerebrum/blood ratio	0.030 ± 0.003	0.030 ± 0.004	0.040 ± 0.010	0.043 ± 0.004	0.040 ± 0.001	0.053 ± 0.008 *
cerebrum/muscle ratio	0.242 ± 0.142	0.335 ± 0.116	0.407 ± 0.270	0.428 ± 0.171	0.422 ± 0.029	0.403 ± 0.100

* = $P<0.05$ wildtype mice compared to APP/PS1 mice.

Table 2. Biodistribution of ^{99m}Tc-pa2H in mice. A bolus injection of 2 µg ^{99m}Tc-pa2H was administered intravenously into 12-14 month old APP/PS1 mice or their wildtype littermates. At three time points after injection the animals were sacrificed and various tissues and entire organs were removed, weighed and counted for radioactivity. Values are expressed as a percentage of the injected dose per gram tissue (mean ± SD).

	t = 3 hr		t = 6 hr		t = 24 hr	
Tissue / organ	**Wildtypes**	**APP/PS1**	**Wildtypes**	**APP/PS1**	**Wildtypes**	**APP/PS1**
blood	0.566 ± 0.003	0.654 ± 0.015	1.009 ± 0.054	1.244 ± 0.123	0.575 ± 0.084	0.696 ± 0.049
heart	0.273 ± 0.121	0.240 ± 0.017	0.623 ± 0.101	0.763 ± 0.031	0.367 ± 0.059	0.393 ± 0.007
lungs	0.843 ± 0.256	0.537 ± 0.010	0.930 ± 0.242	1.088 ± 0.035	0.620 ± 0.160	0.622 ± 0.031
liver	2.615 ± 0.796	1.866 ± 0.016	3.014 ± 1.021	3.392 ± 1.932	1.430 ± 0.402	1.161 ± 0.470
kidneys	9.243 ± 1.787	6.241 ± 0.530	14.306 ± 4.105	15.612 ± 1.042	9.824 ± 2.810	8.608 ± 0.738
spleen	1.515 ± 0.503	1.319 ± 0.060	6.498 ± 1.623	0.258 ± 0.208	3.584 ± 1.381	1.747 ± 0.100
muscle	0.356 ± 0.379	0.054 ± 0.006	0.174 ± 0.022	0.347 ± 0.026	0.102 ± 0.023	0.113 ± 0.018
cerebrum	0.014 ± 0.003	0.017 ± 0.001	0.033 ± 0.005	0.044 ± 0.004	0.027 ± 0.004	0.038 ± 0.002 *
cerebellum	0.023 ± 0.001	0.026 ± 0.001	0.054 ± 0.016	0.067 ± 0.001	0.030 ± 0.007	0.045 ± 0.000 *
cerebrum/blood ratio	0.025 ± 0.005	0.026 ± 0.003	0.033 ± 0.004	0.035 ± 0.004	0.047 ± 0.003	0.055 ± 0.008
cerebrum/muscle ratio	0.083 ± 0.081	0.309 ± 0.067	0.190 ± 0.007	0.177 ± 0.135	0.270 ± 0.032	0.346 ± 0.377

* = $P<0.05$ wildtype mice compared to APP/PS1 mice.

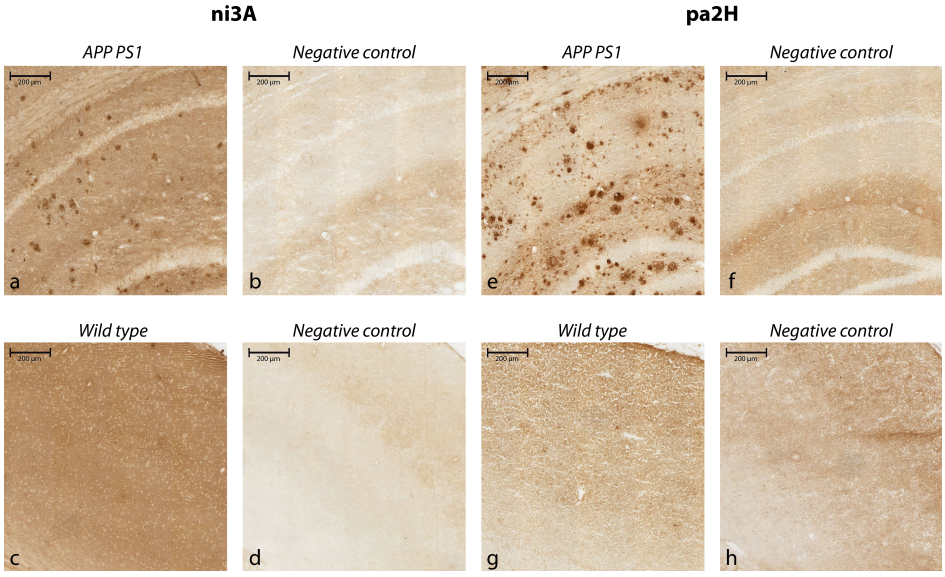

Figure 1. Immunohistochemistry of ni3A and pa2H. The upper panels (**a,b,e,f**) show 10x magnifications of the resulting staining with cryosections of aged APP/PS1 mouse brain tissue including negative controls, while the lower panels (**c,d,g,h**) show similar staining performed with wildtype littermates.

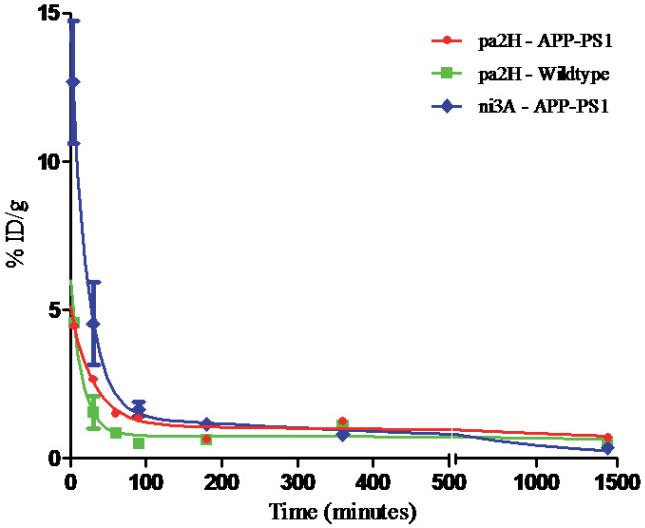

Figure 2. Graphical representation of blood half lives of ^{99m}Tc-ni3A and -pa2H in APP/PS1 mice and wildtype littermates. Data is shown as percentage of injected dose per gram of blood (%ID/g) over time. Based upon this plot the clearance is suggested to consist of a fast and a slow phase.

Table 3. Blood half lives of ^{99m}Tc-ni3A and -pa2H. Half lives were determined by fitting a two phase exponential decay model upon blood obtain from either tail vein and cardiac puncture at several time points after intravenous bolus injection of 2 µg ^{99m}Tc-VHH in 12-14 month old APP/PS1 mice and wildtype littermates.

		Fast t½				Slow t½	
VHH	**genotype**	**(min)**	**(95% C.I.)**	**%**	**(95% C.I.)**	**(min)**	**(95% C.I.)**
ni3A	APP/PS1	14,71	(8.65 - 49.13)	89,7	(72.8 - 100.0)	580	(101.8 - ∞)
	Wildtype	ND		ND		ND	
pa2H	APP/PS1	21,89	(14.24 - 39.38)	79,84	(71.1 - 85.5)	2562	(975.0 - ∞)
	Wildtype	10,78	(7.279 - 20.76)	87,11	(82.0 - 92.3)	5861	(969.3 - ∞)

Table 4. Blood distribution of ^{99m}Tc-pa2H. At different time point after bolus injection of ^{99m}Tc-pa2H blood collected from the tail vein of 12-14 month old APP/PS1 mice or wildtype littermates. Separated into the cell pellet and plasma, samples were counted for radioactivity. Fractions are expressed in percentage of total activity at that time point. No significant differences were calculated using a Student *t*-test (P<0.05).

			APP/PS1		Wildtype	
Sample	**Time p.i. (min)**	**Fraction**	**(%)**	**sd**	**(%)**	**sd**
99mTc-pa2H	10	Supernatant	88,9	6,2	80,3	5,2
		Pellet	11,1		19,7	
	90	Supernatant	83,6	8,7	72,0	8,2
		Pellet	16,4		28,0	

Table 5. Quantitative autoradiography after application of 1 µg ^{99m}Tc- V_HH-2H to human and murine APP/PS1 brain sections. *Statistical difference (P < 0.05) between either murine or human control versus Aβ bearing sections.

		Competion binding	
Brain tissue	**Binding of 99mTc-VHH ng (± sd)**	**Monomeric Aβ ng (± sd)**	**Fibrillar Aβ ng (± sd)**
APP/PS1	98.8 (± 20,7)*	60.1 (± 22.2)	31.4 (± 14.3)
Wildtype	86.4 (± 14.8)	56.4 (± 19.5)	27.1 (± 12.5)
AD human	190.1 (± 73.5)*	81.4 (± N.D.)	42.3 (± 29.2)
Control human	102.3 (± 30.2)	27.2 (± N.D.)	49.9 (± 17.4)

since the half-life was longer than the blood sampling period. In line with the above biodistribution, six hours post-injection the blood levels of ^{99m}Tc-pa2H were remarkably higher compared to earlier time points, which is characteristic for a second passage.

Within the first 90 minutes about 80% of the radiolabeled pa2H remained within the blood plasma. (Table 4) Alterations over time or between the genotypes were not significant.

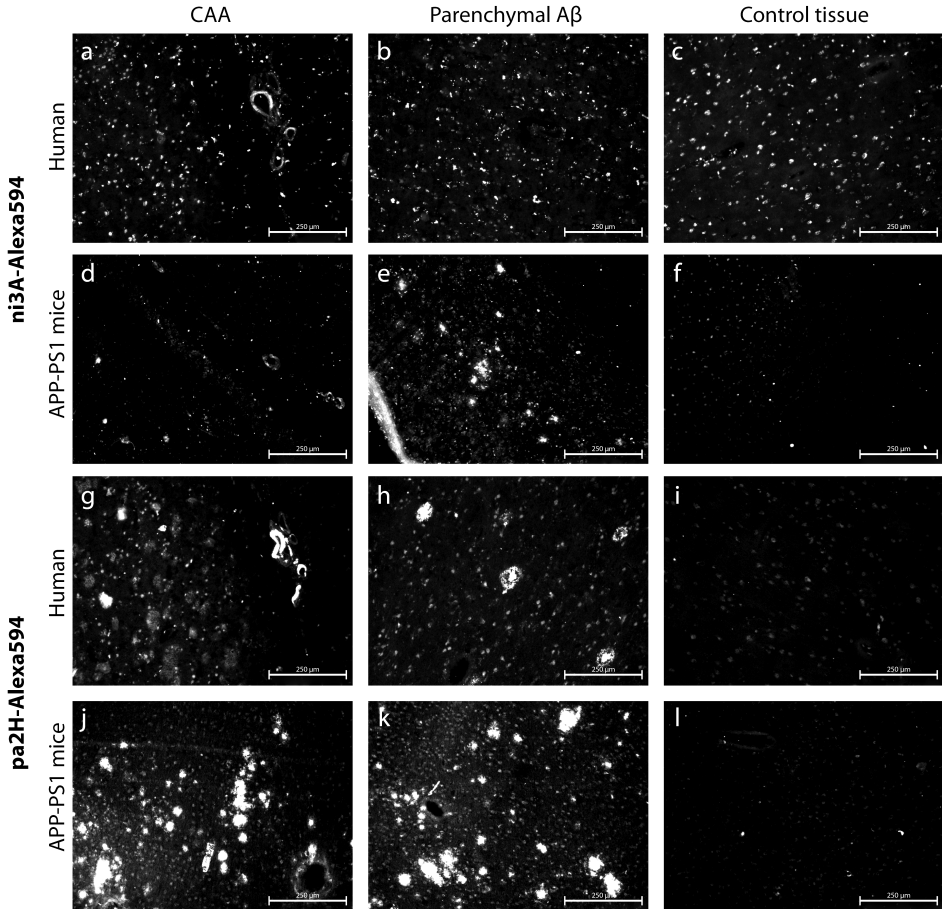

Figure 3. Topical application of ni3A- or pa2H-Alexa594 as visualized over time by intravital multiphoton microscopy in APP/PS1 mice clearly shows the specific *in vivo* labeling of different Aβ deposits. In the *left*, vascular and parenchymal Aβ deposits, detected by prior labeling with Methoxy-X04, colocalize with of ni3A-Alexa594 directly following topical application. One day later, labeling of the plaques has diminished to almost none with some residual left bound to CAA. With interpretation hampered by Methoxy-X04, *middle* images show a similar experiment. Localization of Aβ deposits are visualized based upon autofluorescence, give comparable results and almost complete wash out after two days. Pa2H-Alexa594, as shown in the right images, remains bound to vascular Aβ even two days after application, when the plaques remained undetected. All images are maximum intensity projections of a 3D cortical volume with a field of view 615 x 615 µm.

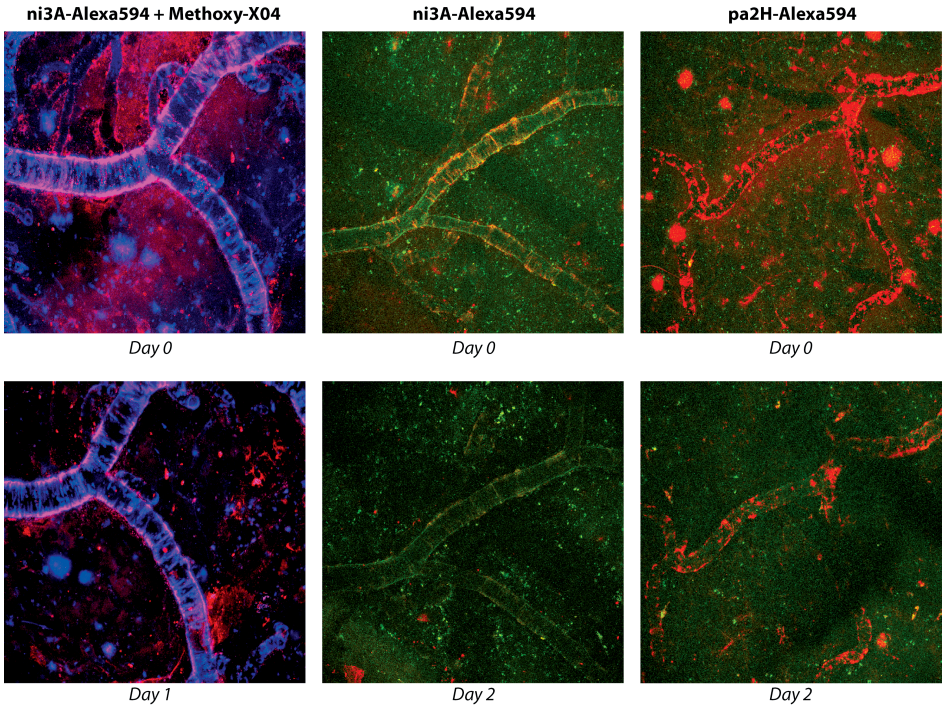

Figure 4. After **disruption of the BBB using a coinjection of 15% mannitol with pa2H-Alexa594 into the right carotid artery of an aged** APP/PS1 mouse sacrificed 2hrs post injection, amyloid plaques are clearly depicted in both hemispheres using a Thioflavin T (ThT) staining (**a**), while the pa2H-Alexa594 signal is only detected in the right hemisphere (**b**). More careful examination shows all Alexa594 signal colocalizes with ThT in the right hemisphere, while in the left only some autofluorescense can be detected. Furthermore, immunofluorescense antiAβ staining of the plaques using Alexa488 within the left hemisphere (**c**) results only in green signal, while within the right hemisphere (**d**) the red signal from pa2H-Alexa594 nicely colocalizes within the plaques. Experiments performed in a similar setting but sacrificed 24hrs post injection, showed similar results with pa2H-Alexa594 still nicely corresponding to the green labeling of the anti-Aβ staining within the right hemisphere (**e**).

Specificity of radiolabeled pa2H

In addition, after radiolabeling V_HH's specificity for Aβ was unaffected, as shown by scintigraphic analysis; binding of ^{99m}Tc-pa2H was higher in those sections including Aβ. (Table 5) Furthermore, binding was significantly ($p<0.001$) reduced when the tracer was pre-incubated with either monomeric or oligomeric Aβ.

In vivo Aß targeting by V_HH

In vivo Aß imaging by topical application

After direct application onto the exposed brain, fluorescent V_HH were followed up for at least 48 hours by *in vivo* multiphoton microscopy. (Fig. 3) Specific *in vivo* labeling of CAA and Aβ plaque by ni3A-Alexa594 was initially confirmed by colocalization

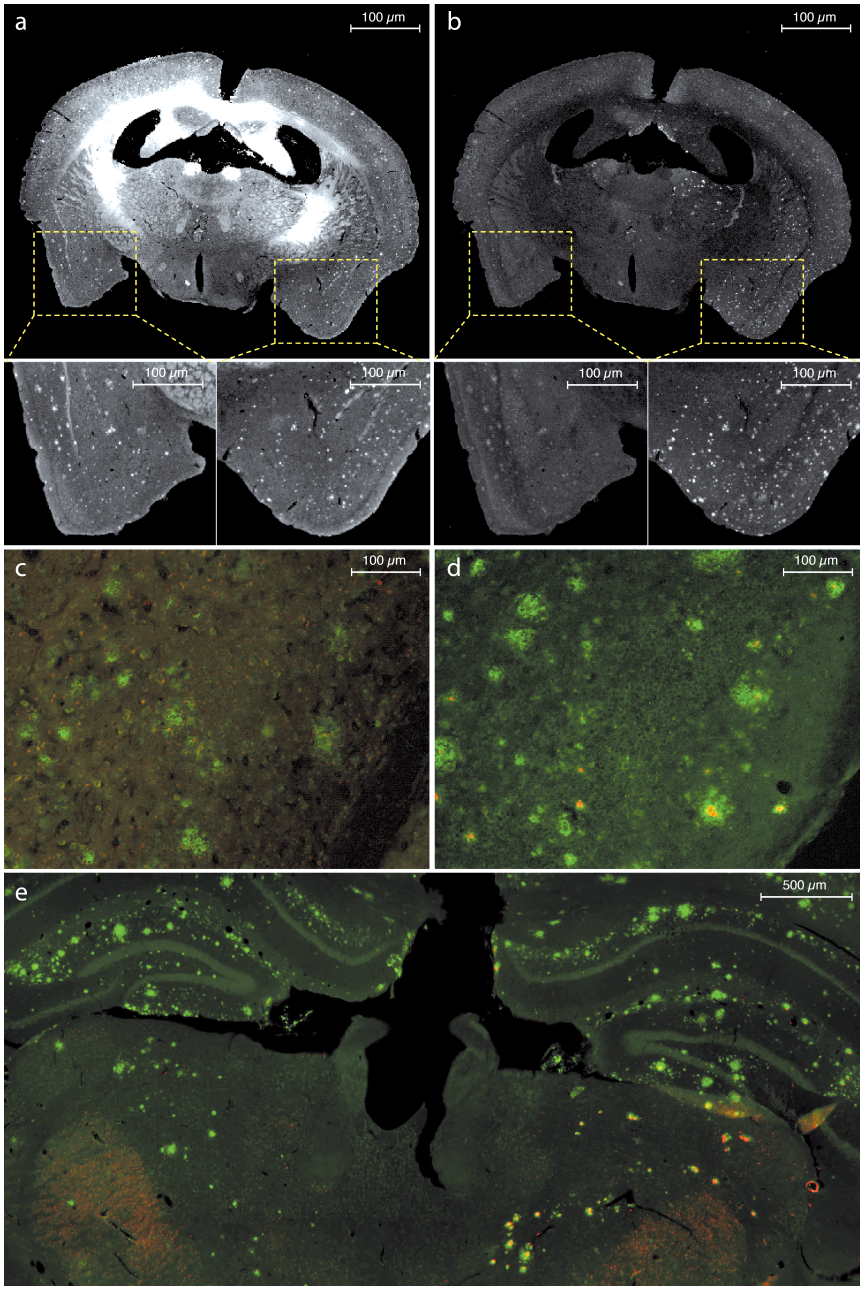

Figure 5. Immunofluorescence of ni3A- and pa2H-Alexa594 on cryosections of APP/PS1 murine and human AD/CAA brain tissue, including wildtype or healthy controls. Both V_HH stain positive for CAA in all sections (**a**,**d**,**g**,**j**). Only ni3A-Alexa594 is negative for human parenchymal Aβ (**b**), while pa2H is positive for several types of parenchymal Aβ deposits (**h**,**i**,**k**,**l**) in both humans and mice. in either human of murine control tissue no such staining patterns were observed.

with Methoxy-X04, a known *in vivo* amyloid targeting fluorophore. (Fig. 3 *left*) Beside possible binding competition with the V_HH, Methoxy-X04 hampered good validation due to signal cross-over into the red channel. However, colocalization based on the typical autofluorescence patterns of the different Aβ depositions resulted in similar findings. (Fig. 3 *middle*) Selectivity was confirmed by lack of unspecific background signal. Although both labeled V_HH were capable of targeting Aβ *in vivo*, only pa2H-Alexa594 was detectable after two days, mainly bound to vascular amyloid.

Specific in vivo Aß binding after BBB disruption

Based on the above findings, co-injections with mannitol to study the *in vivo* characteristics throughout the brain were only conducted with pa2H-Alexa594. Mannitol is known to selectively open the BBB in the ipsilateral side after intracarotid injection. Two hours after right i.c. injection, fluorescence was detected in the right hemisphere, and colocalized with Aβ. (Fig.4a-d) Even within the deeper brain structures, no unspecific binding could be observed. Aβ related fluorescent signal remained detectable for at least 24 hours post-injection. Without BBB disruption no apparent Aβ labeling could be detected. In wild type animals, no fluorescence was observed with or without BBB disruption.

Immunofluorescence using V_HH-Alexa594

Selectivity for specific Aβ deposits was not altered after fluorescent labeling of the V_HH, since immunostaining showed that on human sections, ni3A-Alexa594 selectively stained vascular Aβ. (Fig. 5a-f) Presence of parenchymal and vascular Aβ was confirmed by pa2H- Alexa594. (Fig. 5g-l) Similar to the above immunostaining, in the murine material all Aβ depositions were stained by both fluorescent V_HH.

DISCUSSION

In this study, we assessed our previously selected V_HH for their potential to distinctively detect the different Aβ depositions *in vivo*. Both V_HH stained positive for Aβ upon APP/PS1 brain sections confirming appropriate use of this transgenic model. However, previously shown selectivity for solely vascular Aβ in human post-mortem brain sections by ni3A was not observed within this mouse model. Fluorescent or radiolabeling prior *in vivo* use did not affect their specificity. Bolus injections of radiolabeled V_HH revealed rapid renal clearance, and resulted in a small but significantly higher brain uptake of ^{99m}Tc- pa2H in APP/PS1 animals one day post injection. Specific *in vivo* binding to parenchymal and vascular Aβ was confirmed when the BBB was circumvented. Signal remained detectable for at least 24 hours while *in vivo* pa2H showed a high affinity combined with a low off-rate. All together, these data provide initial evidence that V_HH have the ability to target different Aβ depositions *in vivo*, and make them promising diagnostic tools for the distinctive detection of Aβ related neurodegenerative diseases, like CAA and AD.

The unique specific reactivity of ni3A for vascular amyloid deposition upon human brain material is not yet completely understood.[32] However, this selectivity was no longer present within transgenic APP/PS1 mice.(Fig. 1,3,5) Although plaque formation within transgenic models mimic many aspects of the human disease, differences in morphology and composition might help to understand ni3A's specific reactivity.[10,14] In humans, plaques consist of discontinuous patches with decreased density and random fibrillar orientation within the amyloid core; murine plaques are generally built up by long organized fibrils, resulting in densely packed amyloid plaques with a relatively large core. [39] The diffuse plaques contain a mixture of human and mouse Aβ, while the dense plaques consist of a human core surrounded by mouse Aβ.[39] Besides morphological differences, posttranslational modifications of Aβ differ from mouse to man leading to alterations of the Aβ molecule itself. [5,10,30] Furthermore, a difference in metal ion content has been found, which is known to influence the tertiary structure.[2,28]

Previous epitope mapping revealed that ni3A has no other cross reaction but to Aβ(1-42)[32], which is highly abundant in parenchymal and vascular deposits in both humans and APP/PS1 mice. Therefore, the presented data and the cited literature lead to the conclusion that the selectivity reactivity of ni3A must depend on the structural presentation of Aβ(1-42), in which case murine parenchymal plaques probably show structural similarities to human CAA.

The presented results show that a small bolus injection of ^{99m}Tc-pa2H led to a significant difference in brain uptake in APP/PS1 animals after one day. For both V_HH, higher brain levels were already detected 3 hours post injection in both genotypes, suggesting initial unspecific brain uptake. The relatively low brain uptake may be partially due to the rapid renal clearance. Even though beneficial for imaging purposes, a short blood residential time effectively reduces the blood-to-brain transfer.

Specific brain uptake is the resultant of the V_HH – BBB transfer kinetics, its affinity for Aβ, and the washout of unbound label from the brain. We therefore postulate that the favorable *in vivo* characteristics of pa2H, like high affinity and washout, resulted in a significant difference detected after 24 hours due the presence of Aβ. In contrast, the level of ni3A in the brain dropped significantly after one day in both genotypes, probably due to its lower affinity for Aβ. As this study investigated organ uptake only at three time points, it remains to be investigated whether maximal specific cerebral uptake might be observed at a different time point. The current brain uptake levels were insufficient to assess the uptake kinetics *in vivo* with SPECT imaging (data not shown).

Previous *in vitro* data suggested that our V_HH actively migrated across the BBB in a more efficient way than FC5, an reported VHH specifically selected to pass the BBB.[32] However, *in vivo* studies with FC5 listed up to 4 %ID/g brain uptake, which is much higher than our findings. [29] This discrepancy may be due to the lower dose that we used, but several other factors may also play a part. For FC5 it is known it uses receptor-mediated endocytosis via the α(2,3)-sialoglycoprotein [1]. For our V_HH, we know that *in vitro* active transport mechanisms were involved, but the specific receptors are up to now unknown. As a result, besides the fast half-life, the *in vivo* BBB passage may be limited by the availability of these receptors.

In line with previous reports [12,18], the renal retention was relatively high for both compounds (~9 % ID/g) after 24 hours. Such non-specific renal accumulation is typically seen for peptides and proteins smaller than the filtering threshold of the glomerular membrane (<60kDa). [3] For future imaging prospects this is not necessarily problematic as the main area of interest, the brain, is not in close proximity of the kidneys. However, to increase BBB transmigration in order to reach significant brain uptake for imaging, a possible future solution would be to increase the blood circulation time; the simplest approach would be to increase the injection dose either directly or by slow infusion. Such protocols, however, need to balance the protein load with the renal accumulation and possible toxicity , e.g. by coinjection of gelofusion and lysine.[37]

Currently used contrast agents, like ^{11}C-PiB, are based upon histological stains like Congo Red or Thioflavin, and allow the detection of amyloid rather than Aβ, while they bind specifically to the β-pleated sheet structures within Aβ plaques. In contrast, selectivity of our V_HH depends on the specific epitope presentation of the different forms of Aβ. Thus, we already showed that these V_HH are more specific to a certain type of Ab accumulation. Further selection may allow the *in vivo* detection of the full range of Aβ from oligomers to dense core to CAA. However, similar to the low affinity of ^{11}C-PiB seen with transgenic mice [26], differences between men and mice requires careful interpretation when testing them in AD/CAA mouse models, as shown again in our study.

Besides possible diagnostics, several V_HH have shown their therapeutic value. Preliminary research indicated that similar V_HH were able to prevent protein aggregation of amyloid fibrils, oligomeric forms of Aβ and polyA-binding protein nuclear 1. [6,8,27,41] In the latter even complete clearance of existing aggregates has been observed. Whether V_HHs used in this study possess similar abilities is currently under investigation. However, within the data presented here, we observed that several Aβ plaques as detected by their autofluorescence, could no longer be seen two days after V_HH application. (Fig.4) Whereas current passive immunotherapies targeting Aβ are hampered by unwanted immunogenic side effects, repetitive administration of V_HH has shown to be non-immunogenic. [21,36] Furthermore, their selective binding to different Aβ species, like ni3A's specific binding for CAA, could shift Aβ brain efflux in the favored direction, which could be used to tailor anti-Aβ therapy to further reduce therapy-induced complications, e.g. CAA related microbleeds.[13,21,26]

In conclusion, these initial *in vivo* studies to investigate whether Aβ specific V_HH can be exploited as diagnostic tools show promising results for further development. Here we showed that V_HH are capable of strong specific binding *in vivo*, though issues regarding higher brain uptake and rapid clearance need to be addressed in the future. Possible optimization strategies would include creating multimers, which simultaneously increases affinity and possibly also BBB transmigration. Multimers could also consist of our Aβ-targeting V_HH linked with other V_HH that possess different useful properties, like FC5 to increase BBB transport, or an albumin-recognizing V_HH to increase serum half-life. [7,38]

ACKNOWLEDGEMENTS

This research was supported by the Center for Translational Molecular Medicine (LeARN), IOP Genomics (IGE05005), the Center for Medical Systems Biology (CMSB2), and NWO Athena (700.58.801).

REFERENCE LIST

1. A. Abulrob*, et al.*, "The blood-brain barrier transmigrating single domain antibody: mechanisms of transport and antigenic epitopes in human brain endothelial cells," J. Neurochem. **95**(4), 1201 (2005).
2. P. A. Adlard and A. I. Bush, "Metals and Alzheimer's disease," J. Alzheimers. Dis. **10**(2-3), 145 (2006).
3. T. M. Behr, D. M. Goldenberg, and W. Becker, "Reducing the renal uptake of radiolabeled antibody fragments and peptides for diagnosis and therapy: present status, future prospects and limitations," Eur. J. Nucl. Med. **25**(2), 201 (1998).
4. K. Blennow, M. J. de Leon, and H. Zetterberg, "Alzheimer's disease," Lancet **368**(9533), 387 (2006).
5. T. Bussiere*, et al.*, "Morphological characterization of Thioflavin-S-positive amyloid plaques in transgenic Alzheimer mice and effect of passive Abeta immunotherapy on their clearance," Am. J. Pathol. **165**(3), 987 (2004).
6. A. Chartier*, et al.*, "Prevention of oculopharyngeal muscular dystrophy by muscular expression of Llama single-chain intrabodies in vivo," Hum. Mol. Genet. **18**(10), 1849 (2009).
7. K. Coppieters*, et al.*, "Formatted anti-tumor necrosis factor alpha VHH proteins derived from camelids show superior potency and targeting to inflamed joints in a murine model of collagen-induced arthritis," Arthritis Rheum. **54**(6), 1856 (2006).
8. M. Dumoulin*, et al.*, "A camelid antibody fragment inhibits the formation of amyloid fibrils by human lysozyme," Nature **424**(6950), 783 (2003).
9. C. Duyckaerts, B. Delatour, and M. C. Potier, "Classification and basic pathology of Alzheimer disease,"
10. C. Duyckaerts, M. C. Potier, and B. Delatour, "Alzheimer disease models and human neuropathology: similarities and differences," Acta Neuropathol. **115**(1), 5 (2008).
11. G. B. Frisoni*, et al.*, "The clinical use of structural MRI in Alzheimer disease," Nat. Rev. Neurol. **6**(2), 67 (2010).
12. L. O. Gainkam*, et al.*, "Comparison of the biodistribution and tumor targeting of two 99mTc-labeled anti-EGFR nanobodies in mice, using pinhole SPECT/micro-CT," J. Nucl. Med. **49**(5), 788 (2008).
13. S. M. Greenberg, B. J. Bacskai, and B. T. Hyman, "Alzheimer disease's double-edged vaccine," Nat. Med. **9**(4), 389 (2003).
14. A. Guntert, H. Dobeli, and B. Bohrmann, "High sensitivity analysis of amyloid-beta peptide composition in amyloid deposits from human and PS2APP mouse brain," Neuroscience **143**(2), 461 (2006).
15. C. Hamers-Casterman*, et al.*, "Naturally occurring antibodies devoid of light chains," Nature **363**(6428), 446 (1993).
16. J. Hardy and D. J. Selkoe, "The amyloid hypothesis of Alzheimer's disease: progress and problems on the road to therapeutics," Science **297**(5580), 353 (2002).
17. M. M. Harmsen and H. J. De Haard, "Properties, production, and applications of camelid single-domain antibody fragments," Appl. Microbiol. Biotechnol. **77**(1), 13 (2007).
18. L. Huang, S. Muyldermans, and D. Saerens, "Nanobodies(R): proficient tools in diagnostics," Expert. Rev. Mol. Diagn. **10**(6), 777 (2010).
19. C. R. Jack, Jr.*, et al.*, "Hypothetical model of dynamic biomarkers of the

Alzheimer's pathological cascade," Lancet Neurol. **9**(1), 119 (2010).

20. J. L. Jankowsky, *et al.*, "Co-expression of multiple transgenes in mouse CNS: a comparison of strategies," Biomol. Eng **17**(6), 157 (2001).
21. G. A. Jicha, "Is passive immunization for Alzheimer's disease 'alive and well' or 'dead and buried'?," Expert. Opin. Biol. Ther. **9**(4), 481 (2009).
22. K. A. Johnson, *et al.*, "Imaging of amyloid burden and distribution in cerebral amyloid angiopathy," Ann. Neurol. **62**(3), 229 (2007).
23. A. Kadir and A. Nordberg, "Target-specific PET probes for neurodegenerative disorders related to dementia," J. Nucl. Med. **51**(9), 1418 (2010).
24. B. Kazemier, *et al.*, "Determination of active single chain antibody concentrations in crude periplasmic fractions," J. Immunol. Methods **194**(2), 201 (1996).
25. W. E. Klunk, *et al.*, "Imaging Abeta plaques in living transgenic mice with multiphoton microscopy and methoxy-X04, a systemically administered Congo red derivative," J. Neuropathol. Exp. Neurol. **61**(9), 797 (2002).
26. W. E. Klunk, *et al.*, "Binding of the positron emission tomography tracer Pittsburgh compound-B reflects the amount of amyloid-beta in Alzheimer's disease brain but not in transgenic mouse brain," J. Neurosci. **25**(46), 10598 (2005).
27. P. Lafaye, *et al.*, "Single-domain antibodies recognize selectively small oligomeric forms of amyloid beta, prevent Abeta-induced neurotoxicity and inhibit fibril formation," Mol. Immunol. **46**(4), 695 (2009).
28. A. C. Leskovjan, A. Lanzirotti, and L. M. Miller, "Amyloid plaques in PSAPP mice bind less metal than plaques in human Alzheimer's disease," Neuroimage. **47**(4), 1215 (2009).
29. A. Muruganandam, *et al.*, "Selection of phage-displayed llama single-domain antibodies that transmigrate across human blood-brain barrier endothelium," FASEB J. **16**(2), 240 (2002).
30. J. A. Richardson and D. K. Burns, "Mouse models of Alzheimer's disease: a quest for plaques
31. E. M. Robbins, *et al.*, "Kinetics of cerebral amyloid angiopathy progression in a transgenic mouse model of Alzheimer disease," J. Neurosci. **26**(2), 365 (2006).
32. K. S. Rutgers, *et al.*, "Transmigration of beta amyloid specific heavy chain antibody fragments across the in-vitro blood brain barrier," Unknown (2010).
33. K. S. Rutgers, *et al.*, "Differential recognition of vascular and parenchymal beta amyloid deposition," Neurobiol. Aging (2009).
34. J. Skoch, *et al.*, "Development of an optical approach for noninvasive imaging of Alzheimer's disease pathology," J. Biomed. Opt. **10**(1), 11007 (2005).
35. E. E. Smith and S. M. Greenberg, "Beta-amyloid, blood vessels, and brain function," Stroke **40**(7), 2601 (2009).
36. B. Stijlemans, *et al.*, "Efficient targeting of conserved cryptic epitopes of infectious agents by single domain antibodies. African trypanosomes as paradigm," J. Biol. Chem. **279**(2), 1256 (2004).
37. L. O. Tchouate Gainkam, *et al.*, "Localization, mechanism and reduction of renal retention of technetium-99m labeled epidermal growth factor receptor-specific nanobody in mice," Contrast Media & Molecular Imaging (2010).
38. B. M. Tijink, *et al.*, "Improved tumor targeting of anti-epidermal growth factor receptor Nanobodies through albumin binding: taking advantage of modular Nanobody technology," Mol. Cancer Ther. **7**(8), 2288 (2008).
39. T. van Groen, A. J. Kiliaan, and I. Kadish, "Deposition of mouse amyloid beta in human APP/PS1 double and single AD model transgenic mice," Neurobiol. Dis. **23**(3), 653 (2006).
40. S. van Koningsbruggen, *et al.*, "Llama-derived phage display antibodies in the dissection of the human disease oculopharyngeal muscular dystrophy," J. Immunol. Methods **279**(1-2), 149 (2003).
41. P. Verheesen, *et al.*, "Prevention of oculopharyngeal muscular dystrophy-associated aggregation of nuclear polyA-binding protein with a single-domain intracellular antibody," Hum. Mol. Genet. **15**(1), 105 (2006).

42. Y. Z. Wadghiri, *et al.*, "Magnetic resonance imaging of amyloid plaques in transgenic mice," Methods Mol. Biol. **299**, 365 (2005).

43. D. M. Walsh and D. J. Selkoe, "A beta oligomers - a decade of discovery," J. Neurochem. **101**(5), 1172 (2007).

44. R. O. Weller, *et al.*, "Cerebral amyloid angiopathy in the aetiology and immunotherapy of Alzheimer disease," Alzheimers. Res. Ther. **1**(2), 6 (2009).

45. M. M. Welling, *et al.*, "Kit with technetium-99m labelled antimicrobial peptide UBI 29-41 for specific infection detection," Journal of Labelled Compounds & Radiopharmaceuticals **48**(9), 683 (2005).

46. M. M. Welling, *et al.*, "Technetium-99m labelled antimicrobial peptides discriminate between bacterial infections and sterile inflammations," Eur. J. Nucl. Med. **27**(3), 292 (2000).

47. S. X. Zhang-Nunes, *et al.*, "The cerebral beta-amyloid angiopathies: hereditary and sporadic," Brain Pathol. **16**(1), 30 (2006).

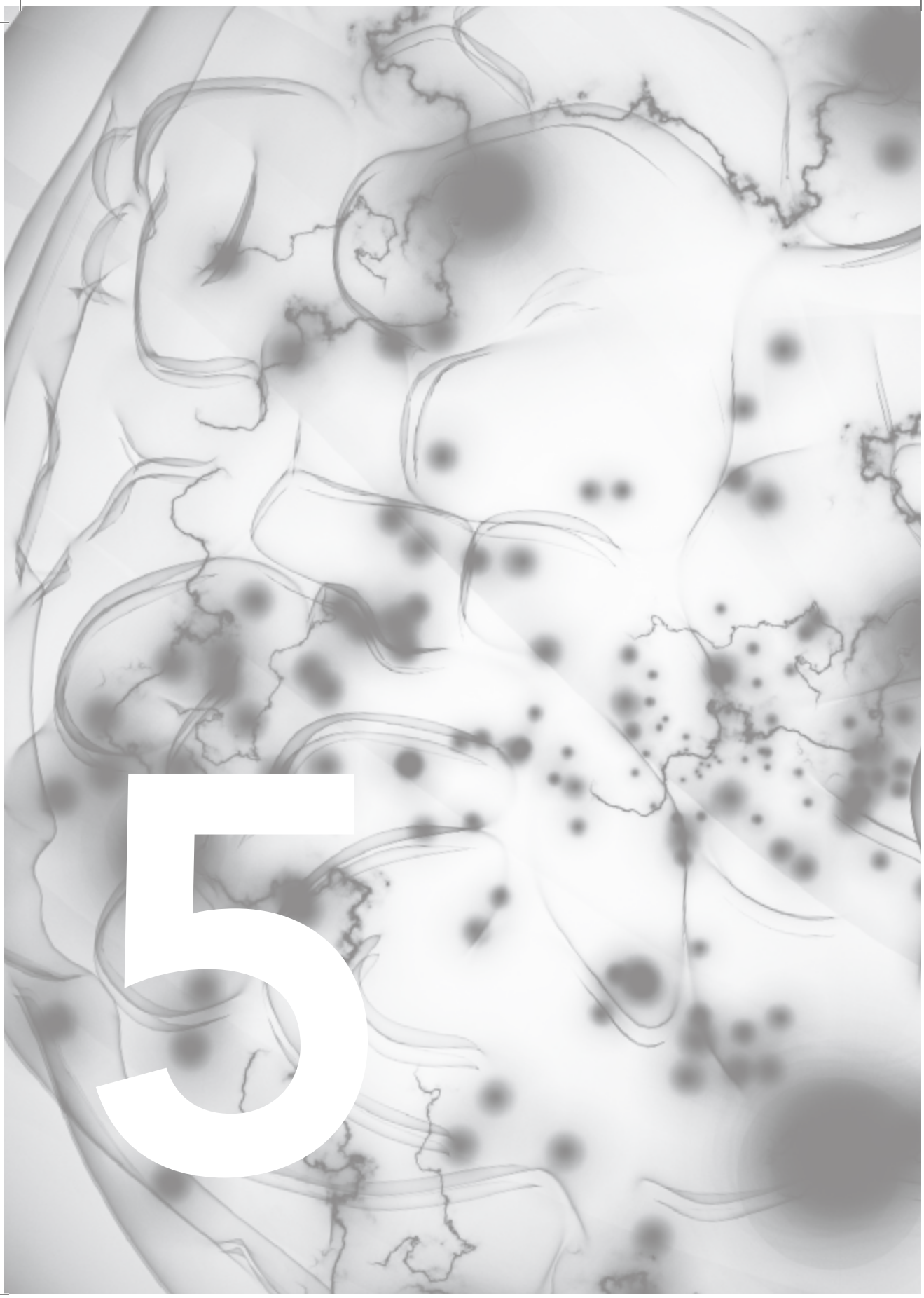
5

CHAPTER 5 | GENERAL DISCUSSION

INVOLVEMENT OF ASS IN NEURODEGENERATIVE DISORDERS LIKE AD, SPORADIC AND HEREDITARY CAA (HCHWA-D)

Alzheimer disease (AD) is the most common cause of dementia and therefore one of the major health problems in the world. The disease is histologically characterized by the accumulation of aggregated proteins in the brain, progressive neuronal loss, inflammation, and leading to the progressive and irreversible decline of memory and cognition. The major component of the protein aggregates is beta amyloid (Aβ). Studies on this protein led to the postulation of the amyloid cascade hypothesis, which proposes that amyloid fibrils and plaques in the brain are drivers of the neurodegeneration [1]. Although in a decade of research the hypothesis changed from the focus on Aβ fibrils to small soluble aggregates of Aβ, the central focus is still on Aβ. The deposition of Aβ is also the primary neuropathologic feature of cerebral amyloid angiopathy (CAA). Different from AD, in CAA the Aβ deposits are located primarily in the cerebral vessel walls [1,2]. A hereditary form of CAA is Hereditary Cerebral Hemorrhage with Amyloidosis-Dutch type (HCHWA-D) [3]. AD and CAA are two distinct diseases with cerebral Aβ accumulation as primary neuropathalogic feature [1,2]. The availability of diagnostic probes for early differential detection of cerebral Aß in living patients would contribute significantly to the early diagnosis and treatment of this group of disorders. These probes ideally have to be small, easy and cost effective to produce, straightforward to modify and have little off target effects with little immunogenicity.

VHH with the ability to differential recognize vascular Aß

In chapter two the generation of antibody fragments (VHH), derived from heavy chain Camelidea IGgs, directed against Aß is described. These immunologic reagents were selected with the ultimate goal to develop tools for the early non-invasive differential in vivo imaging of AD and CAA. The initial selected VHH were derived from a non-immune library (niVHH). This selection yielded niVHH that selectively recognize vascular Aβ of AD and CAA patients, sporadic and hereditary. In order to obtain affinity binders with a higher affinity, directed against vascular Aβ, VHH (vaVHH) were additionally selected from a vascular HCHWA-D immune library. The vaVHH obtained from this library recognized selectively vascular Aβ as well. The difference between the two pools of antibodies is the strong preference of the immune library-derived vaVHH for vascular HCHWA-D. The commonality is their recognition of vascular Aβ. This vascular Aβ specificity could be due to high affinity of the VHH for Aβ40, because this is the major component of vascular Aβ in this group of diseases [4]. The different VHH were therefore tested for affinity preference for different Aβ peptides by phage-ELISA (figure 1 chapter 2). Unexpectedly, most VHH showed higher affinity for Aβ1-42 rather than Aβ 1-40. Therefore, the cause of the preferential recognition of vascular Aβ, which consists largely of Aβ 1-40, could not be selective

affinity for Aβ 1-40. Consequently, the reason for the affinity preference for Aβ in the vessels of HCHWA-D patients could be caused by differences in epitope availability in both vessels and parenchyma and in the different diseases. In addition, from these results became clear that the VHH are not selectively recognizing mutant E22Q Aβ, present in HCHWA-D patients which tissue was used for immunization. Therefore, other explanations for their affinity preferences need to be explored. Amongst others the differences in etiology between the different Aβ depositions, parenchymal plaques and vascular plaques and in the different diseases could be key to the observed differences in affinity of the VHH.

Sequence specificity of vascular Aß recognizing VHH

Since Aβ is folded in an even β-pleated configuration, which is common for a wide variety of proteins, it is important to test whether the VHH are Amyloid structure specific and therefore not Aβ protein sequence specific. VHH were tested on tissue sections of HCHWA-I patients, in which the Amyloid in the vessels is formed by the cystatin-C. There was no recognition of the cystatin-C protein. Therefore, we conclude that the selected VHH, from the naive and vascular library, are sequence specific and specific for a vascular Aβ epitope, present in AD, hereditary (HCHWA-D) and sporadic (Boston patients) CAA.

VHH with additional affinity for Aß located in parenchymal plaques

For the third selection strategy we immunized llama's with brain parenchyma of a patient with extensive AD pathology with the objective to obtain VHH with high affinity preference for Aβ present in parenchymal plaques (paVHH). Surprisingly, the selected VHH showed high affinity for both parenchymal and vascular Aβ. In accordance with the former selections the paVHH derived from the AD grey matter library showed highest affinity for Aβ depositions present in the grey matter of AD patients as judged by the immunohistochemistry results. The reason for this differential recognition could possibly lie in the composition of the parenchymal plaques in HCHWA-D patients. The parenchymal plaques of HCHWA-D patients consist for 50 percent of the mutant form of Aβ and for 50 percent of the wildtype Aβ [5]. Because the VHH were selected against the wildtype Aβ there could be a affinity preference for the wildtype Aβ, although further research is necessary to confirm this. In addition, the parenchymal plaques of HCHWA-D patients have a higher constituent of Aβ 40 and the parenchymal VHH show affinity preference for Aβ 42 [6].

Implementation of Aß specific VHH and future research

Research to understand the pathogenesis of neurodegenerative disorders and for the development of effective therapeutic agents has focused primarily on neurons. Numerous efforts have been undertaken to develop inhibitors of the production or aggregation of Aβ. For example efforts to inhibit β-secretase also called β-site APP-cleaving enzyme (BACE). BACE is responsible for the first step of APP cleaving

though the amyloidogenic pathway that generates, after cleavage by γ-secretase, Aß 1-37/42. Consequently, by the inhibition of BACE the production of Aß decreases.

The role of the blood brain barrier (BBB) in neurodegenerative diseases has gained less attention in these studies. Aβ species have to be removed from the central nervous (CNS) continuously to prevent neurotoxic accumulations in the brain. The maintenance of critical threshold levels of Aβ is important for preventing pathogenic cascades mediating neurovascular and neuronal stress. These events are indicated to be the start of the development of cerebral and neurovascular β-amyloidosis and dementia in AD and CAA patients. The BBB maintains the homeostasis of the brain and preserves therewith the neuronal integrity. Therefore the BBB does not allow free passing of polar substances like Aβ across its interface. Specialized receptors at the BBB shuttle Aβ across the BBB. The low-density lipoprotein receptor related protein 1 (LRP) and the receptor for advanced end glycation products (RAGE) have the ability to rapidly transport Aβ from and to the brain and are respectively down and up regulated in AD and APP transgenic mouse models of AD [7-9]. Consequently, as AD and related diseases might be caused by an imbalance between Aβ production and clearance, LRP and RAGE are interesting targets for therapy.

As described above the primary transporter of Aβ from the brain, across the BBB, into systemic circulation is thought to be LRP [7]. In order to increase transport of Aβ from the brain into the circulation a VHH directed against LRP, with the goal to up regulate this receptor, may help in Aβ clearing from the brain. However, Aβ is present in the brain of symptom free people, where it likely performs an important physiological function and only small oligomers are indicated to be the neurotoxic. Therefore, a specific targeting of those small toxic oligomers would be preferable. Bi-functional bihead VHH could be developed against on one side Aβ toxic oligomers and on the other side the receptor binding VHH. The development of this bi-head could be an approach resulting in specific clearance of the toxic Aβ oligomers. Known functional bi-heads with distinct specificity are VHH directed against anti-tumor necrosis factor alpha and serum albumin, this bihead targets respectively inflamed joints of patients with induced arthritis and increases the serum half life of the agent [10].

Nevertheless, it is technically difficult to obtain VHH that selectively recognize Aβ oligomers. However it is not impossible, and it could be manageable by selecting on oligomers subtracted from the human AD brain. After preparation of the brain homogenates, the oligomers can be revealed by consecutive IP and western blotting (WB) as previously described [11]. The WB can be used for the oligomeric specific selection. As this is the closest by an *in vivo* situation, which is important as Aβ seems to behave dissimilar in every different experimental approach. The disadvantage of this approach is the difficulty of crossing the BBB.

As described above the primary transporter of Aβ from the systemic circulation, across the BBB, to the brain is thought to be RAGE [7]. Based on this transport hypothesis the development of VHH which inhibit the RAGE- Aβ interaction at the BBB, could reduce Aβ transport into the brain and consequently reduction of neuroinflammation and neuronal impairment [12]. The advantage of this approach is that difficult BBB

crossing is circumvented. A known functional VHH directly influencing receptor activity is directed against the CD16 FC-receptor on natural killer (NK) cells. These VHH were able to bind to the receptor and induce activity of the NK cells and are considered good candidates, in a bi-specific format, to recruit NK cells to the tumor and destroy the malignant cells [13].

Delivery of diagnostic and/or therapeutic agents behind the selective interface entitled the BBB

An important step in the development of imaging/diagnostic tools for neurodegenerative disorders like AD and CAA is the delivery of those moieties over the BBB. The selective interface located between the blood and the brain is accomplished by unique features, such as tight junctions, low vesicular transport and high metabolic activity [14]. Only molecules with a molecular weight lower than ~400 Da are able to pass the BBB [15]. Consequently, it is difficult to transmigrate high molecular weight drugs or imaging agents, such as recombinant proteins, over the BBB. However, these agents could be delivered behind the BBB through transcytosis [16]. This is a form of vesicular transport that starts with endocytosis at the luminal surface of the cerebral endothelial cells (CEC), through the endothelial cytoplasm, and exocytosis at the abluminal side of the CEC.

Studies have shown that there are different endocytic pathways in CEC: macropinocytosis, a random pathway of internalization of large proteins in large droplets underneath extensions (ruffles) of the cell surface. Adsorptive-mediated endocytosis (AME), in which uptake is driven by non-specific charge-based interactions. And receptor mediated endocytosis (RME), which is initiated through specific interaction with receptors [16,17] It has been shown that VHH are able to cross the blood brain barrier in vitro. VHH FC5 recognizes α(2,3)-sialoglycoprotein and undergoes RME via clathrin-coated vesicles [18]. In addition, VHH have several favorable characteristics when used for the development of therapeutic or diagnostic agents which have to be transcytosed behind the BBB. VHH have small a size of ~ 15kDa, they lack the Fc domain and as a consequence the expected interaction with tissues expressing Fc receptors (e.g. spleen, liver) is low and expected to result in low immunogenicity. Furthermore, they are remarkable stable against high temperature, pH, salts and show high expression levels in micro organisms like *E. coli* which are favorable production characteristics [19]. Therefore, VHH have the propensity to serve as tools for non invasive *in vivo* imaging and drug targeting tools in patients neurological and neurodegenerative diseases like AD or CAA. If VHH selected against Aβ could cross the BBB, they could serve as promising tools for AD and CAA diagnosis and/ or therapy.

Propensity of Aβ specific VHH to pass the BBB

In chapter three the VHH selected against Aβ are assessed for their ability to cross the BBB in vitro. The system we used consists of co-cultures of fully differentiated

primary cultures of Bovine Cerebral Endothelial Cells (BCEC) and astrocytes, since in those cells BBB properties are better maintained. In addition, tumor cell lines and immortalized cells are sub-optimal for the use in a BBB model since they mimic a BBB with disease-like properties. Astrocytes induce and preserve BBB properties in endothelial cells and are therefore essential for the in vitro BBB model.

Unexpectedly Ni3A showed the highest crossing efficiency compared to all other VHH at 37°C, even when compared to FC5 which was specifically selected for the purpose to transmigrate over the BBB. Interestingly, there was a significant difference in crossing efficiency between ni3A and ni8B, although those VHH differ only three amino acids in the N-terminal Framework 1. These results instigated studies addressing the influence of these three amino acids on BBB passage. For this purpose VHH 3A2E was constructed. 3A2E consists of Framework 1 of ni3A, containing the three anomalous amino acids and the C-terminus (Complementary Determining Region 1-Framework 4) of va2E, an Aβ recognizing VHH with no crossing ability. 3A2E displayed significantly enhanced crossing abilities compared to va2E, intermediate between ni3A and va2E. Consequently, we conclude that the unique amino acids in ni3A have a positive influence on the crossing ability. However, the crossing was not as efficient as that of ni3A. Therefore, the three amino acids are not the sole contributors of the high crossing ability of ni3A and other specific sequences of ni3A are of influence as well.

The reason for the effect of the three amino acids remains to be elucidated. From numerous studies on enhancement of drug transport it is known that hydrophobic and positively charged molecules can increase the BBB permeability and transport into the brain [20]. The grand average of hydropathicity index (GRAVY), indicates the solubility of the proteins: with a positive GRAVY a protein can be characterized as hydrophobic and with a negative GRAVY a protein is hydrophilic [21]. Ni3A and ni8B have respectively a GRAVY -0.545 and -0.455. From these results we can conclude that ni3A has even a lower hydrophobicity than ni8B and therefore favorable higher hydrophobicity could not be the cause of the enhanced transport of ni3A. Ni3A has 18 positively charged amino acids and ni8B 17, however if this is counteracted by the amount of negatively charged amino acids, for ni3A and ni8B respectively 13 and 11 has to be determined from the tertiary structure and all the accompanied interactions. Further structural analysis is necessary after this tertiary structure and the interaction between the different molecules to determine the nature of the higher transport rate of ni3A.

5. IN VIVO IMAGING OF ASS SPECIFIC VHH

In the next step the niVHH were tested on tissue sections of 13-14 month old APP-PS1 mice. On those sections the niVHH could not distinguish between vascular and parenchymal Aβ depositions. This in contrast to the ability to differentiate between the different Aβ depositions in human tissue.

An explanation for the observed divergence in reactivity between human AD and the APP/PPS1 mouse model could be that there are dissimilarities reported in the plaque morphology and consistence between human AD and the APP/PS1 mouse model [22,23]. The human AD plaques consist of discontinuous patches with decreased density and the amyloid core has a random fibrillar orientation. The structure of amyloid in transgenic mouse plaques is densely packed and the amyloid forms long and organized fibrils. The decreased compactness in the human AD plaques results in gaps that are seldom present in the transgenic mouse plaques. In addition, plaques of similar size have a larger center core of dense compact amyloid in APP/PS 1 mice compared to human AD.

Besides structure differences, distribution of human and mouse amyloid are intermingled in diffuse plaques found in the APP/PS1 mouse model and dense plaques are composed of human core surrounded by mouse amyloid [24].

Furthermore, there are differences in posttranslational modifications between the APP/PS1 mouse model and the human situation. This leads to alterations in the Aβ molecule and consequently to affinity differences of our antibody fragments [22,25,26].

While it is unknown precisely how Aβ plaque aggregation occurs, it is known that metalions play a role especially regarding its toxicity [27]. The differences in morphology and iron constitution reported between human AD and transgenic APP/PS1 plaques may indicate a dissimilar genesis. This could influence the tertiary structure and consequently the availability of the diverse epitopes. The affinity of the antibody fragment for the amyloid present is dependent on this epitope availability.

The differences between the plaques raises the question for translating the APP/PS1 models data to the human AD. Therefore knowledge of the differences between the mouse model and the human situation is essential to translate and interpret the data correctly when using a such mouse model.

The first step toward *in vivo* imaging was to assess whether the VHH maintained their properties when applied in the APP/PS1 mouse model. From the results of this study we can conclude that the Aβ specificity of the VHH is preserved *in vivo* and their ability to recognize vascular and parenchymal Aβ discussed above is confirmed. In order to monitor this Aβ specificity, Aβ depositions were labeled with Methoxy-X04 prior to application of the VHH. When Methoxy-X04 was applied first, binding of the VHH was not visible. The influence of Methoxy-X04 on the binding properties of the VHH could indicate competition between the two binders and denote towards affinity for the same epitope. Future competition experiments are necessary to elucidate the exact epitope recognized by the VHH.

In addition, many of the Aβ plaques visualized with the VHH at day 0, remained undetected two days later. Although presence of the VHH was not tested after the experiment and should therefore not be excluded as a cause, this could indicate disentanglement of the plaque itself. Preliminary research indicated that VHH could prevent protein aggregation of amyloid fibrils polyA-binding protein and oligomeric forms of Aβ and , even clear existing aggregates [28,29].

Additionally a biodistribution study was performed. The results of this study show a significant difference in cerebral activity of ^{99m}Tc-VHH between wild type and transgenic animals 24hrs past the injection of pa2H. Although, enhancement of the actual amounts of VHH within the brain should be accomplished in future research, these data provide preliminary evidence that these VHH have the ability to target Aβ depositions *in vivo*. The presence of soluble amyloid in the blood of transgenic animals, and also to lesser extent in wild type mice [30], could lead to the binding of the relative small amount VHH in the blood and decrease the amount of VHH found in the brain. In order to prevent this, higher amounts of unlabeled VHH could be pre-injecting or slow infusion experiments have to be performed.

In addition the VHH were tested in a more systemic approach. With disrupting the BBB, VHH pa2H-Alexa594 could be detected to label, up to at least 24hrs post injection into the right internal carotic artery of aged APP-PS1 mice, the cerebral Aβ. Unfortunately, the VHH could not be detected without BBB disruption. Because the biodistribution study indicates towards BBB crossing potential of the VHH, the failing ability to cross in this experimental setup could be caused by a combination of not sufficient transmigration of the VHH and the sensitivity of the detection technique. VHH transport could be improved by giving the protein an overall higher positive charge, without losing affinity for Aβ, as positively charged molecules can increase the BBB permeability. In addition, BBB crossing efficiency could be improved by linking Aβ recognizing VHH to a serum albumin recognizing VHH, a bispecific VHH is created with increased serum half life [10].

GENERAL CONCLUSION

Overall, the results obtained from three different selections indicate that the selected VHH can detect a difference in conformational structures of Aβ between parenchymal plaques and vascular Aβ depositions. In addition, the VHH are able to pass the BBB *in vitro* and biodistribution studies indicate towards possible *in vivo* passage. Moreover, it can be concluded that the VHH maintain their functionality in an *in vivo* system.

VHH are known for their ability to recognize small and not easily accessible epitopes. Therefore, the difference in recognition of the VHH between the diverse Aβ depositions in the different disease conditions could well be a trait specific for VHH. When this is indeed the case, it makes them a potentially unique tool for further research into the role of Aβ in sporadic and hereditary forms of AD and CAA.

The VHH selected from different libraries show high affinities preferentially for the immunization material used. Different affinities between Aβ depositions in the plaques and the vessels and between AD/CAA and HCHWA-D were observed. Therefore, with the use of these different immune libraries it became evident that is it possible to select against the same antigen in a different appearance and fine tune the selection of VHH by the choice of the immunization material. Therefore, this selection strategy has potential to be used to develop imaging probes for a wide scope

of neurodegenerative disorders. The VHH selected in this study have potential as highly specific diagnostic probes for early and differential detection of cerebral Aß in living patients.

REFERENCE LIST

1. Hardy,J. & Selkoe,D.J. The amyloid hypothesis of Alzheimer's disease: progress and problems on the road to therapeutics. *Science* **297**, 353-356 (2002).
2. van Duinen,S.G. *et al.* Hereditary cerebral hemorrhage with amyloidosis in patients of Dutch origin is related to Alzheimer disease. *Proc. Natl. Acad. Sci. U. S. A* **84**, 5991-5994 (1987).
3. Bornebroek,M. *et al.* Hereditary cerebral hemorrhage with amyloidosis-Dutch type: better correlation of cognitive deterioration with advancing age than with number of focal lesions or white matter hyperintensities. *Alzheimer Dis. Assoc. Disord.* **10**, 224-231 (1996).
4. Gravina,S.A. *et al.* Amyloid beta protein (A beta) in Alzheimer's disease brain. Biochemical and immunocytochemical analysis with antibodies specific for forms ending at A beta 40 or A beta 42(43). *J. Biol. Chem.* **270**, 7013-7016 (1995).
5. Prelli,F. *et al.* Expression of a normal and variant Alzheimer's beta-protein gene in amyloid of hereditary cerebral hemorrhage, Dutch type: DNA and protein diagnostic assays. *Biochem. Biophys. Res. Commun.* **170**, 301-307 (1990).
6. Herzig,M.C. *et al.* Abeta is targeted to the vasculature in a mouse model of hereditary cerebral hemorrhage with amyloidosis. *Nat. Neurosci.* **7**, 954-960 (2004).
7. Deane,R. *et al.* RAGE mediates amyloid-beta peptide transport across the blood-brain barrier and accumulation in brain. *Nat. Med.* **9**, 907-913 (2003).
8. Shibata,M. *et al.* Clearance of Alzheimer's amyloid-ss(1-40) peptide from brain by LDL receptor-related protein-1 at the blood-brain barrier. *J. Clin. Invest* **106**, 1489-1499 (2000).
9. Herz,J. & Marschang,P. Coaxing the LDL receptor family into the fold. *Cell* **112**, 289-292 (2003).
10. Coppieters,K. *et al.* Formatted anti-tumor necrosis factor alpha VHH proteins derived from camelids show superior potency and targeting to inflamed joints in a murine model of collagen-induced arthritis. *Arthritis Rheum.* **54**, 1856-1866 (2006).
11. Shankar,G.M. *et al.* Amyloid-beta protein dimers isolated directly from Alzheimer's brains impair synaptic plasticity and memory. *Nat. Med.* **14**, 837-842 (2008).
12. Banks,W.A., Robinson,S.M., Verma,S. & Morley,J.E. Efflux of human and mouse amyloid beta proteins 1-40 and 1-42 from brain: impairment in a mouse model of Alzheimer's disease. *Neuroscience* **121**, 487-492 (2003).
13. Behar,G. *et al.* Isolation and characterization of anti-FcgammaRIII (CD16) llama single-domain antibodies that activate natural killer cells. *Protein Eng Des Sel* **21**, 1-10 (2008).
14. Rubin,L.L. & Staddon,J.M. The cell biology of the blood-brain barrier. *Annu. Rev. Neurosci.* **22**, 11-28 (1999).
15. Pardridge,W.M. Blood-brain barrier biology and methodology. *J. Neurovirol.* **5**, 556-569 (1999).
16. Pardridge,W.M. Drug and gene delivery to the brain: the vascular route. *Neuron* **36**, 555-558 (2002).
17. Abbott,N.J. & Romero,I.A. Transporting therapeutics across the blood-brain barrier. *Mol. Med. Today* **2**, 106-113 (1996).
18. Abulrob,A., Sprong,H., Bergen en,H.P. & Stanimirovic,D. The blood-brain barrier transmigrating single domain antibody: mechanisms of transport and antigenic epitopes in human brain endothelial cells. *J. Neurochem.* **95**, 1201-1214 (2005).
19. Muyldermans,S., Cambillau,C. & Wyns,L. Recognition of antigens by single-domain antibody fragments: the

superfluous luxury of paired domains. *Trends Biochem. Sci.* **26**, 230-235 (2001).

20. Pardridge,W.M. Blood-brain barrier delivery. *Drug Discov. Today* **12**, 54-61 (2007).
21. Kyte,J. & Doolittle,R.F. A simple method for displaying the hydropathic character of a protein. *J. Mol. Biol.* **157**, 105-132 (1982).
22. Duyckaerts,C., Potier,M.C. & Delatour,B. Alzheimer disease models and human neuropathology: similarities and differences. *Acta Neuropathol.* **115**, 5-38 (2008).
23. Guntert,A., Dobeli,H. & Bohrmann,B. High sensitivity analysis of amyloid-beta peptide composition in amyloid deposits from human and PS2APP mouse brain. *Neuroscience* **143**, 461-475 (2006).
24. van Groen,T., Kiliaan,A.J. & Kadish,I. Deposition of mouse amyloid beta in human APP/PS1 double and single AD model transgenic mice. *Neurobiol. Dis.* **23**, 653-662 (2006).
25. Bussiere,T. *et al.* Morphological characterization of Thioflavin-S-positive amyloid plaques in transgenic Alzheimer mice and effect of passive Abeta immunotherapy on their clearance. *Am. J. Pathol.* **165**, 987-995 (2004).
26. Richardson,J.A. & Burns,D.K. Mouse models of Alzheimer's disease: a quest for plaques and tangles. *ILAR. J.* **43**, 89-99 (2002).
27. Ghribi,O., Golovko,M.Y., Larsen,B., Schrag,M. & Murphy,E.J. Deposition of iron and beta-amyloid plaques is associated with cortical cellular damage in rabbits fed with long-term cholesterol-enriched diets. *J. Neurochem.* **99**, 438-449 (2006).
28. Dumoulin,M. *et al.* A camelid antibody fragment inhibits the formation of amyloid fibrils by human lysozyme. *Nature* **424**, 783-788 (2003).
29. Verheesen,P. *et al.* Reliable and controllable antibody fragment selections from Camelid non-immune libraries for target validation. *Biochim. Biophys. Acta* **1764**, 1307-1319 (2006).
30. Takeda,S. *et al.* Elevation of plasma beta-amyloid level by glucose loading in Alzheimer mouse models. *Biochem. Biophys. Res. Commun.* **385**, 193-197 (2009).

ADDENDUM | SUMMARY
SAMENVATTING
CURRICULUM VITAE
DANKWOORD

SUMMARY

Accumulation and Aggregation of amyloid-forming proteins are fundamental to a rising group of progressive and chronic diseases, collectively known as cerebral amyloidoses. The aggregates are all arranged in an equally structured manner, termed amyloid. Alzheimer's disease (AD) and cerebral amyloid angiopathy (CAA) are diseases that are histologically characterized by amyloid deposits.

AD is one of the major health problems in the world and the most common form of dementia. By post-mortem analysis of human AD brains the first indication of the mechanisms involved in this disease were acquired. Based on these investigations the histological hallmarks of AD were identified: senile plaques consisting of extracellular amyloid-β (Aβ) deposits, and neurofibrillary tangles associated with tau aggregates in the regions of the brain responsible for memory and cognition. Apart from the appearance in senile plaques, fibrillar amyloid deposition is also often detected in medium-sized and small cerebral vessel walls, causing CAA. This vascular amyloid deposition causes vascular dysfunction, which is postulated to be a major contributor to age-related neurodegeneration.

CAA is most frequently caused by Aβ aggregates and, analogous to AD, mutations in the Aβ precursor protein (APP), presenilin 1 en 2 (PS1 and PS2) genes underlie familial forms of CAA. The most severe forms of CAA are observed in cases with the Flemisch, Iowa or Dutch mutation in APP. The Dutch mutation in APP (guanine-to-cytosine transversion at codon 693) causes the disorder known as hereditary cerebral hemorrhage with amyloidosis-Dutch type (HCHWA-D). As HCHWA-D is an autosomal dominant disease, causing early deposition of amyloid, HCHWA-D is a good model for research of early diagnosis of AD and CAA.

The mere presence of Aβ is not responsible for setting off the Aβ-inflicted neurodegeneration pathway, because the Aβ protein is also present in the brain and cerebrospinal fluid of healthy individuals throughout life. Therefore, the exact nature of Aβ toxicity is still an object of debate. The ability to self-associate appears to instigate neurotoxicity of Aβ. Earlier it was assumed that amyloid fibrils were the toxic species of Aβ. However the soluble Aβ oligomer levels correlate better with the degree of synaptic loss and severity of cognitive impairment than the number of senile plaques, which consist of Aβ fibrils. In addition, small Aβ oligomers exhibit in general much higher cytotoxicity than Aβ fibrils. Therefore, efforts to develop therapeutic approaches for early targeting of Aβ neurotoxicity should be primarily directed against the oligomeric forms of Aβ. The difficulty in targeting Aβ is that all imaging or therapeutic moieties have to be able to pass the blood brain barrier (BBB), which is formed by different types of cells that regulate transport selectively in order to protect the brain against pathogenic molecules and organisms. Therefore, small molecules that can cross the BBB and recognize Aβ depositions could be valuable tools for AD imaging and therapy.

This thesis aimed at the development of affinity binders for non-invasive in vivo imaging of neurodegenerative disorders like AD and CAA.

Camelidae express, in addition to the conventional immunoglobulin repertoire, unusually shaped antibodies which are devoid of light chains: the so-called heavy chain antibodies. Their single N-terminal domain (VHH) is fully capable of antigen binding. The favourable properties of VHHs make them good candidates as tool for non-invasive, early and differential *in vivo* Aß detection in the brain, because of their small size VHHs rapidly pass the renal filter resulting in a fast blood clearance and rapid tissue penetration, they are reported to be able to cross the BBB, and they have not shown any immunogenicity in mice.

In ***chapter two*** the generation of antibody fragments directed against Aß is described. The llama-derived VHHs were selected by phage display. For this selection, non-immune and immune libraries were used. The VHHs were tested for their beta amyloid recognizing properties by phage-ELISA, immunohistochemistry and affinity measurements. Eight distinct VHHs were identified with high beta amyloid affinity and specificity. Three VHHs displayed affinity for vascular and parenchymal beta amyloid deposits and five VHHs specifically recognized vascular beta amyloid. VHHs that were selected from different libraries showed differential affinity for different epitopes when used for immunohistochemistry. These observations indicate that the VHHs are the first immunologic probes with the capacity to differentiate between parenchymal and vascular beta amyloid aggregates. Consequently, this infers that vascular and parenchymal beta amyloid deposits are heterogeneous in epitope presence/availability. The described properties of these VHHs make them potential candidates for use in differential *in vivo* diagnosis of AD and CAA.

Subsequently, the amyloid beta specific VHHs were assessed for their potential to cross the BBB, in ***chapter three***, using an established *in vitro* BBB co-culture system. Bovine brain capillary endothelial (BCEC) cells and newborn rat astrocytes are used in this *in vitro* BBB co-culture system to mimic the BBB *in vitro*. VHH ni3A showed the highest transmigration efficiency of all tested VHHs. This transport is, in part, facilitated by a 3 amino acid substitution in its N-terminal domain. Additional studies indicated that the mechanism of transcellular passage of ni3A is by active transport. VHH ni3A combines the ability to recognize amyloid beta and to cross the BBB and has consequently potential as a tool for non-invasive *in vivo* imaging in patients suffering from neurodegenerative disorders like AD and CAA.

The VHHs were evaluated for their *in vivo* properties in ***chapter four***. VHH ni3A and pa2H recognized murine parenchymal Aβ depositions in post mortem brain sections of a mouse model for AD and CAA. However, the selectivity of ni3A for CAA was not confirmed for this transgenic model. This result underlines the divergence between murine and human plaque formation. In addition, *in vivo* behavior in terms of clearance and biodistribution was monitored. Radioactive ^{99m}Technicium-labeled VHHs showed fast renal clearance after tail vein injection. Administration of a small bolus of radiolabeled pa2H resulted in a significantly higher brain uptake 24 hours post injection in transgenic versus wild type animals. *In vivo* binding properties

were assessed using fluorescently labeled VHHs. In these experiments, the BBB was bypassed either by craniotomy combined with intravital microscopy, or disrupted using intracarotid co-injections of mannitol. Both VHHs showed specificity for parenchymal and vascular Aβ plaques *in vivo*. Pa2H displayed the highest affinity for Aβ deposits. In contrast to ni3A, the higher affinity of pa2H *in vivo* resulted in detection of Aβ deposits even 24 hours or more past injection. The data described in ***chapter four*** provides preliminary proof that these VHHs have the capacity to target Aβ depositions *in vivo*. Consequently, the VHHs are promising tools for further development as imaging agents for the differential diagnosis of Aβ-related neurodegenerative diseases like CAA and AD.

The results of the experiments described in the first four chapters of this thesis are discussed in ***chapter five***. The results obtained from the three different selections indicate that the selected VHHs are able to detect differences in conformational structures between parenchymal plaque and vascular Aβ depositions. Additionally, the VHHs have shown to transmigrate the BBB *in vitro* and biodistribution studies point towards possible *in vivo* passage. Moreover, it can be concluded that the VHHs maintain their functionality in an *in vivo* system.

The difference in detection of the VHHs between the various Aβ depositions in the different disease conditions could well be a trait specific for VHHs, since the ability to recognize small and not easily accessible epitopes is a characteristic feature of VHHs. Consequently, VHHs are a potentially unique tool for further research into the role of Aβ in sporadic and hereditary forms of AD and CAA.

The VHHs discussed in this thesis show different affinities for Aβ depositions in the plaques and the vessels and between AD/CAA and HCHWA-D. From this we can conclude that the immunization material, which forms the foundation for the different libraries, is essential for the affinity preference of the selected VHH. Therefore, with the use of these different immune libraries it became evident that it is possible to select against the same antigen in a different appearance and fine tune the selection of VHHs by the choice of the immunization material. This selection strategy has potential for the development of imaging probes for a wide scope of neurodegenerative disorders. The VHHs developed in this study possess a special high specificity. Consequently, these VHHs could be developed to be potent diagnostic probes for early and differential detection of cerebral Aß in living patients.

SAMENVATTING

Accumulatie en aggregatie van amyloïd-vormende eiwitten zijn essentieel voor een groeiende groep van progressieve en chronische ziekten, gezamenlijk bekend als amyloidoses. De aggregaten zijn allemaal op zeer gestructureerde wijze gerangschikt, in het zogenoemde amyloïd. De ziekte van Alzheimer (AD) en cerebrale amyloïd angiopathie (CAA) zijn ziekten die histologisch onder andere worden gekenmerkt door amyloïd afzettingen. AD is één van de belangrijkste gezondheidsproblemen in de wereld en de meest voorkomende vorm van dementie. Het eerste inzicht in de mechanismen achter deze ziekte werd verworven door post-mortem analyse van de menselijke hersenen van Alzheimer patiënten. Op basis van dit onderzoek werden de histologische kenmerken van AD geïdentificeerd: seniele plaques bestaande uit extracellulaire amyloid-β (Aß) deposities en tangles geassocieerd met tau aggregaten in de regio van de hersenen die verantwoordelijk zijn voor het geheugen en cognitie.

Naast deze kenmerken, worden fibrillaire amyloïd afzetting ook vaak aangetroffen in middelgrote en kleine cerebrale vaatwanden, waar het CAA veroorzaakt. Deze vasculaire amyloïd afzetting veroorzaakt vasculaire dysfunctie die wordt gepostuleerd als een van de belangrijkste mechanismen achter neurodegeneratie. Het levert daarom een belangrijke bijdrage aan de pathogenese van de ziekte. CAA word meestal veroorzaakt door Aß aggregaten en analoog aan AD, liggen mutaties in het Aß precursor eiwit (APP), presenilin 1 en 2 (PS1 en PS2) genen ten grondslag aan de familiale vormen van CAA. De meest ernstige vormen van CAA zijn waargenomen in patiënten met de Vlaamse, Iowa of Nederlandse mutatie in APP. De Nederlandse mutatie in APP (guanine-to-cytosine transversie op codon 693) veroorzaakt de aandoening die bekend staat als hereditary cerebral hemorrhage with amyloidosis-Dutch type (HCHWA-D). Omdat er bij HCHWA-D een genetische oorzaak ten grondslag ligt aan de ziekte, waarbij alle dragers van de mutatie (jong) last zullen krijgen van amyloid afzettingen, is HCHWA-D een goed model voor onderzoek naar de vroegdiagnostiek van AD en CAA.

Gezien het feit dat het Aß-eiwit ook aanwezig is in de hersenen en de cerebrospinale vloeistof van gezonde individuen gedurende het hele leven, is de loutere aanwezigheid van Aß niet verantwoordelijk voor de toedracht van Aß aan de neurodegeneratie. Daarom is de precieze aard van Aß toxiciteit nog steeds een onderwerp van debat. Het vermogen tot zelf-aggregatie lijkt de agitator van de neurotoxiciteit van Aß. Er werd eerst van uitgegaan dat amyloïde fibrillen de giftige vormen van Aß waren. Echter, de oplosbare Aß oligomeer-concentraties zijn sterk gecorreleerd met de mate van synaptisch verlies en de ernst van cognitieve stoornissen, terwijl de correlatie veel minder sterk aanwezig is met het aantal seniele plaques, bestaande uit Aß fibrillen. Bovendien vertonen kleine Aß oligomeren in het algemeen veel hogere cytotoxiciteit dan de Aß fibrillen. Bijgevolg moet therapie met als doel vroege neutralisatie van Aß neurotoxiciteit gericht zijn tegen deze oligomeren. De moeilijkheid bij de targeting van Aß is dat alle beeldvormende of therapeutische middelen in staat moeten zijn om de bloed-hersenbarrière (BHB) passeren, een barrière van verschillende celtypen

die selectief transport toelaten om zo de hersenen te beschermen tegen pathogene moleculen en organismen. Daarom zouden kleine moleculen die in staat zijn de BHB te passeren en Aß kunnen herkennen waardevolle hulpmiddelen voor AD imaging en therapie zijn.

Het doel van de in dit proefschrift beschreven experimenten is de ontwikkeling van affiniteitsbinders voor niet-invasieve *in vivo* imaging van neurodegeneratieve aandoeningen zoals AD en CAA. De affiniteitsbinders die uitermate geschikt zijn voor dit doel zijn afgeleiden van Lama antilichamen.

Kameelachtigen produceren in aanvulling op het conventionele antilichaam repertoire, bijzondere gevormde antilichamen die zijn verstoken van lichte ketens: de zogenaamde zware keten antilichamen. Hun N-terminale domein (VHH) is volledig in staat om antigenen te binden. Verschillende gunstige eigenschappen van VHHs maken hen tot goede kandidaten voor niet-invasieve, vroegtijdige en differentiële *in vivo* detectie van Aß in de hersenen: vanwege hun kleine formaat passeren VHHs snel het renale-filter wat resulteert in een snelle bloedklaring en snelle weefselpenetratie, ze zijn volgens de literatuur in staat om de BHB te passeren, en ze tonen geen immunogeniciteit bij muizen.

In ***hoofdstuk twee*** wordt de ontwikkeling van antilichaamfragmenten gericht tegen Aß beschreven. De lama-afgeleide VHHs werden geselecteerd door faag display. Voor deze selectie werden niet-immuun en immuun bibliotheken van VHHs gebruikt. De geselecteerde VHHs werden getest op hun beta-amyloïd herkennende eigenschappen door middel van faag-ELISA, immunohistochemie en affiniteitsstudies. Acht verschillende VHHs werden geïdentificeerd met een hoge affiniteit en specificiteit for beta-amyloïd. Drie VHHs lieten affiniteit voor vasculaire en parenchymale beta-amyloïd afzettingen zien en vijf VHHs toonden specificiteit voor vasculaire beta-amyloïd deposities. VHHs die werden geselecteerd uit verschillende bibliotheken bleken differentiële affiniteit voor verschillende epitopen te bezitten wanneer deze getest werden door middel van immunohistochemie. Deze waarnemingen geven aan dat de VHHs de eerste immunologische moleculen zijn met het vermogen om onderscheid te maken tussen parenchymale en vasculaire beta-amyloïd aggregaten. Bijgevolg wijst dit op heterogeniteit tussen vasculaire en parenchymale beta-amyloïd deposities in epitoop aanwezigheid/beschikbaarheid. De beschreven eigenschappen van deze VHHs maakt hen potentiële kandidaten voor gebruik in differentiële *in vivo* diagnose van AD en CAA.

De ontwikkelde beta-amyloïd specifieke VHHs werden beoordeeld op hun potentieel om de BHB te passeren met behulp van een erkend *in vitro* BHB co-cultuur systeem in ***hoofdstuk drie***. Om de BHB na te bootsen *in vitro*, worden in dit BHB co-cultuur systeem Capillaire Runder Endotheelcellen (CREC) en pasgeboren rat astrocyten gebruikt. VHH ni3A toonde de hoogste BHB transmigratie efficiëntie van alle geteste VHHs. Dit transport wordt voor een deel gefaciliteerd door een substitutie van 3 aminozuren in het N-terminale domein van VHH ni3A. Additionele studies gaven aan dat het mechanisme van transcellulaire passage van ni3A actief transport is. VHH ni3A combineert dus de mogelijkheid om amyloïd beta te herkennen en de BHB

te passeren en heeft daarom potentieel als middel voor niet-invasieve *in vivo* imaging bij patiënten die lijden aan neurodegeneratieve aandoeningen zoals AD en CAA.

De VHHs worden beoordeeld op hun *in vivo* eigenschappen in ***hoofdstuk vier***. Middels immunohistochemie werd aangetoond dat VHHs ni3A en pa2H de Aß deposities herkennen in post mortem parenchym van een muismodel voor CAA en AD. De selectiviteit van ni3A voor uitsluitend CAA werd echter niet bevestigd voor dit transgene model. Dit resultaat onderstreept het verschil tussen muis en mens in plaque-vorming. Daarnaast werd het *in vivo* gedrag in termen van klaring en biodistributie bepaald. Radioactief 99mTechnicium gelabelde VHHs toonden snelle renale klaring na intraveneuze injectie. Toediening van een kleine bolus van radioactief gemerkte pa2H resulteerde in een significant hogere brein opname 24 uur na injectie in transgene versus wild-type dieren. *In vivo* bindende eigenschappen werden verder beoordeeld met behulp van fluorescent gelabelde VHHs. In deze experimenten de werd BHB ofwel omzeild door craniotomie gecombineerd met intravitaal microscopie of verstoord met behulp van intracarotid co-injecties met mannitol. Beide VHHs toonden specificiteit voor parenchymale en vasculaire Aß plaques *in vivo*. Pa2H toonde de hoogste affiniteit voor Aß deposities. In tegenstelling tot ni3A, resulteerde de hogere affiniteit van pa2H *in vivo* in de detectie van Aß deposito's, zelfs na 24 uur of meer. De data beschreven in ***hoofdstuk vier*** levert preliminair bewijs dat deze VHHs de capaciteit hebben om *in vivo* Aß afzettingen te herkennen. Bijgevolg zijn de VHHs veelbelovend voor de verdere ontwikkeling als diagnostische middelen voor differentiële detectie van Aß gerelateerde neurodegeneratieve ziekten zoals CAA en AD.

De resultaten van de experimenten beschreven in hoofdstukken 2 t/m 4 van dit proefschrift worden bediscussieerd in ***hoofdstuk vijf***. De uitkomsten van de drie verschillende selecties geven aan dat de geselecteerde VHHs in staat zijn om verschillen in conformationele structuren tussen parenchymale plaque en vasculaire Aß afzettingen op te sporen. Daarnaast zijn de VHHs in staat om *in vitro* over de BHB te passeren, en biodistributie studies wijzen in de richting van mogelijke *in vivo* passage. Bovendien kan worden geconcludeerd dat de VHHs hun functionaliteit *in vivo* behouden.

Het verschil in detectie van de VHHs tussen de verschillende Aß afzettingen in de verschillende aandoeningen zou wel eens een eigenschap kunnen zijn die specifiek is voor VHHs, omdat de mogelijkheid om kleine en niet gemakkelijk toegankelijke epitopen te herkennen één van de gunstige karakteristieken is van VHHs. Bijgevolg zijn VHHs een potentieel uniek instrument voor verder onderzoek naar de rol van Aß bij sporadische en erfelijke vormen van AD en CAA.

De VHHs besproken in dit proefschrift tonen verschillende affiniteiten voor Aß deposities in de plaques en de vaten en tussen AD/CAA en HCHWA-D. Hieruit kunnen we concluderen dat het immunisatiemateriaal, dat de bron vormt voor de verschillende bibliotheken, essentieel is voor de affiniteitsvoorkeur van de geselecteerde VHHs.

Derhalve, is met het gebruik van deze verschillende immuunbibliotheken duidelijk geworden dat het mogelijk is om te selecteren voor het zelfde antigeen in een andere conformatie, en zodoende de selectie van VHHs te optimaliseren door de keuze van het

immunisatiemateriaal. Deze selectiestrategie heeft potentie voor de ontwikkeling van imaging probes met een breed toepassingsgebied, onder andere voor de diagnostiek van neurodegeneratieve aandoeningen. De VHHs ontwikkeld in deze studie beschikken over een hoge specificiteit. Bijgevolg zouden deze VHHs ontwikkeld kunnen worden tot effectieve diagnostische probes voor vroegtijdige en differentiële detectie van cerebraal Aß in levende patiënten.

CURRICULUM VITAE

Kim Rutgers was born on October 3th, 1975, in Nijmegen, The Netherlands. She attended the Canisius College Mater Dei in Nijmegen, where she finished her VWO degree in 1996. Thereupon, she studied Molecular Biology at Leiden University. During her studies she specialized in Biotechnology at the Technical University of Delft in 2001. For her graduation internship she worked on the project: *Phage display and heavy chain antibody fragments* at Utrecht university. This project e.g. heavy chain antibody fragments formed the basis of her PhD project. Kim graduated "*cum laude*" in 2003.

During her Master's studies Kim did volunteer work for the Dutch government plan to help improve knowledge of the Dutch language by allochthonous children from disadvantaged neighborhoods. She was member of the Dies committee in 2002 and vice-chairman in 2003 from the Leiden Biology Study Association.

In 2003 Kim started her PhD research in medical sciences at the Leiden University Medical Center. In 2009 Kim was invited for collaboration with Harvard University and Massachusetts general Hospital to test the affinity binders for Alzheimer's diagnostics, developed during her research, on their *in vivo* applications.

Currently Kim initiated a comprehensive internship/learning program at Standard Tael (a specialized M&A boutique) to enable a career switch from an academic research environment to the business environment of a professional service provider. Program will eventually cover all aspects of the advisory practice i.e. sales & marketing, transaction origination, research and deal execution. From April 1st 2011 Kim lives in Luxembourg with husband Bas and daughter Josephine.

DANKWOORD

Dit proefschrift beschrijft mijn onderzoek van de afgelopen jaren en meer. De voltooiing van dit proefschrift luidt het einde in van een enorm boeiend en leerrijk proces. Tijdens de afgelopen jaren heb ik een beroep kunnen doen op de steun van vele mensen, en bij deze gelegenheid wil ik hen dan ook van harte bedanken. Vooreerst richt ik mij tot mijn promotor Silvere van der Maarel. Bedankt voor de grote vrijheid die je me hebt gegeven in dit onderzoek, voor je advies en voor de verrijkende discussies. Ik heb de kans gekregen een compleet nieuw onderzoek op te bouwen en ons als groep op de kaart te zetten op het gebied van de neuroscience, hartelijk dank voor deze mogelijkheid. Verder zou ik graag Mark van Buchem en Louise van der Weerd willen bedanken. Mark bedankt voor je constructieve feedback en waardevolle suggesties die mij in staat hebben gesteld om deze dissertatie verder te verbeteren.

Binnen dit multidisciplinaire onderzoek heb ik vele samenwerkingsverbanden op mogen bouwen. De afdelingen pathology en neurology van het LUMC, hartelijk dank voor jullie enthousiasme, steun en expertise. Speciaal zou ik Marion Maat-Schieman, Sjoerd van Duinen en natuurlijk Ingrid Hegeman heel hartelijk willen bedanken. Van de universiteit Utrecht zou ik Mohammed willen bedanken voor een bijdrage aan het maken van de immuun banken en Theo Verrips voor het mentoren van de basis in het affinity binder onderzoek die tijdens mijn studietijd gelegd is. Dit onderzoek was niet mogelijk geweest zonder een fantastisch *in vitro* bloed hersen barriere systeem waarvoor de groep van Bert de Boer zorg droeg, ik ben jullie zeer erkentelijk.

Special thanks go to Steven Greenberg for inviting me to Harvard University/ Massachusetts general hospital to start with our *in vivo* experiments in mice. I was given the opportunity to work in the great group of Brian Bacskai, thank you so much for sharing your experience and insights. Matthew Frosch thank you for providing the tissue of the Boston CAA patients and for sharing your expertise.

Tevens zou ik mijn collega's van het LUMC willen bedanken voor de fantastische werkomgeving. Met name alle mensen van de groep Frants: Migraine, Lipiden, FSHD en natuurlijk proteomics: Ilona, Laure, Maarten, Maartje, Marco en Rinse een buitengewoon team. En niet te vergeten de oud proteomics leden: Antoine, Antonietta, Paula en Smiriti. Sjoerd en Silvia dank jullie wel voor de gezelligheid en leuke discussies. In dit rijtje mogen natuurlijk Marjolein en Jeroen niet ontbreken, dank jullie wel voor jullie support en output. Anita bedankt voor de coördinatie van alle administratieve zaken. Alexandra dank je wel voor onze uiterst belangrijke koffie momenten, steun en ook output binnen het project. En natuurlijk wil ik Rob bedanken voor de mooie resultaten die we met het *in vivo* werk behaald hebben en de leuke tijd in Boston. Veel succes binnen dit mooie project. Tevens wil ik mijn studenten bedanken voor hun bijdrage.

Uiteraard horen ook mijn vrienden in dit rijtje thuis. Bedankt ook voor jullie interesse en de continue steun. Speciaal de meisjes uit Leiden, Mas, dank je dat je mijn paranimf wilt zijn. Mijn bestuursmaatjes: Maaike en Marjolein. Mijn familie en

schoonfamilie wil ik ook bedanken. Bob, Agnes, Oma, Charlotte en Mark. Maria en Jos bedankt voor steun en boeiende gesprekken ;-) die me opnieuw energie gaven en tezelfdertijd hielpen om de dingen in perspectief te zien.

Tot slot wil ik voor mij de twee allerbelangrijkste mensen op deze wereld bedanken Josephine en Bas. Josephientje je hebt nu al zo'n krachtige en vrolijke persoonlijkheid, die mij bergen met geluk geeft. Bas bedankt voor je nooit aflatende steun. Je geeft me altijd stapels met vertrouwen die me de kracht hebben gegeven om dit traject te doorlopen en een fantastisch resultaat neer te zetten. Het is niet altijd makkelijk mijn man te zijn ;-), zeker niet wanneer ik door mijn focus soms de wereld om me heen een beetje vergeet.

&

Amor omnia vincit.

Het is gemakkelijker een atoom te splitsen dan een vooroordeel weg te nemen.

Albert Einstein